Soil Stabilization Phase Report No. 8

EFFECT OF MOLDING CONDITIONS ON THE EFFECTIVE STRESS-STRENGTH BEHAVIOR OF A STABILIZED CLAYEY SILT

by

Anwar E.Z. Wissa
Samuel Feferbaum-Zyto
Jose Guillermo Paniagua

Sponsored by

U.S. Army Materiel Command
DA Project No. I-T-O-1451-B-52-A30

Conducted for

U.S. Army Engineer Waterways Experiment Station
Vicksburg, Mississippi

under

Contract No. DA IT06111102B52A-01

Research Report No. R69-55
Soil Mechanics Division
Department of Civil Engineering
Massachusetts Institute of Technology

January, 1970

Soils Publication No. 242

FOREWORD

This report is the eighth in a series of reports on soil stabilization issued by the Massachusetts Institute of Technology for the U.S. Army Materiel Command under Project Number DA IT061102B52A-01. The work was conducted during fiscal years 1966-1968 under Contract No. DA-22-079-eng-465 between the U.S. Army Engineer Waterways Experiment Station, Vicksburg, Mississippi, and the Soils Research Laboratory of the Department of Civil Engineering at the Massachusetts Institute of Technology.

The work covered by this report was conducted by Mr. Samuel Feterbaum-Zyto, and Mr. Jose Guillermo Paniagua, both Research Assistants in Soils, under the direct supervision of Dr. Anwar E.Z. Wissa, Associate Professor of Civil Engineering. Dr. Wissa and Mr. Paniagua prepared the report.

The contract was monitored by Mr. Royce C. Eaves, Chief Stabilization Section, Expedient Surfaces Branch, under the general supervision of Mr. J.P. Sale, Chief, Soils Division, W.E.S. Contracting Officer was Col. L.A. Brown, C.E.

LIST OF SOIL STABILIZATION PHASE REPORTS

Phase Report	Title
No. 1	"Engineering Behavior of Partially Saturated Soils", May 1963.
No. 2	"Triaxial Equipment and Computer Program for Measuring the Strength Behavior of Stabilized Soils", September 1963.
No. 3	"Effective Stress-Strength Behavior of Compacted Stabilized Soils", July 1964.
No. 4	"Chemical Stabilization of Selected Tropical Soils (From Puerto Rico and Panama)", October 1964.
No. 5	"Shear Strength Generation in Stabilized Soils", June 1965.
No. 6	"Compressibility-Permeability Behavior of Untreated and Cement-Stabilized Clayey Silt", December 1968.
No. 7	"A Durability Test for Stabilized Soils", June 1969.
No. 8	"Effect of Molding Conditions on the Effective Stress-Strength Behavior of a Stabilized Clayey Silt", January 1970.

TABLE OF CONTENTS

LIST OF TABLES

LIST OF FIGURES

Appendix A STRESS-STRAIN BEHAVIOR

BLANK PAGE

SUMMARY

The influence of molding water content, as-molded dry density, and delay time prior to compaction after mixing in of the molding water on the effective stress-strength behavior of a clayey silt stabilized with hydrated lime and portland cement is presented in this report. This investigation used the results of high pressure consolidated-undrained triaxial compression tests with pore water pressure measurements.

It is shown that molding conditions have no significant effect on the Mohr-Coulomb effective stress-strength parameters, $\bar{c}$ and $\bar{\Phi}$, of the untreated compacted soil. For both the cement and lime stabilized systems, the effective cohesion intercept, $\bar{c}$, significantly increases with increases in as-molded dry density while $\bar{\Phi}$ does not change. Molding water content per se does not influence either $\bar{c}$ or $\bar{\Phi}$.

For a given compactive effort, delay time prior to compaction produces a drop in the as-molded dry density of the cement stabilized soil which shows up primarily as a drop in the effective angle of shearing resistance, $\bar{\Phi}$. It also lowers the strains required to reach Mohr-Coulomb failure, which is an undesirable characteristic.

At ultimate failure (large strains), it is shown that neither molding conditions nor delay time prior to compaction have any

significant effect on the effective stress-strength parameters of the stabilized systems.

DEFINITIONS OF SYMBOLS

Symbol	Definition
A	Skempton A Factor or pore pressure coefficient A.
$\bar{A}$	Skempton $\bar{A}$ Factor or pore pressure coefficient $\bar{A}$. $\bar{A} = AB$
B	Skempton B Factor or pore pressure coefficient B. Also called pore pressure response when given as a percentage.
c	Cohesion intercept in terms of total stresses. kg/cm^2.
$\bar{c}$	Effective cohesion intercept of Mohr-Coulomb effective stress envelope, kg/cm^2.
E	Initial tangent modulus or Young's modulus, kg/cm^2.
L.L.	Liquid limit, %.
M-21	Massachusetts clayey silt
Subscript$_M$	At maximum stress difference
P.I.	Plasticity index, %
P.L.	Plasticity limit, %.
p	Maximum Axial Load in Unconfined Test, kg/cm^2
$\bar{p}$	Effective normal stress on 45° plane, kg/cm^2 . $\bar{p} = 1/2\ (\bar{\sigma}_1 + \bar{\sigma}_3)$
q	Shear stress on 45° plane or half principal stress difference, kg/cm^2 . $q = 1/2\ (\sigma_1 - \sigma_3)$
S	Degree of saturation, %
u	Pore Pressure, kg/cm^2
Δu	Change in pore pressure, kg/cm^2

DEFINITIONS OF SYMBOLS (Continued)

Symbol	Definition
w	Water content, %
$\tan \alpha$	Slope of total stress envelope on p versus q plot. $\tan \alpha = \sin \phi$
$\tan \bar{\alpha}$	Slope of effective stress envelope on p versus q plot. $\tan \bar{\alpha} = \sin \bar{\phi}$. Also slope of axial strain contours on $\bar{p}$ versus q plot.
$\tan \bar{\alpha}_{ult}$	Slope of effective stress versus strength relation at ultimate conditions on $\bar{p}$ versus q plot
ε	Axial strain, %
ε_M	Axial strain at maximum principal stress difference, %
σ	Total normal stress, kg/cm^2
$\bar{\sigma}$	Normal effective stress, kg/cm^2
σ_o	Cell pressure, kg/cm^2
$\Delta\sigma_o$	Increment of cell pressure, kg/cm^2
$\bar{\sigma}_o$	Consolidation pressure, kg/cm^2
σ_1	Total major principal stress, kg/cm^2
$\bar{\sigma}_1$	Effective major principal stress, kg/cm^2
σ_3	Total minor principal stress, kg/cm^2
$\bar{\sigma}_3$	Effective minor principal stress, kg/cm^2
$\bar{\sigma}_1/\bar{\sigma}_3$	Effective principal stress ratio (obliquity) Shear stress, kg/cm^2

DEFINITIONS OF SYMBOLS (Continued)

Symbols	Definition
ϕ	Angle of shearing resistance in terms of total stresses, and degrees
$\bar{\phi}$	Angle of shearing resistance in terms of effective stresses, degrees
$\tan \bar{\phi}_{ult}$	Slope of effective normal stress versus shear stress relation at maximum stress difference
γ_d	Dry Density, lb/cu ft

BLANK PAGE

Chapter 1

INTRODUCTION

Numerous investigators have shown that the unconfined compressive strength of lime or cement stabilized fine-grained soils is influenced to a large extent by the as-molded dry density and molding water content. Usually, the maximum unconfined compressive strength of a stabilized soil for a given compaction effort occurs close to the optimum water content for maximum dry density, and therefore it is common practice to specify field compaction at optimum water content. In previous phase reports Wissa and Ladd (1964 and 1965)* have shown that the unconfined compression test is of limited use in studying the strength behavior of stabilized soils since it measures strength under only one specific set of testing conditions that does not usually represent the most critical conditions in the field.

In order to overcome most of the limitation inherent in the unconfined compression test, M.I.T. is using consolidated-drained triaxial tests with volume-change measurements and consolidated-undrained triaxial tests with pore pressure

---

* Items indicated thus, (Wissa and Ladd, 1964) or Wissa and Ladd (1965), refer to corresponding entries arranged alphabetically in the List of References.

measurements to study the strength behavior of stabilized soils. From such test results it is possible to apply the effective stress principle (Terzaghi, 1923) to determine the strength behavior of stabilized soils under a variety of field conditions.

In previous phase reports (Wissa and Ladd, 1964 and 1965), the influence of soil type, type and amount of stabilizer, curing time, and curing history, on the strength behavior of stabilized soils was investigated. It was shown that for a given soil-stabilized system, the frictional resistance in terms of effective stresses is independent of environmental changes during curing and testing; whereas the cohesive resistance is very sensitive to these changes. It was also shown that, in the case of granular soils, lime and cement stabilization has only a minor influence on the effective angle of shearing resistance of the soil; whereas in the case of fine-grained soils, the stabilizers cause a large increase in the angle of shearing resistance. It was hypothesized that the increase in the frictional resistance of fine-grained soils is due to the formation of strongly cemented soil aggregates formed by soil particles surrounding nuclei of high cement particle concentrations. The formation of these cemented soil aggregates causes fine-grained soils to behave like granular materials having high effective angles of shearing resistance. The weaker cementation between

aggregates is responsible for the increase in effective cohesion, which is influenced by environmental conditions such as curing time and cycles of wet-dry or freeze-thaw.

This report is an extension of the work described in Phase Reports No. 3 and 5* and is a study of the influence of molding water content and as-molded dry density as well as delay time of compaction on the strength behavior of stabilized fine-grained soils. The testing procedures followed in this study are basically the same as those used in the previous reports, and the results are examined in terms of the same hypotheses and concepts.

---

* See Wissa and Ladd (1964) and (1965).

Chapter 2

MATERIALS AND TESTING PROCEDURES

2.1 SOIL

The soil used for this investigation was Massachusetts clayey silt M-21, the fine fraction (material passing No. 40 sieve size) of a glacial till from a drumlin overlooking Logan International Airport in East Boston. The particle size distribution of the batch of soil used for this investigation differed slightly from that used in the previous studies (Fig2.1). While the percentages of sand, silt, and clay were essentially the same, the silt fraction in this batch was coarser than in the previous batch. The properties of the soil are given in Table 2.1 and 2.2.

2.2 TYPE AND AMOUNT OF STABILIZER

The two chemical stabilizers used were reagent grade calcium hydroxide (hydrated lime) and portland cement Type I (commercial grade). The influence of molding conditions was studied for untreated soil and soil stabilized with five per cent lime or five per cent cement by weight.

2.3 MIXING PROCEDURES

The stabilizers were mixed with the air-dry soil until homogeneous mixtures were obtained. About 1 per cent extra water, above the desired amount, was added to all the mixes to compensate for evaporation losses that occurred during mixing. The water was mixed in by hand for about five minutes.

2.3.1 Untreated Soil

After addition of the desired amount of water and mixing, the mixes were allowed to equilibrate for one day in sealed glass containers prior to compaction.

2.3.2 Soil-Lime Mixes

A batch of soil-lime for 4 or 5 compacted samples was prepared at a time. The lime was added to the pulverized air-dry soil and thoroughly mixed in with a spoon until no traces of lime could be observed. The desired amount of water was then added and thoroughly mixed with the soil-lime mixture. While each sample was being compacted,the remaining soil was kept covered with a moist towel and intermittently remixed. All samples from a batch were compacted within four hours after addition of the mixing water. A water content of the mix was taken before compacting each sample.

2.3.3 Soil-Cement Mixes

The soil for each compacted sample was mixed separately and compacted immediately after mixing. The cement and water were added in the same manner as for the lime-stabilized samples. Two water contents of the mix were taken for each sample, one before and one after compaction. The time between first mixing in of the water and final compaction was not allowed to exceed fifteen minutes, when studying the influence of molding conditions.

For the delay time prior to compaction study, after adding and mixing in the water for each sample, the mixture was sealed in a plastic bag for five hours prior to compaction. During this delay time the mixtures were hand kneaded in the bags at half-hour intervals.

2.4 COMPACTION PROCEDURE

All test specimens were prepared by two-end static compaction. A compaction effort of 400 psi or 800 psi was gradually applied to the two rams by means of a hydraulic press. The full pressure was maintained on the samples for approximately one minute before releasing the load off the rams. Sufficient mix was placed in the mold such that neither ram reached the end of its travel when the full compactive effort was applied. Precautions were taken to prevent the

top and bottom rams from moving together at different rates so that neither ram reached the end of its travel under the full load.

2.4.1 Compaction Effort

To investigate the effect of molding water content and dry density on the effective stress-strength behavior of the stabilized systems, the samples were prepared using a compaction effort of 400 psi. The mold was Teflon lined to minimize wall friction during compaction,and it had guided top and bottom plungers.

For studying the effect of dry density, per se, samples were prepared using 800 psi instead of 400 psi compaction effort.

To investigate the effect of delayed time of compaction on the effective stress-strength behavior of the portland cement-stabilized system, some samples were prepared using the same compaction effort of 400 psi as the zero delay time samples. Other samples were compacted to the same dry density as the zero delay time samples (at the same molding water content) by increasing the static compaction effort to approximately 800 psi.

The mositure-density relations of the test specimens used in this investigation are plotted in Fig. 2.2.

2.4.2 Size of Specimens

The size of the mold used to compact the specimens was:

Length = 3.150 in.

Diameter = 1.405 in.

Volume = 80 cc.

2.5 CURING PROCEDURES

In the investigation of the effect of molding water content and dry density on the stress-strength behavior of the stabilized systems, the lime-stabilized samples were humid cured in glass containers at 100 per cent relative humidity and at room temperature for 243 days minimum. The portland cement-stabilized samples were subject to an accelerated humid curing by storing them in glass containers at 100 per cent relative humidity and at a temperature of 70°C. These samples were allowed to cure for 14 days prior to testing. The untreated samples were not stored before testing.

In the investigation of the effect of delay time of compaction on the stress-strength behavior of the portland cement-stabilized system, the samples were humid cured in glass containers at 100 per cent relative humidity and at room temperature for a time no less than 83 days.

2.6 TESTING PROCEDURE

The method used to test the samples was the same as that presented in previous reports (Phase Reports Nos. 3 and 5) with the following variations:

a) The untreated samples were saturated and tested under back pressure of 150 psi.

b) Stabilized samples were saturated and tested under back pressures of 200 psi or 220 psi.

c) The cell pressures were applied first to a pressure level a little above the back pressure, at which time the back pressure was applied to the samples and immediately following, the cell pressure was increased to achieve the desired effective consolidation pressure.

Table 2.1

PROPERTIES OF UNTREATED M-21

Textural Composition, % by wt.	
Sand 2mm to 0.06m	42
Silt 0.06mm to 0.002m	43
Clay 0.002mm	15
Physical Properties	
Liquid Limit %	20.5
Plastic Limit %	14.7
Plastic Index %	5.8
Specific Gravity	2.75
Max. Dry Density (1) lb/cu ft.	122.5
Optimum Water Content (1)%	12.9
Classification	
Unified	CL-ML
AASHO	A-4(0)
Chemical Properties (2)	
Organic Matter, % by wt.	0.2
Gation Exchange Capacity meq/100 gm	10
Glycol Retention mg/gm	22
Mineralogic Composition (3)	
Clay Composition, % by wt.	30
Illite: Montmorillonoid	1:0
Free Iron Oxide, $\%Fe_2O_3$	2.9

(1) Static Compaction, 400 psi effort

(2) For minus No. 200 sieve (0.074mm) fractions obtained from a different batch of soil.

(3) Most montmorillonoid mineral is montmorillonite.

Table 2.2

ATTERBERG LIMITS FOR M-21 SYSTEMS

System	Liquid Limit W_L%	Plastic Limit W_P%	Plasticity Index P.I.%
Untreated M-21	20.5	14.7	5.8
M-21+5% Lime*	22.5	19.4	3.1
M-21+5% Cement*	21.2	17.6	3.6

* Determined immediately after mixing in of the water

FIG. 2.1 GRAIN SIZE DISTRIBUTION OF UNTREATED MASSACHUSETTS CLAYEY SILT

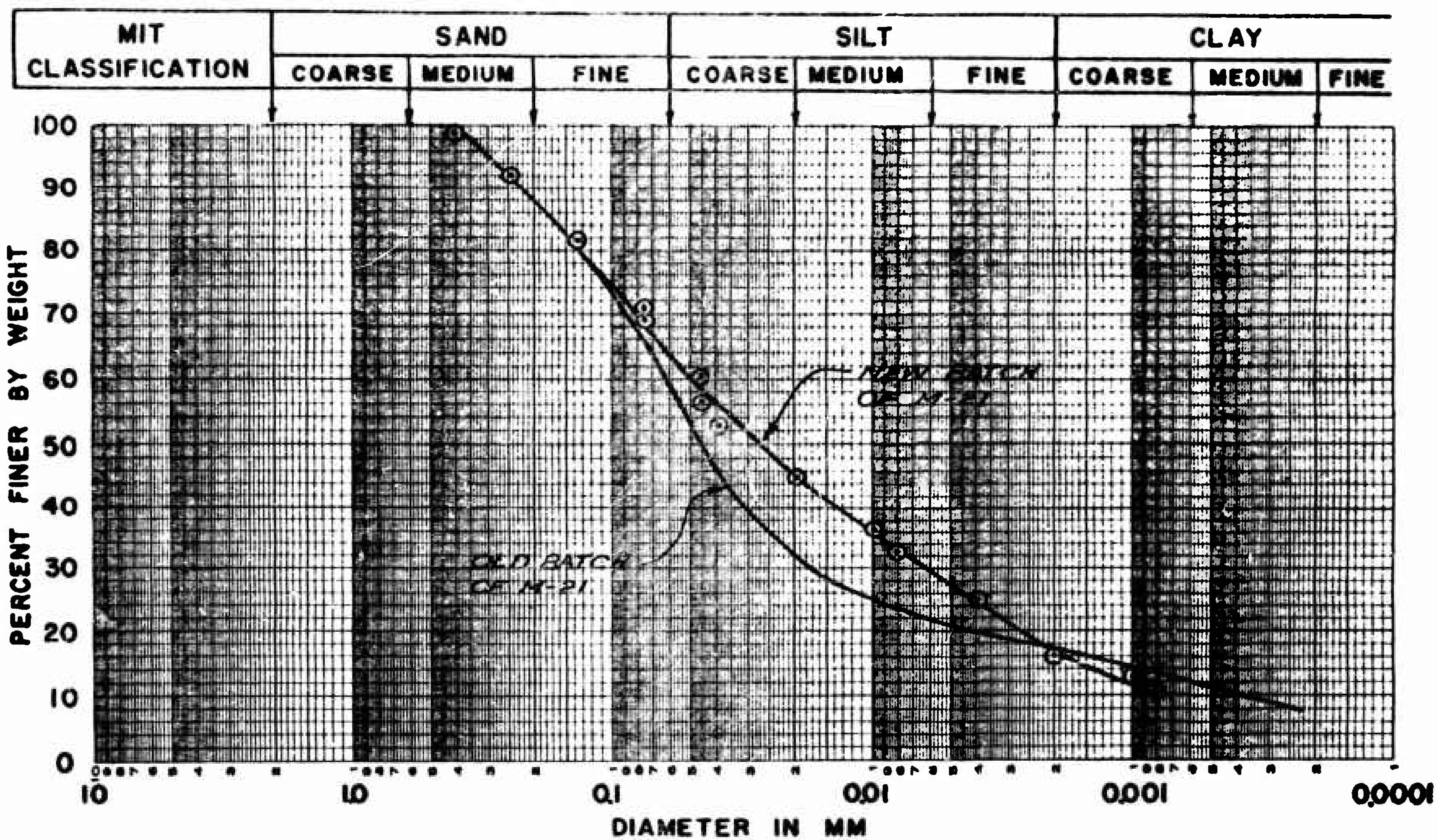

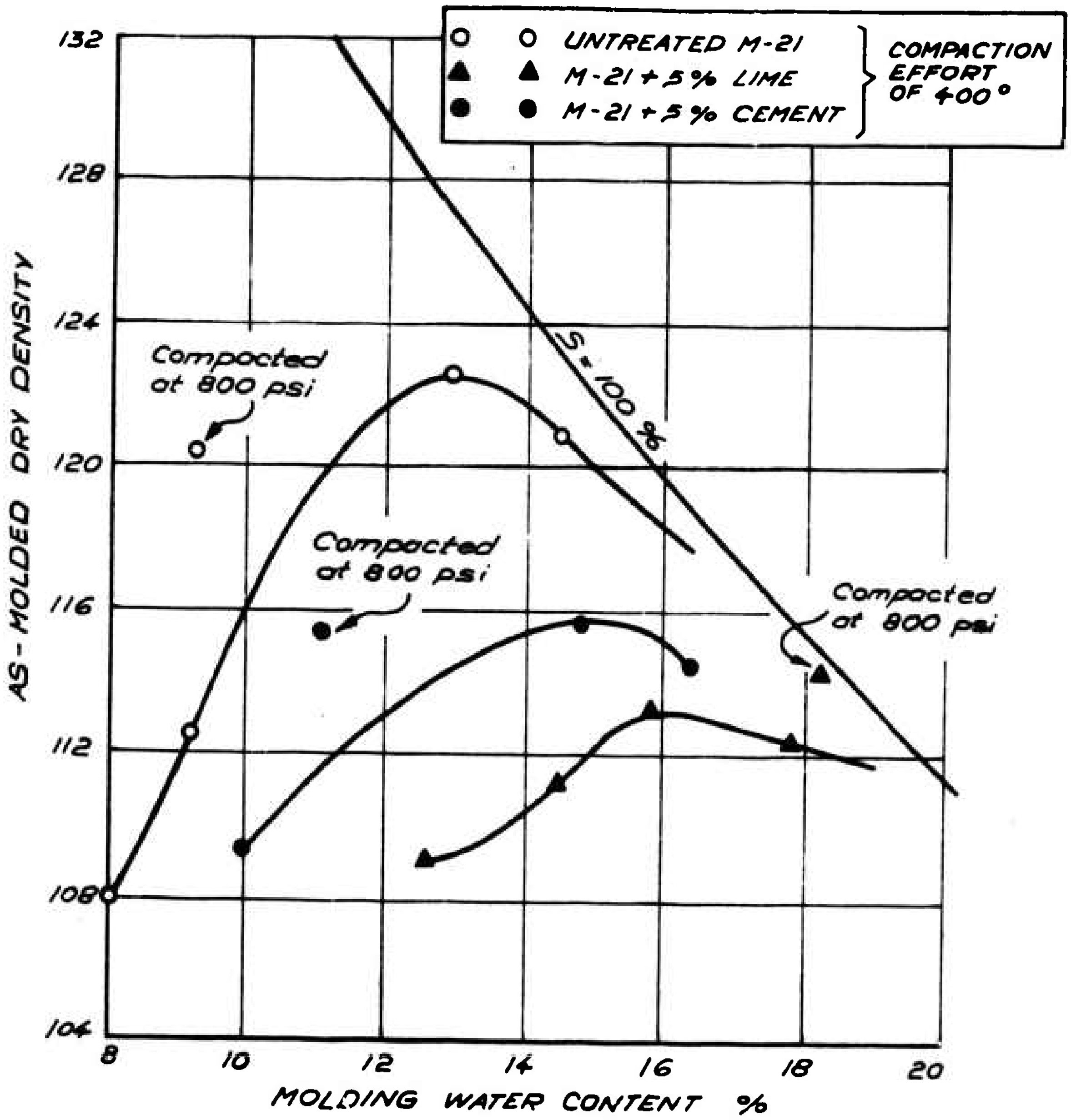

FIG. 2.2 MOISTURE - DENSITY RELATIONSHIP AT COMPACTION FOR M-21 SYSTEMS STATIC COMPACTION METHOD.

Chapter 3

INFLUENCE OF MOLDING WATER CONTENT AND DRY DENSITY

3.1 EFFECTIVE-STRESS-STRENGTH BEHAVIOR

3.1.1 Untreated Soil

Table 3.1 summarizes preshear data for the untreated M-21.

The Mohr-Coulomb effective stress-strength envelope of untreated Massachusetts clayey silt at the various molding conditions shown in Fig. 2.2 are given in Figs. 3.1 through 3.5. Over the wide range of consolidation pressures used in this investigation the envelopes at all molding conditions were straight lines having no measureable effective cohesion intercepts. As summarized in Fig. 3.6a molding conditions only slightly influenced the effective Mohr-Coulomb angle of shearing resistance, $\bar{\Phi}$. For a molding water content ranging from 8 per cent to 14.5 per cent and an as-molded dry density ranging from 108 lb/cu ft. to 123 lb/cu ft. the change in $\bar{\Phi}$ was only 2.5°, which, from a practical point of view, is not significant.

The small differences in $\bar{\Phi}$ due to molding conditions are probably caused by small differences in soil fabric still remaining in the failure zone at the time Mohr-Coulomb failure is reached. However, by the time ultimate conditions are reached at larger shear strains, these minor differences

in fabric have been eliminated and then the effective angle of shearing resistance is independent of molding conditions as shown in Figs. 3.7 and 3.6b ($\bar{\phi}_{ult}$ for this soil was 32°).

In summary it can be said that molding conditions do not significantly influence the effective stress-strength envelope of this fine-grained soil.

3.1.2 Stabilized Soil

The preshear data for the stabilized soils are shown in tables 3.2 and 3.3.

The effective stress-strength behavior of Massachusetts clayey silt M-21, stabilized with 5 per cent lime and 5 per cent cement at the various molding conditions given in Fig. 2.2,are shown in Figs. 3.8 through 3.12 and Figs. 3.13 through 3.16 respectively. Over the wide range of molding conditions investigated with each stabilizer,the Mohr-Coulomb effective angle of shearing resistance, $\bar{\phi}$, varied by only 1.5° (Figs. 3.17a and 3.17b, and 3.18a and 3.18b), which is probably within experimental error. However, the Mohr-Coulomb effective cohesion intercepts, $\bar{c}$, increased significantly with increasing as-molded dry density (Figs. 3.17c and 3.18c).

Molding water content, per se, did not control $\bar{c}$ since samples at approximately the same as-molded dry density, compacted dry and wet of optimum water content, had the same

$\bar{c}$. Further, an increase in as-molded dry density both dry and wet of optimum water content (caused by an increase in compaction effort) caused an increase in $\bar{c}$ that corresponded to the $\bar{c}$ obtained at a lower compaction effort and a different molding water content.

This behavior can be explained by the mechanistic picture proposed in Phase Report No. 5 (Wissa and Ladd, 1965). It was hypothesized that, even under ideal mixing conditions in the laboratory, cementing agents, such as portland cement and hydrated lime, do not get uniformly distributed in fine-grained soils. Strongly cemented soil aggregates thus form around nuclei of high cement particle concentration. These cemented aggregates cause the fine-grained soil to behave like a cemented granular material having a high effective angle of shearing resistance. Distribution of the cementing agent in the pulverized soil primarily occurs during the dry mixing process, and further mixing during addition of the molding water and during static compaction has very little influence on redistributing the cementing agent in the soil. A change in the molding water content and/or in the compaction effort will therefore cause no significant change in the size gradation of the cemented soil aggregates and thus no large change in effective angle of shearing resistance occurs. The cementation between soil aggregates will increase with increasing molding dry density, since the area of contact

and the number of contacts between adjacent aggregates increases. This causes the effective cohesive resistance of the stabilized soil to increase with increasing dry density.

By the time ultimate conditions are reached at large strains, the weaker cementation between the strongly cemented soil aggregates is completely destroyed in the failure zone, and the soil then behaves like a granular material having zero effective cohesion intercept and a high effective angle of shearing resistance, $\bar{\phi}_{ult}$. Since molding conditions apparently do not influence the aggregation, $\bar{\phi}_{ult}$ of the stabilized soil is independent of molding conditions as shown in Figs. 3.19 and 3.20.

Figs. 3.21 and 3.22 show the influence of molding conditions on the effective principal stress ratio of the cemented soil systems at Mohr-Coulomb and ultimate conditions, as a function of effective minor principal stress. At Mohr-Coulomb failure, the effective principal stress ratio is a function of both $\bar{\sigma}_3$ and molding conditions, because the cemented soil possesses an effective cohesion intercept, $\bar{c}$, which is a function of molding conditions. At ultimate, $\bar{\sigma}_1/\bar{\sigma}_3$ is independent of $\bar{\sigma}_3$, since $\bar{c}$ is zero and $\bar{\phi}$ ultimate is independent of molding conditions.

For the lime-stabilized soil, $\bar{\phi}_{ult}$ was 37.5° and for the cement-stabilized soil, it was 38.5°. This compares with

$\bar{\phi}_{ult}$ of 32° for the untreated soils (see Fig. 3.23). Figures 3.24 and 3.25 show the influence of molding dry density on the undrained strength of both the cement and the lime stabilized systems.

3.2 PORE PRESSURE RESPONSE

3.2.1 Pore Pressure Response Prior to Shear

The pore pressure response, B ($B = \Delta u/\Delta\sigma_c$)*, was determined after consolidation and saturation, but prior to shear, to check that complete saturation had been achieved. Since B was often less than 100 per cent, (see Tables 3.1 through 3.3) several consecutive 2 kg/cm^2 increments of cell pressure were used to insure that B values less than 100 per cent were due to the rigidity of the soil skeleton and not due to entrapped air (Wissa, 1969).

No correlation appeared to exist between molding conditions and B for both the stabilized and the untreated soil as can be seen from Figs. 3.26, 3.27, and 3.28. In general the pore pressure response prior to shear, B_o, decreased with increasing consolidation pressure, since the rigidity of the soil skeleton increases with increasing consolidation pressure (Wissa 1969). This can be seen from Figs. 3.26b, 3.27b and 3.28b, which are plots of B_o versus initial tangent modulus, E, obtained from the undrained stress-strain

---

* See Skempton (1954).

curves. The large scatter in the results is believed to be due to the large seating imperfections at the initial stages of shear, which made it difficult to obtain accurate values of E (see Tables 3.4 through 3.6). The pore pressure responses of the samples compacted dry of optimum were not usually lower than those of the samples compacted wet of optimum. This is further evidence that all samples were completely saturated prior to shear. A possible exception was the untreated samples compacted very dry of optimum.

3.2.2 Pore Pressure Response after Shearing

After shearing, the test specimens were unloaded at constant cell pressure without allowing drainage. The excess pore pressures existing after unloading were allowed to equalize overnight and then the final pore pressure response, B_f, determined in a similar manner to B_o. Plots of B_o versus B_f are shown in Figs. 3.26c, 3.27c and 3.28c. In most cases B_f was greater than B_o, since the results plotted above the 45° line shown in the figures. In the case of the untreated samples, the effective stresses after shear and unloading were usually lower than the effective consolidation pressures prior to shear, since positive residual excess pore pressures remained in the test specimens. The lower effective stress after shear causes a decrease in the rigidity of the soil skeleton and consequently an increase in B. This also

occurred with most of the stabilized test specimens; however, in addition, for stabilized specimens, a breakdown of the cemented soil skeleton also occurs during shear resulting in a further decrease in the rigidity of the soil skeleton that would also cause B_f to be higher than B_o.

In summary a back pressure of 200 psi was sufficient to ensure complete saturation prior to shear at all molding conditions investigated. Since the rigidity of the soil skeleton is changing during undrained shear, the pore pressure response also changes during shear; and therefore, the initial pore pressure response prior to shear cannot be used to correct for the rigidity of the soil skeleton on the excess pore pressures developed during shear.

3.3 PORE PRESSURE DURING SHEAR

3.3.1 Untreated Soil

According to Lambe (1958) and Seed et al (1960), fine-grained soils compacted dry of optimum have a more flocculated fabric than when compacted wet of optimum. Seed et al showed that at low consolidation pressures (up to 2.0 kg/cm^2), the excess pore water pressures developed during undrained shear were lower for samples compacted dry of optimum than for samples compacted wet of optimum. Their explanation for the

observed behavior was that a flocculated fabric is more resistant to applied stress and consequently lower excess pore pressures develop during undrained shear.

Fig. 3.29 shows the influence of molding water content and molding dry density (using 400 psi static compaction) on the effective minor principal stress* of untreated Massachusetts clayey silt at ultimate failure in undrained shear. (Similar trends existed at maximum principal stress difference and at tangency with the effective Mohr-Coulomb envelope.) Over the wide range of consolidation pressures investigated, the effective minor principal stress at a given consolidation pressure increased with increasing molding water content. In other words, the more flocculated the soil fabric after compaction, the larger the excess pore pressures developed during undrained shear. This behavior is contrary to that reported by Seed et al, and is probably due to the fact that Seed et al only investigated the behavior of compacted soils at low consolidation pressures up to 2.0 kg/cm^2, while these results are for higher consolidation pressures ranging from 5 kg/cm^2 to 50 kg/cm^2. The pore pressure developed during

* Since the total minor principal stress was kept constant during consolidation and shear, the excess pore pressure developed during undrained shear is equal to the consolidation pressure minus the effective minor principal stress.

undrained shear is dependent on the change in fabric that occurs during shear. The change in fabric during shear is not only dependent on the initial fabric but also on the applied stresses and strains required to produce failure. The higher the stresses and the larger the strains at failure, the greater is the tendency for the soil to develop a preferred orientation (dispersed fabric) and consequently, the larger the change of fabric during shear. At low consolidation pressures, the stresses and strains required to reach Mohr-Coulomb failure are relatively small, and therefore, only a small change in fabric has occured by the time failure is reached. Under these conditions samples compacted dry of optimum, having a higher resistance to the applied stresses, will produce smaller excess pore pressures during shear than samples compacted wet of optimum as reported by Seed et al. However, higher consolidation pressures were used in this investigation. The applied stresses and strains required to produce failure were larger, and therefore, the tendency for a dispersed fabric to occur during shear is consequently greater than would have existed at lower consolidation pressures. At a given consolidation pressure, the samples compacted dry of optimum, therefore, developed much larger excess pore pressures during shear than samples compacted wet of optimum since their initial fabric after compaction was more flocculated than samples compacted wet of optimum and consequently

underwent larger changes in fabric during shear. From Fig. 3.30 it is apparent that for a constant compaction effort of 400 psi molding water content rather than molding dry density controls the pore pressure behavior of the untreated soil.

The influence of an increase in dry density due to increasing the compaction effort from 400 psi to 800 psi is shown in Fig. 3.31. This figure consists of plots of molding water content and as-molded dry density versus the normalized effective minor principal stress at ultimate, $(\bar{\sigma}_3 ult/\bar{\sigma}_c)$, for the samples consolidated to 25 kg/cm^2 and 50 kg/cm^2. Here again molding water content primarily controls the pore pressures. At a molding water content of about 9.2 per cent, the high-density samples had about the same excess pore pressures at failure as the low-density samples (Fig. 3.31a). However, from Fig. 3.31b it is apparent that at the same as-molded dry density of about 118 lb/cu ft., samples compacted to 400 psi corresponding to a molding water content of about 11.3 per cent developed a lower excess pore pressure during shear than the samples compacted to 800 psi at a molding water content of 9.2 per cent. This is reasonable, since static compaction does not induce very large shear stresses during molding and consequently an increase in compaction effort does not significantly alter the soil fabric after compaction. Fig. 3.32

shows the influence of molding water content on the A-factor of untreated M-21 at maximum stress difference and at tangency with the effective Mohr-Coulomb envelope. The use of the A-factor* rather the excess pore pressure or minor effective principal stress to describe the pore pressure behavior adjusts the excess pore pressures for the effect of differences in the magnitude of the applied principal stress difference. Once the prestress effects due to compaction were overcome at the higher consolidation pressures, the A-factor was independent of consolidation pressure and was solely a function of molding water. (The low consolidation pressure test results are not included in this figure.) The change in A-factor with changes in molding water content indicates that the differences in magnitude of the applied shear stresses do not solely account for the differences in the excess pore pressures but also differences in the soil fabric existing prior to shear influence the pore pressures generated.

In summary, molding water content rather than molding dry density controls the pore pressure behavior of compacted untreated Massachusetts clayey silt in undrained shear. At consolidation pressures ranging from 5 kg/cm^2 to 50 kg/cm^2, samples compacted dry of optimum develop higher pore pressures

---

* See Skempton (1954).

during undrained shear than samples compacted wet of optimum because they have a more flocculated fabric prior to shear and consequently undergo a larger change in fabric during shear.

3.3.2 Stabilized Soils

As shown in Figs. 3.33a and 3.34a molding conditions had no significant influence on the effective minor principal stress, and consequently the excess pore pressure, of the stabilized soil at Mohr-Coulomb failure. This was also the case at the maximum principal stress difference. However, the A-factors at a given consolidation pressure decreased with increasing as-molded dry density (Figs. 3.35 and 3.36 because (σ_1 - σ_3) at tangency and at maximum stress difference increased with increasing dry density due to the influence of molding dry density on the effective cohesion of the cemented soil.

At ultimate conditions when the cementation between soil aggregates was completely destroyed, $\bar{\sigma}_3$ increased and consequently the excess pore pressure decreased with increasing dry density (Figs. 3.33c and 3.34c). The A-factor also decreased (Fig. 3.37). This is similar to the influence of density on the pore pressure and A-factor behaviors of uncemented sands. It is interesting to note that at ultimate

conditions, the same relation existed between as-molded dry density and A-factor for both the lime-and cement-stabilized soil.

In summary as-molded dry density rather than molding water content controls the pore pressure behavior of cemented fine-grained soils. This is further evidence that molding water content does not significantly influence the fabric of stabilized soils. However, it should be noted that static compaction was used in this investigation and it is possible that if kneading compaction had been used, molding water content might have had an influence on the pore pressure behavior since with untreated fine-grained soils kneading compaction causes a greater change in fabric as a function of molding water content than does static compaction (Seed et al 1960).

3.4 TOTAL STRESS-STRENGTH BEHAVIOR

3.4.1 Untreated Soil

The influence of molding conditions on the total stress-strength behavior of untreated Massachusetts clayey silt is shown in Fig. 3.38. Even though the effective angle of shearing resistance is not significantly influenced by molding conditions, the excess pore pressure developed during undrained

shear is a function of molding water content and consequently, the angle of shearing resistance in terms of total stress, ϕ, is influenced by molding conditons. At a given consolidation pressure, the higher the pore pressures developed during shear the lower the angle of shearing resistance in terms of total stresses. For this soil ϕ* at maximum stress difference ranged from 13.5° dry of optimum to 22.5° wet of optimum and from 13° to 21° at ultimate. Comparing this with a 2.5° variation of the angle of shearing resistance in terms of effective stresses is a good demonstration of the advantage of using effective stress-strength parameters rather than total stress-strength parameters to define the strength behavior of compacted soils.

3.4.2 Stabilized Soil

In the case of the stabilized soil, both the cohesion intercept, c, and angle of shearing resistance, ϕ, in terms of total stresses are influenced by molding conditions (Figs. 3.39 and 3.40). This is due to the fact that both the effective cohesion intercept and the pore water pressures developed during undrained shear are influenced by the as-molded dry density.

---

* Note that the angles shown in Fig. 3.35 are in terms of α rather than ϕ. ($\tan\alpha = \sin\phi$).

It is of interest to note that while the effective cohesion intercept of the cemented soils at ultimate was zero at all molding conditions, it had an appreciable value in terms of total stresses and was also a function of molding dry density (Figs. 3.39b and 3.40b). Since the cementation between soil aggregates in the failure zone has been completely destroyed by the time ultimate conditions are reached at large strains, this apparent cohesion intercept is not a measure of the cementation but rather reflects the influence of the pore pressures on the ultimate shear resistance of the soil.

3.5 STRESS-STRAIN BEHAVIOR

Stress-strain data for the untreated and stabilized M-21 systems during undrained shear are summarized in Tables 3.4 through 3.6.

3.5.1 Initial Tangent Modulus

As can be seen in Tables 3.4 through 3.6, seating corrections had to be applied to the stress-strain curves of most of the stabilized soils test specimens. This made it impossible to determine the influence of molding conditions on the initial tangent modulus.

3.5.2 Axial Strain to Reach Maximum Stress Difference

The influence of molding conditions on the axial strain required to reach maximum stress difference, ε_m, for untreated M-21, M-21 plus 5% lime, and M-21 plus 5% cement is shown in

Fig. 3.41. With the exception of the samples compacted very dry of optimum, molding conditions had no influence on ε_m of the untreated soil. In the case of the stabilized soils, ε_m increased with increasing molding water content but did not appear to be a function of the as-molded dry density. While no definite explanation can be given for this trend, it is believed to reflect the volume changes that occured during humid curing. Samples compacted dry of optimum tend to swell during humid curing, while samples compacted wet of optimum tend to shrink. The shrinkage cracking that takes place during curing and soaking of the wet samples makes it necessary for them to undergo larger strains during shear before the sum of their frictional and cohesive resistance reaches a maximum. In order to verify the above hypothesis, it would be necessary to prevent any changes in moisture during curing and then check that molding water content no longer had an effect on ε_m. Stress-strain curves, as well as change in pore pressure and A-factor versus percentage of axial strain, are presented in Appendix A.

3.5.3 Friction and Cohesion

Figs. 3.42, 3.43, and 3.44 are plots of mobilization of the effective frictional and the effective cohesive resistance as a function of axial strain. For the untreated soil (Fig. 3.42), the rate at which the frictional resistance increased

with increasing axial strain appears to be a function of the molding water content. The flocculated soil fabrics (dry of optimum) appear to develop their frictional resistance at a slower rate than the dispersed fabrics (wet of optimum). In the case of the stabilized soils (Figs. 3.43 and 3.44). no general trend was apparent as a function of molding conditions. This is probably due to the large influence seating imperfections have on the slopes and intercepts of the strain contours at small strain levels.

TABLE 3.1

PRESHEAR DATA FOR UNTREATED M-21

SAMPLE No.	COMPACTIVE EFFORT PSI	AS-MOLDED		CONSOLIDATION PRESSURE $\bar{\sigma}_o$ Kg/cm^2	FINAL WATER CONTENT %	PORE PRESSURE RESPONSE B %
		ω %	γ_d lb/ft^3			
2001	400	8.0	108	10.0	10.6	96.0
2002	400	8.0	108	25.0	13.0	83.0
2003	400	8.0	108	50.0	11.5	71.0
2004	400	9.2	112.2	4.96	15.0	100
2005	400	9.0	112.0	10.0	13.9	92.0
2006	400	9.2	113.0	25.0	13.0	100
2007	400	9.2	112.5	50.0	—	90.0
2008	400	13.0	123.3	4.93	13.1	100
2009	400	12.8	122.3	10.0	12.5	96.0
2010	400	13.2	122.7	25.0	11.6	95.0
2011	400	12.7	122.4	50.0	10.7	84.0
2012	400	14.6	120.1	4.95	12.6	100
2013	400	14.6	121.1	10.0	11.5	90.0
2014	400	14.2	121.1	25.0	11.0	95.0
2015	400	14.5	121.0	50.0	10.2	85.0
2016	800	9.3	120.4	5.0	15.6	98.0
2017	800	9.2	120.6	10.0	13.0	95.0
2018	800	9.2	118.0	25.0	13.1	92.0
2019	800	9.1	118.2	50.0	13.2	86.0

TABLE 3.2

PRESHEAR DATA FOR M-21 + 5% LIME

SAMPLE No.	COMPACTIVE EFFORT PSI	AS-MOLDED ω %	AS-MOLDED γ_d lb/ft^3	CURING TIME: HUMID CURE, DAYS	CURING TIME: SOAKING, DAYS	CURING TIME: TOTAL CURE, DAYS	CONSOLIDATION PRESSURE $\bar{\sigma}_o$ Kg/cm^2	FINAL WATER CONTENT %	PORE PRESSURE RESPONSE B %
1005	400	12.6	109.0	251	23	274	5.0	21.1	100
1003	400	12.7	108.9	243	20	263	10.0	20.5	86.7
1009	400	12.6	109.0	243	47	290	25.0	20.8	76.0
1007	400	12.5	109.0	251	22	273	50.0	20.2	83.0
1004	400	14.8	111.1	251	14	265	5.0	20.0	100
1010	400	14.1	112.0	251	40	291	10.0	20.0	80.0
1002	400	14.5	111.4	251	10	261	25.0	18.9	—
1006	400	14.5	111.1	260	11	271	50.0	19.1	—
1015	400	17.8	112.8	284	41	325	5.0	18.0	98.0
1016	400	17.8	112.0	284	16	300	10.0	18.7	83.0
1017	400	17.8	112.3	290	23	313	25.0	18.2	80.0
1018	400	17.8	112.0	277	10	287	50.0	17.8	71.0
1019	400	15.8	113.6	281	12	293	5.0	17.6	87.5
1012	400	15.8	113.7	291	33	324	10.0	17.5	82.0
1024	400	15.8	113.3	287	91	278	25.0	18.9	77.5
1014	400	16.1	112.4	281	13	294	50.0	18.5	71.8
1020	800	17.8	114.5	266	10	276	5.0	17.4	100
1021	800	18.0	114.4	271	7	278	10.0	17.2	76.0
1022	800	18.2	114.2	266	16	282	25.0	17.4	75.0
1023	800	18.5	114.0	266	18	284	50.0	17.9	78.0

TABLE 3.3

PRESHEAR DATA FOR M-21 + 5% CEMENT

SAMPLE No.	COMPACTIVE EFFORT PSI	AS-MOLDED		CURING TIME			CONSOLIDATION PRESSURE $\bar{\sigma}_o$ Kg/cm^2	FINAL WATER CONTENT %	PORE PRESSURE RESPONSE B %
		ω %	γ_d lb/ft^3	HUMID CURE, DAYS	SOAKING, DAYS	TOTAL CURE, DAYS			
3001	400	9.9	109.4	14	10	24	49.65	19.1	78.0
3002	400	9.9	109.0	14	10	24	24.8	19.6	81.0
3003	400	10.1	108.5	14	10	24	7.95	20.4	89.0
3021	400	11.0	110.5	14	10	24	10.28	19.3	92.0
3007	400	16.3	114.6	14	10	24	49.9	16.4	82.0
3008	400	16.5	114.5	14	10	24	25.7	16.7	82.0
3009	400	16.4	114.0	14	10	24	10.0	16.9	89.0
3010	400	16.5	114.6	14	10	24	5.0	16.7	84.0
3011	400	14.9	115.7	14	7	21	50.0	15.4	78.0
3012	400	14.9	115.3	14	7	21	25.7	16.6	78.0
3013	400	14.7	115.3	14	7	21	10.0	16.6	79.0
3014	400	14.6	115.3	14	8	22	5.0	16.9	89.0
3016	800	11.2	115.5	14	8	22	50.0	16.9	80.0
3017	800	11.0	115.1	14	8	22	25.6	17.9	79.4
3018	800	10.9	115.0	14	8	22	10.0	17.7	92.0
3019	800	11.2	115.6	14	10	24	5.0	17.9	80.0

TABLE 3.4 SUMMARY OF STRESS - STRAIN CHARACTERISTICS FOR UNTREATED M-21

SAMPLE No	CONSOLIDAT PRESS $\bar{\sigma}_o$ kg/cm²	INITIAL TANG MOD E kg/cm²	AT MAXIMUM DIFFERENCE $(\bar{\sigma}_1 - \bar{\sigma}_3)_M$							AT FIRST TANGENCY WITH ENVELOPE							AT ULTIMATE				FINAL B FACTOR %	REMARKS
			AXIAL STRAIN %	$\bar{\sigma}_3$ kg/cm²	$\bar{\sigma}_1 - \bar{\sigma}_3$ kg/cm²	Δu kg/cm²	$\bar{A}$	q kg/cm²	$\bar{p}$ kg/cm²	AXIAL STRAIN %	$\bar{\sigma}_3$ kg/cm²	$\bar{\sigma}_1 - \bar{\sigma}_3$ kg/cm²	Δu kg/cm²	$\bar{A}$	q kg/cm²	$\bar{p}$ kg/cm²	q kg/cm²	Δu kg/cm²	$\bar{p}$ kg/cm²	$\bar{A}$		
2001	100	5440	12	51	60	49	085	30	81	120	28	58	72	124	29	57	3.0	7.3	5.7	1.22	96.5	SEATING CORRECT
2002	250	6590	16	98	130	152	116	65	163	74	53	116	198	170	58	111	6.0	20.0	11.0	1.67	99.3	
2003	500	13200	11.4	105	240	386	160	120	23.4	125	11.5	240	385	160	120	235	12.0	38.5	23.5	1.53	99.3	SEATING CORRECT
2004	4.96	2650	14	25	36	25	070	18	43	100	1.3	32	36	117	1.6	29	1.6	3.6	3.0	1.13	100	"
2005	10.2	4285	15.5	32	86	70	078	43	75	90	32	81	68	083	4.1	72	4.4	6.8	7.6	0.77	97.0	"
2006	250	6310	16.3	75	162	175	106	81	156	110	70	156	180	1.15	78	148	8.2	17.4	15.8	1.06	100	"
2007	500	11110	16.1	151	327	348	110	164	315	135	148	31.8	35.2	116	15.9	307	16.4	34.8	31.6	1.06	100	"
2008	4.93	2810	18	25	56	24	041	28	53	18	25	56	24	0.41	2.8	5.3	2.4	1.9	5.4	0.40	100	"
2009	100	2750	16.1	47	107	53	050	54	100	108	43	98	54	058	4.9	92	5.4	5.3	100	0.55	100	"
2010	25.0	6690	15.0	108	250	142	056	125	233	96	97	232	15.3	065	11.6	21.5	12.6	14.3	25.3	0.62	976	
2011	500	9220	16.5	208	462	292	065	231	439	106	188	432	312	072	21.6	40.4	23.3	29.6	43.7	0.64	900	SEATING CORRECT
2012	4.95	2800	32	24	55	26	048	28	52	32	24	55	26	048	2.7	5.1	2.3	1.7	5.6	0.28	100	
2013	100	4870	16.4	71	178	29	016	89	160	69	53	132	4.7	037	66	11.9	8.8	2.9	16.0	0.19	95.7	SEATING CORRECT
2014	25.0	6770	16.1	12.9	310	12.1	039	15.5	28.4	7.2	108	25.0	14.2	058	12.5	23.3	16.0	12.0	28.9	0.43	97.5	"
2015	50.0	9130	15.6	25.8	623	242	0.39	31.2	570	6.6	210	53.2	290	0.55	26.6	47.6	31.3	24.1	57.1	0.45	84.1	
2016	5.0	4625	1.3	35	63	15	024	32	6.6	11.0	2.4	6.0	2.6	0.43	30.0	5.4	3.1	2.6	5.5	0.48	98.0	SEATING CORRECT
2017	10.0	4950	16.5	4.6	10.8	5.4	0.49	5.4	10.0	11.7	4.6	10.8	5.4	0.50	5.4	10.0	5.5	5.2	10.0	0.50	95.0	"
2018	25.0	5310	16.0	13.3	14.6	11.7	0.80	7.5	20.6	11.0	6.0	13.6	19.0	1.40	6.8	12.8	6.8	18.9	12.9	1.39	95.0	"
2019	50.0	7660	16.5	12.0	27.3	38.0	1.37	13.7	25.7	12.6	11.7	26.6	38.3	1.45	13.3	25.0	13.7	38.1	25.6	1.47	90.0	"

TABLE 3.5 SUMMARY OF STRESS-STRAIN CHARACTERISTICS FOR M-21 + LIME

SAMPLE No	CONSOLIDAT. PRESS $\bar{\sigma}_0$ kg/cm²	INITIAL TANG MOD. E kg/cm²	AT MAXIMUM DIFFERENCE $(\sigma_1-\sigma_3)_M$							AT FIRST TANGENCY WITH ENVELOPE							AT ULTIMATE				FINAL B FACTOR %	REMARKS
			AXIAL STRAIN %	$\bar{\sigma}_3$ kg/cm²	$\bar{\sigma}_1-\bar{\sigma}_3$ kg/cm²	Δu kg/cm²	$\bar{A}$	q kg/cm²	$\bar{p}$ kg/cm²	AXIAL STRAIN %	$\bar{\sigma}_3$ kg/cm²	$\bar{\sigma}_1-\bar{\sigma}_3$ kg/cm²	Δu kg/cm²	$\bar{A}$	q kg/cm²	$\bar{p}$ kg/cm²	q kg/cm²	Δu kg/cm²	$\bar{p}$ kg/cm²	$\bar{A}$		
1005	5.0	11850	1.2	5.8	28.2	-0.8	-0.03	14.1	19.9	0.4	2.75	25.8	2.23	0.08	12.9	15.7	11.1	-0.70	16.8	-0.05	98.2	SEATING CORRECT.
1003	10.0	16460	1.1	5.1	27.45	4.9	0.18	13.7	18.9	0.4	3.5	25.6	6.5	0.26	12.8	16.4	10.4	4.4	15.9	0.28	98.0	"
1009	25.0	19600	0.6	8.1	37.9	16.9	0.44	19.0	27.1	1.1	8.4	36.3	16.6	0.46	18.2	26.6	13.6	17.7	20.9	0.91	89.0	
1007	50.0	31800	0.7	18.6	54.7	31.4	0.57	27.4	46.0	1.0	17.1	57.0	32.9	0.58	28.5	45.6	19.4	39.4	30.0	1.35	94.0	SEATING CORRECT.
1004	5.0	21750	4.5	8.7	41.1	-3.7	-0.08	20.6	29.3	0.6	2.2	35.7	2.8	0.08	17.8	20.1	19.2	-5.2	29.4	-0.16	97.0	"
1010	10.0	8750	3.0	9.8	45.6	0.2	0.02	22.8	32.7	0.86	3.1	40.4	6.9	0.17	20.2	23.5	21.8	-1.6	33.4	-0.05	94.5	"
1002	25.0	13150	1.7	10.4	48.4	14.6	[illegible]	24.2	34.6	0.96	8.2	47.5	16.8	0.36	23.8	32.0	21.0	12.9	33.1	0.41	86.0	"
1006	50.0	28000	0.82	16.7	62.7	33.3	0.54	31.3	48.1	1.0	16.3	62.3	33.7	0.54	31.1	48.4	25.8	33.6	42.2	0.89	93.0	"
1015	5.0	9700	7.5	10.7	45.1	-8.7	-0.12	22.6	33.2	0.86	2.2	38.8	2.7	0.05	19.4	21.6	21.3	-7.9	34.2	-0.20	100	"
1016	10.0	17530	10.7	16.2	54.9	-6.2	-0.11	27.4	43.7	1.05	4.0	42.0	6.0	0.14	21.0	25.0	26.0	-7.0	43	-0.17	100	"
1017	25.0	17250	9.5	17.0	55.5	8.0	0.14	27.8	44.8	1.0	7.5	44.7	17.5	0.39	22.3	29.8	27.6	7.4	45.3	0.17	91.0	"
1018	50.0	35600	6.0	20.3	65.5	29.7	0.46	32.7	53.0	1.45	15.5	65.0	34.5	0.54	31.5	97.1	32.2	28.3	53.9	0.56	86.0	"
1019	5.3	14680	7.5	13.3	53.1	-8.0	-0.15	26.5	39.8	0.70	2.3	41.3	3.0	0.07	20.6	22.9	24.7	-8.9	38.8	-0.23	100	
1012	10.0	13200	6.0	11.0	53.0	-1.0	-0.20	26.5	37.5	0.90	3.3	44.5	6.7	0.14	22.2	25.6	26.9	-1.2	38.1	-0.02	90.0	SEATING CORRECT.
1024	25.0	22700	4.0	15.0	58.2	10.0	0.16	29.1	44.1	0.72	6.6	51.8	18.4	0.36	25.9	32.5	27.3	7.6	44.8	0.18	100	"
1014	50.0	37200	1.5	15.6	65.1	34.4	0.52	32.6	48.2	1.3	15.3	65.2	34.7	0.53	32.6	47.8	31.6	30.0	51.7	0.66	100	"
1020	5.0	11800	10.1	12.7	50.6	-7.7	-0.11	25.3	37.9	1.25	4.3	45.7	0.75	0.01	22.9	27.1	20.6	-7.5	33.0	-0.20	93.5	"
1021	10.0	33900	2.2	11.5	55.0	-1.5	-0.03	27.5	39.0	0.88	4.6	50.5	5.4	0.11	25.3	29.9	25.2	-4.5	39.8	-0.11	100	
1022	25.0	23250	5.1	17.5	65.2	7.5	0.12	32.6	50.1	1.10	7.2	56.5	17.8	0.32	28.2	35.4	30.2	6.2	49.0	0.13	86.8	SEATING CORRECT
1023	50.0	20640	4.5	18.9	68.9	31.1	0.45	39.5	53.3	1.15	12.0	63.7	38.1	0.59	31.8	43.8	32.8	29.2	53.7	0.59	94.0	"

TABLE 3.6 SUMMARY OF STRESS - STRAIN CHARACTERISTICS FOR M-21 + 5% CEMENT

SAMPLE No	CONSOLIDAT PRESS $\bar{\sigma}_o$ kg/cm^2	INITIAL TANG. MOD E kg/cm^2	AT MAXIMUM DIFFERENCE $(\sigma_1 - \sigma_3)_M$							AT FIRST TANGENCY WITH ENVELOPE							AT ULTIMATE				FINAL B FACTOR %	REMARKS
			AXIAL STRAIN %	$\bar{\sigma}_3$ kg/cm^2	$\bar{\sigma}_1 - \bar{\sigma}_3$ kg/cm^2	Δu kg/cm^2	$\bar{A}$	q kg/cm^2	$\bar{p}$ kg/cm^2	AXIAL STRAIN %	$\bar{\sigma}_3$ kg/cm^2	$\bar{\sigma}_1 - \bar{\sigma}_3$ kg/cm^2	Δu kg/cm^2	$\bar{A}$	q kg/cm^2	$\bar{p}$ kg/cm^2	q kg/cm^2	Δu kg/cm^2	$\bar{p}$ kg/cm^2	$\bar{A}$		
3001	49.65	22000	1.2	18.65	43.0	31.0	0.73	21.5	40.2	3.0	14.15	41.0	35.5	0.86	20.5	34.65	17.0	37.7	29.0	1.27	92.8	SEATING CORRECT
3002	24.80	15600	0.8	9.9	27.0	14.9	0.53	13.5	23.4	3.0	7.3	25.0	17.5	0.70	12.5	19.8	10.6	18.8	16.6	1.06	90.5	"
3003	7.96	8300	2.7	4.3	21.2	3.7	0.60	10.6	14.9	3.0	4.36	21.2	3.6	0.17	10.6	15.0	8.6	3.9	12.1	0.27	92.0	"
3021	10.28	9750	0.8	6.5	25.0	3.8	0.15	12.5	19.0	3.0	6.28	23.0	4.0	0.18	11.5	17.8	10.0	5.0	15.3	0.30	87.0	"
3007	49.90	16000	7.0	20.9	79.0	29.0	0.38	39.5	60.4	2.6	12.9	66.8	37.0	0.53	33.4	46.3	37.2	26.8	60.3	0.38	92.7	"
3008	25.70	25000	3.7	13.2	66.7	12.5	0.18	33.3	46.6	1.3	4.7	60.0	21.0	0.41	30.0	34.7	32.0	7.5	50.1	0.13	87.0	"
3009	10.00	8800	8.3	15.9	64.2	-5.9	-0.10	32.1	16.2	2.6	6.6	56.0	3.4	0.06	28.0	34.6	28.8	- 6.2	45.0	0.12	97.0	"
3010	5.00	10000	—	—	—	—	—	—	—	—	—	—	—	—	—	—	—	—	—	—	—	"
3011	50.00	10400	5.5	21.0	71.4	29.0	0.42	35.7	56.7	2.3	18.0	68.0	32.0	0.49	34.0	52.0	35.4	26.4	59.0	0.46	93.4	"
3012	25.70	10300	6.0	16.2	58.8	9.5	0.16	29.4	45.6	1.4	7.4	48.8	18.3	0.39	24.4	31.8	27.5	8.3	44.9	0.17	98.0	"
3013	10.00	8900	7.7	12.6	47.0	- 2.6	-0.05	23.5	36.1	0.9	4.0	36.6	6.0	0.14	18.3	22.3	22.4	-3.5	35.8	-0.09	100	
3014	5.00	3700	6.5	11.0	47.0	- 6.0	-0.14	23.5	34.5	1.0	3.0	34.2	2.0	0.06	17.1	20.1	20.7	-6.8	32.5	-0.19	90.0	SEATING CORRECT.
3016	50.00	12500	4.5	19.5	70.0	30.5	0.43	35.0	54.5	2.0	18.0	69.2	32.0	0.47	34.1	52.1	34.0	29.2	54.8	0.51	94.0	
3017	25.60	20800	3.5	12.9	50.8	12.7	0.26	25.4	38.5	0.7	8.9	49.2	16.7	0.34	24.6	33.5	24.2	11.6	38.2	0.30	94.0	
3018	10.00	10500	5.3	10.7	44.0	-0.70	-0.012	22.0	32.7	0.7	3.6	37.4	6.4	0.16	18.7	22.3	21.0	-1.6	32.6	-0.05	90.0	SEATING CORRECT.
3019	5.00	6250	4.0	9.7	41.0	-4.7	-0.15	20.5	30.2	0.8	2.8	35.8	2.2	0.06	16.9	19.7	20.1	-6.9	32.1	-0.24	90.7	"

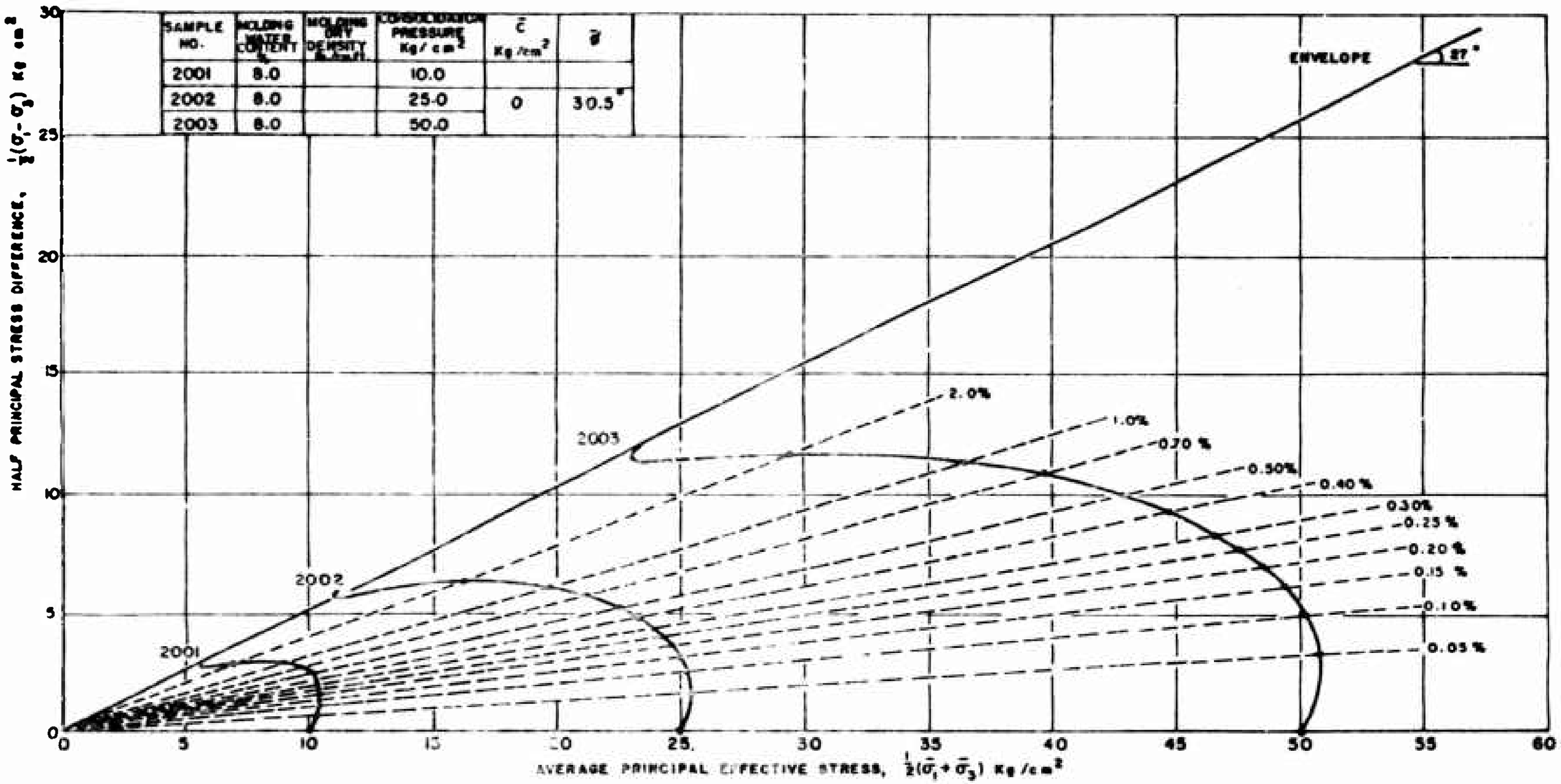

FIGURE 31 EFFECTIVE STRESS-STRENGTH BEHAVIOR OF UNTREATED M-21 COMPACTED DRY OF OPTIMUM

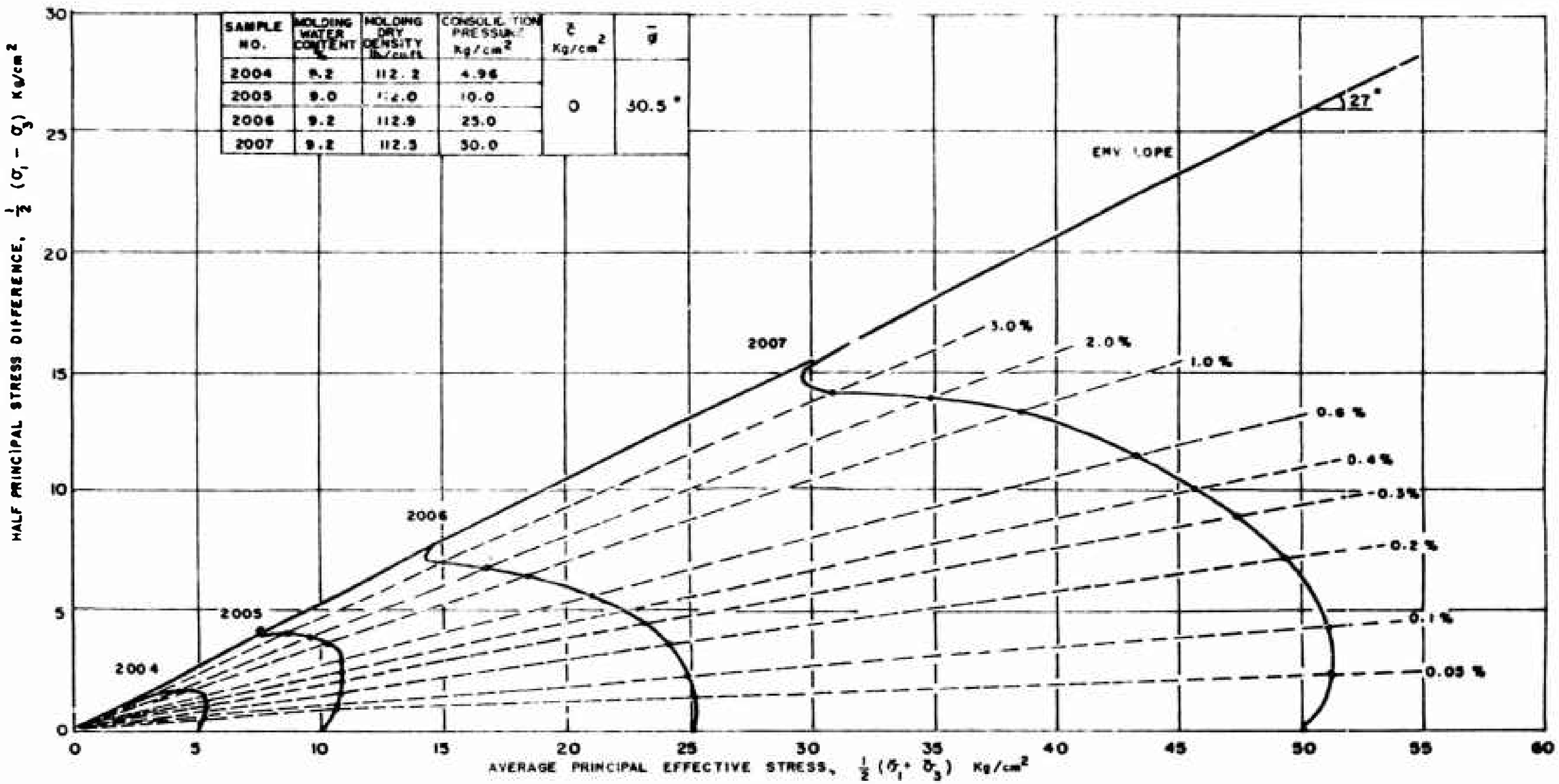

FIGURE 3.2 EFFECTIVE STRESS – STRENGTH BEHAVIOR OF M-21 COMPACTED DRY OF OPTIMUM

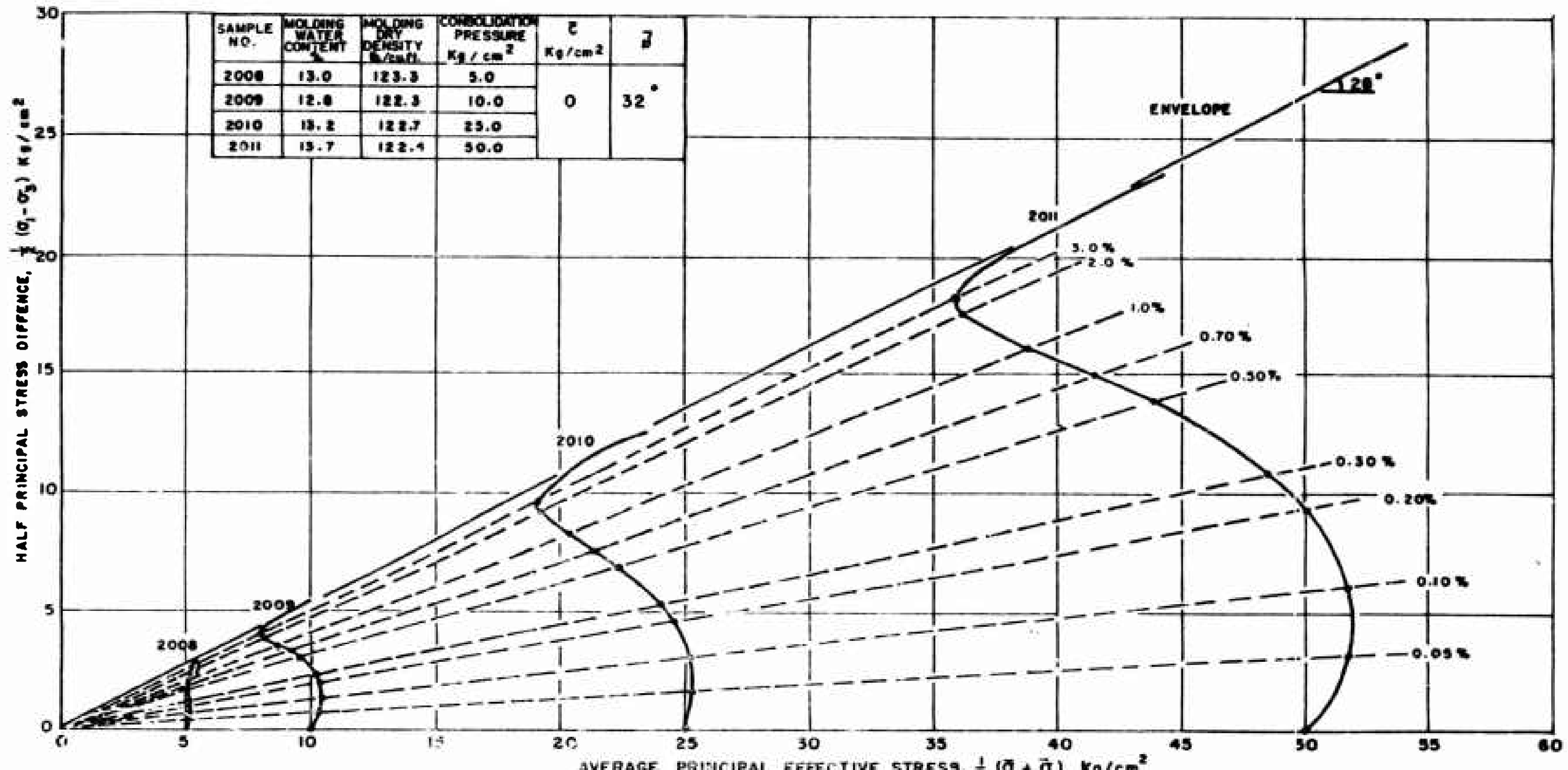

SAMPLE NO.	MOLDING WATER CONTENT %	MOLDING DRY DENSITY lb/cu.ft.	CONSOLIDATION PRESSURE Kg/cm²	$\bar{c}$ Kg/cm²	$\bar{\phi}$
2008	13.0	123.3	5.0	0	32°
2009	12.8	122.3	10.0		
2010	13.2	122.7	25.0		
2011	13.7	122.4	50.0		

FIGURE 3.3 EFFECTIVE STRESS–STRENGTH BEHAVIOR OF UNTREATED M-21 COMPACTED AT OPTIMUM

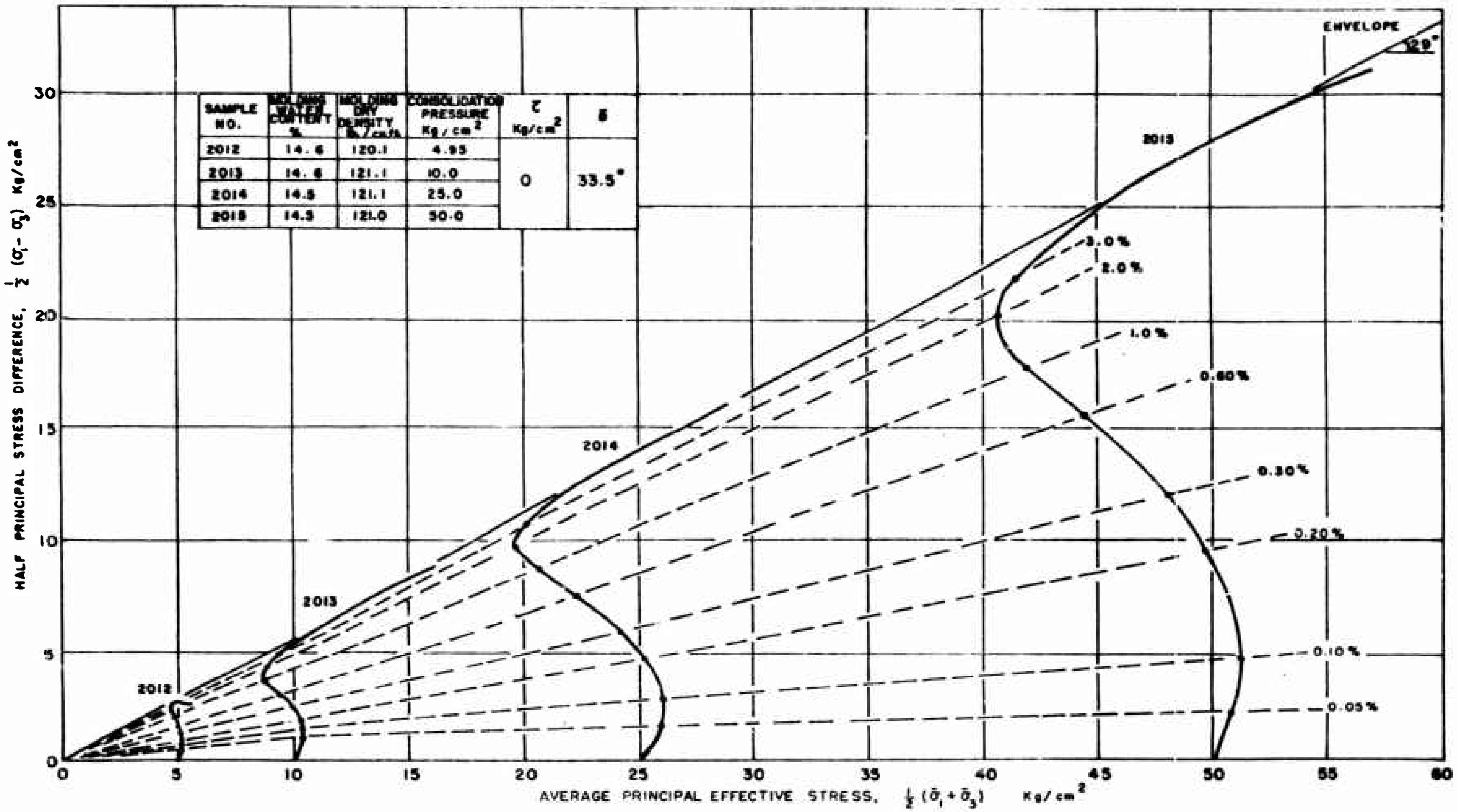

FIGURE 3.4 EFFECTIVE STRESS – STRENGTH BEHAVIOR OF UNTREATED M-21 COMPACTED WET OF OPTIMUM

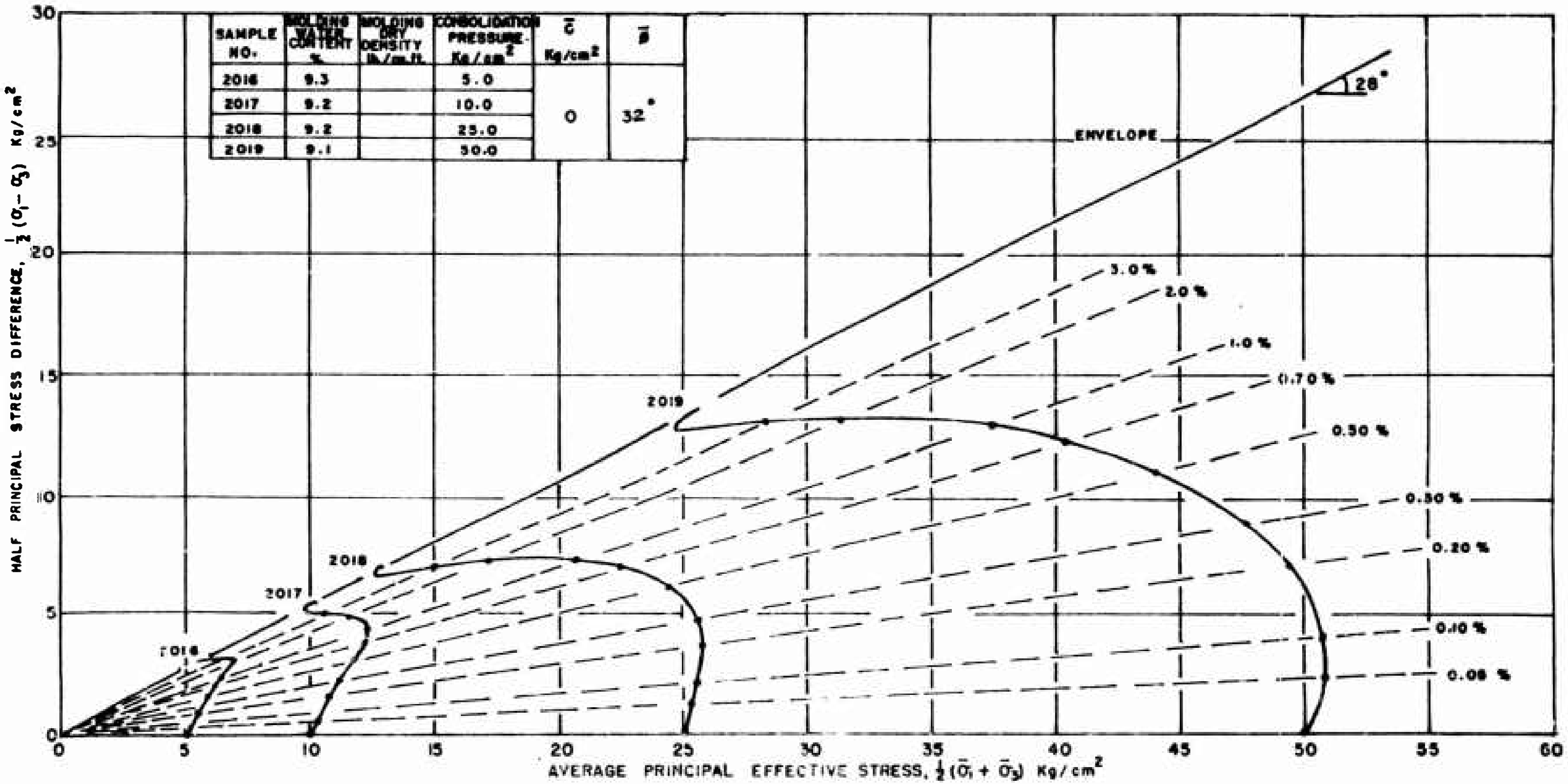

SAMPLE NO.	MOLDING WATER CONTENT %	MOLDING DRY DENSITY lb/cu.ft.	CONSOLIDATION PRESSURE Kg/cm²	$\bar{c}$ Kg/cm²	$\bar{\phi}$
2016	9.3		5.0	0	32°
2017	9.2		10.0		
2018	9.2		25.0		
2019	9.1		50.0		

FIGURE 3.5 EFFECTIVE STRESS-STRENGTH BEHAVIOR OF UNTREATED M-21 COMPACTED TO HIGH DENSITY

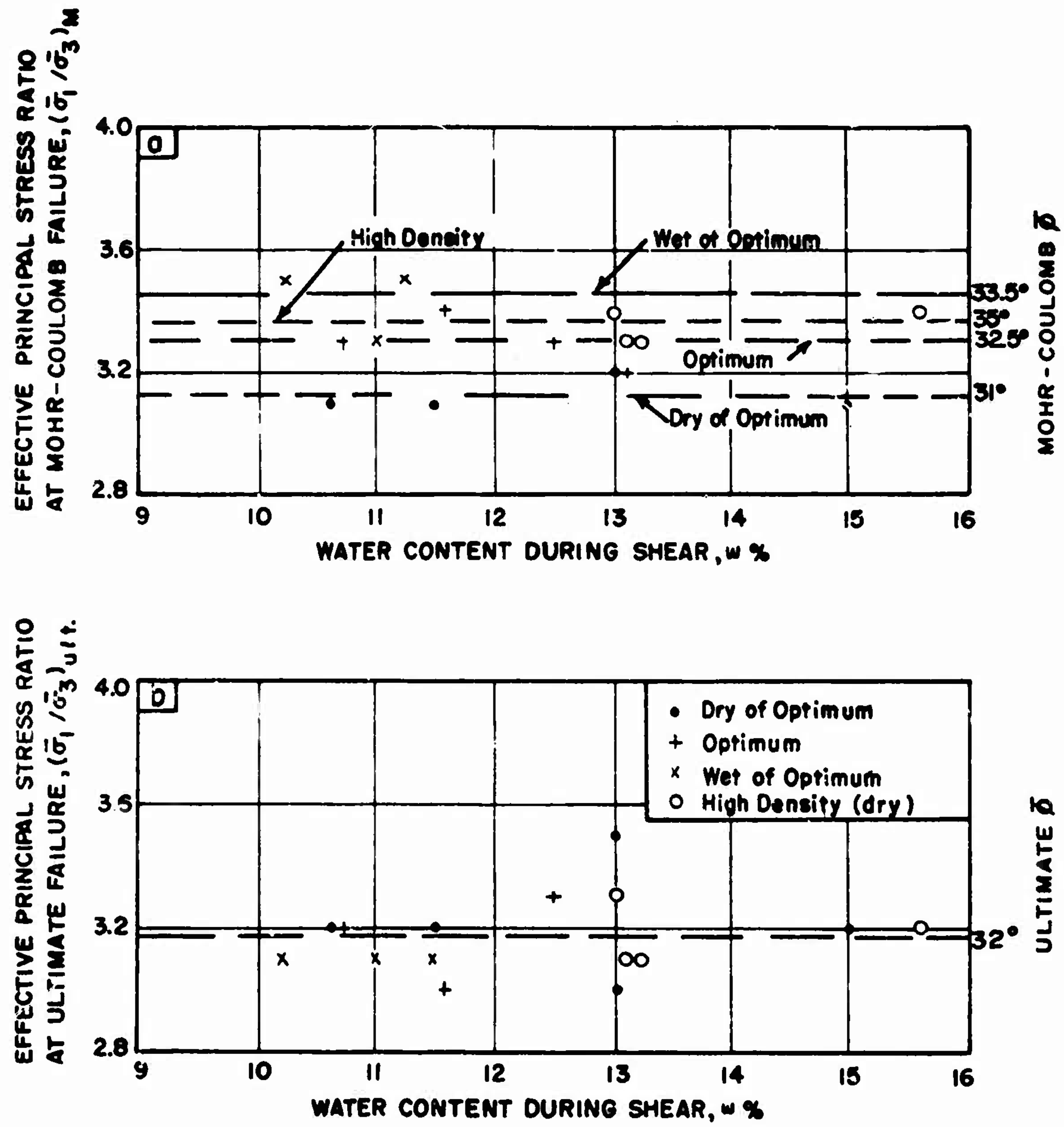

FIG.3.6 INFLUENCE OF WATER CONTENT DURING SHEAR ON THE EFFECTIVE PRINCIPAL STRESS RATIO OF UNTREATED MASSACHUSETTS CLAYEY SILT AS A FUNCTION OF MOLDING CONDITIONS

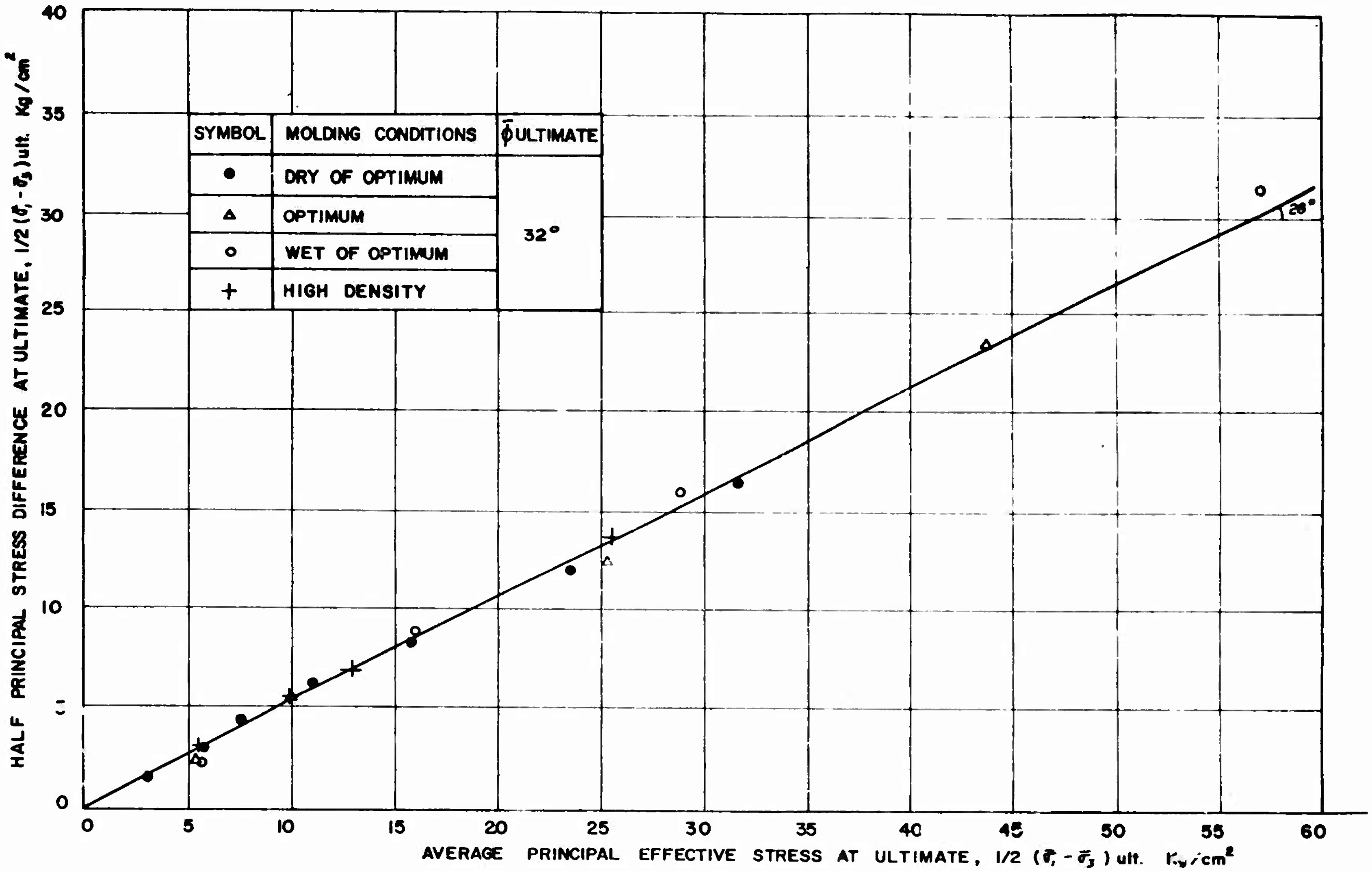

FIGURE 3.7 INFLUENCE OF MOLDING CONDITIONS ON THE EFFECTIVE STRESS–STRENGTH RELATION OF UNTREATED MASSACHUSETTS CLAYEY SILT AT ULTIMATE

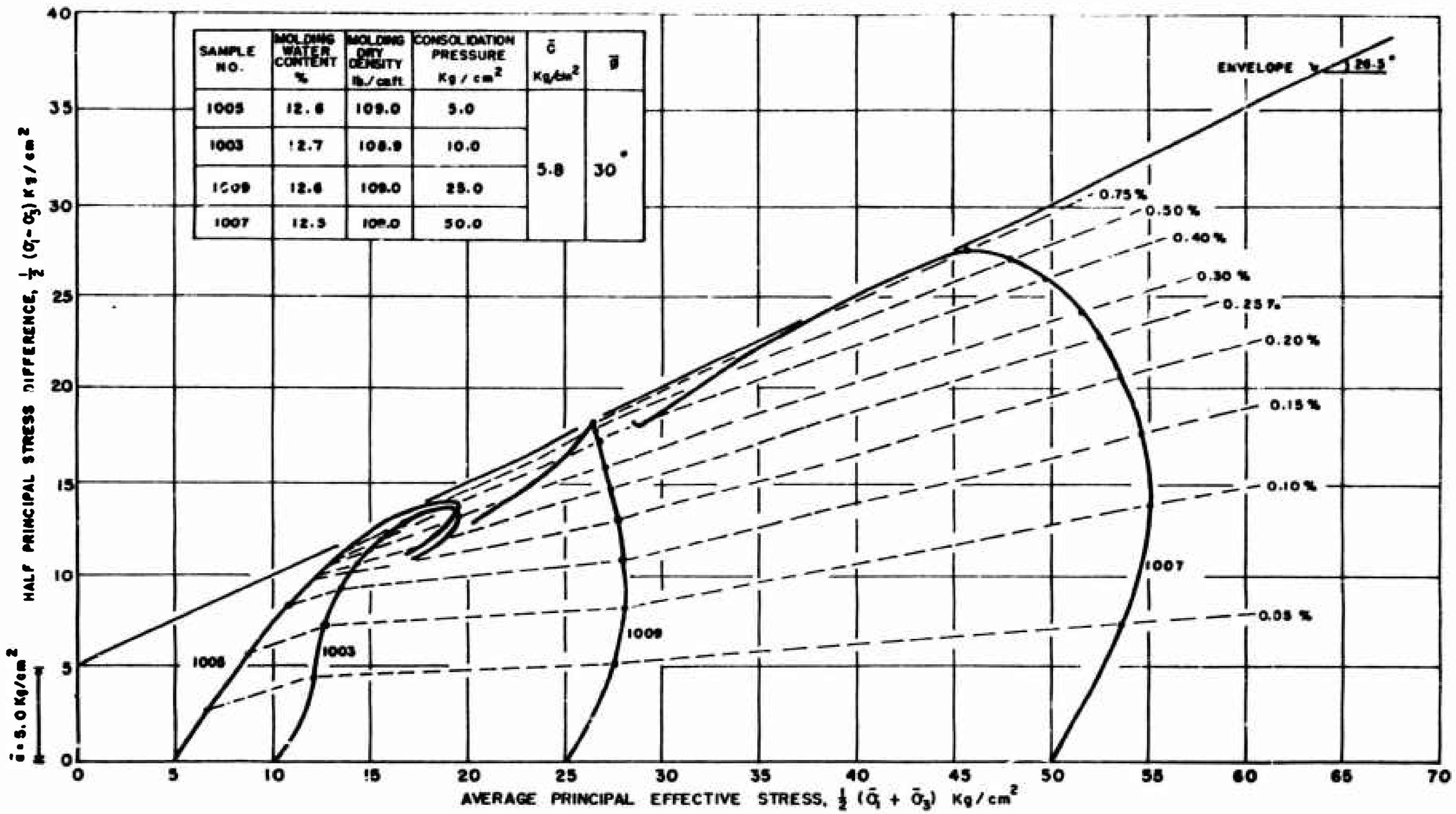

SAMPLE NO.	MOLDING WATER CONTENT %	MOLDING DRY DENSITY lb./cu.ft.	CONSOLIDATION PRESSURE Kg/cm²	$\bar{c}$ Kg/cm²	$\bar{\phi}$
1005	12.6	109.0	5.0	5.8	30°
1003	12.7	108.9	10.0		
1009	12.6	109.0	25.0		
1007	12.5	109.0	50.0		

FIGURE 3.8 EFFECTIVE STRESS-STRENGTH BEHAVIOR OF M-21 + 5% LIME COMPACTED VERY DRY OF OPTIMUM

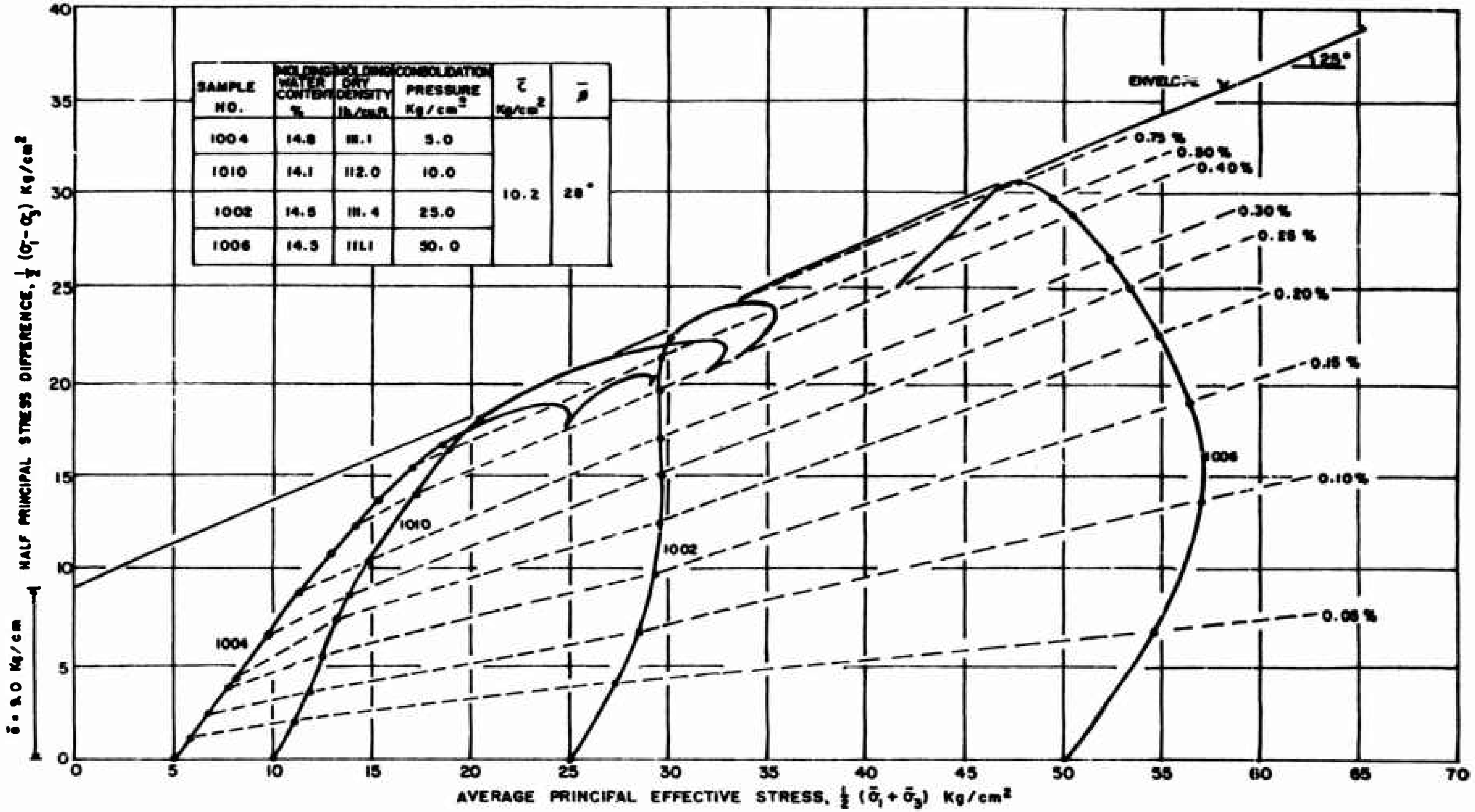

SAMPLE NO.	MOLDING WATER CONTENT %	MOLDING DRY DENSITY lb/cu.ft	CONSOLIDATION PRESSURE Kg/cm²	$\bar{c}$ Kg/cm²	$\bar{\phi}$
1004	14.8	111.1	5.0	10.2	28°
1010	14.1	112.0	10.0		
1002	14.5	111.4	25.0		
1006	14.5	111.1	50.0		

FIGURE 3.9 EFFECTIVE STRESS-STRENGTH BEHAVIOR OF M-21 + 5 % LIME COMPACTED DRY OF OPTIMUM

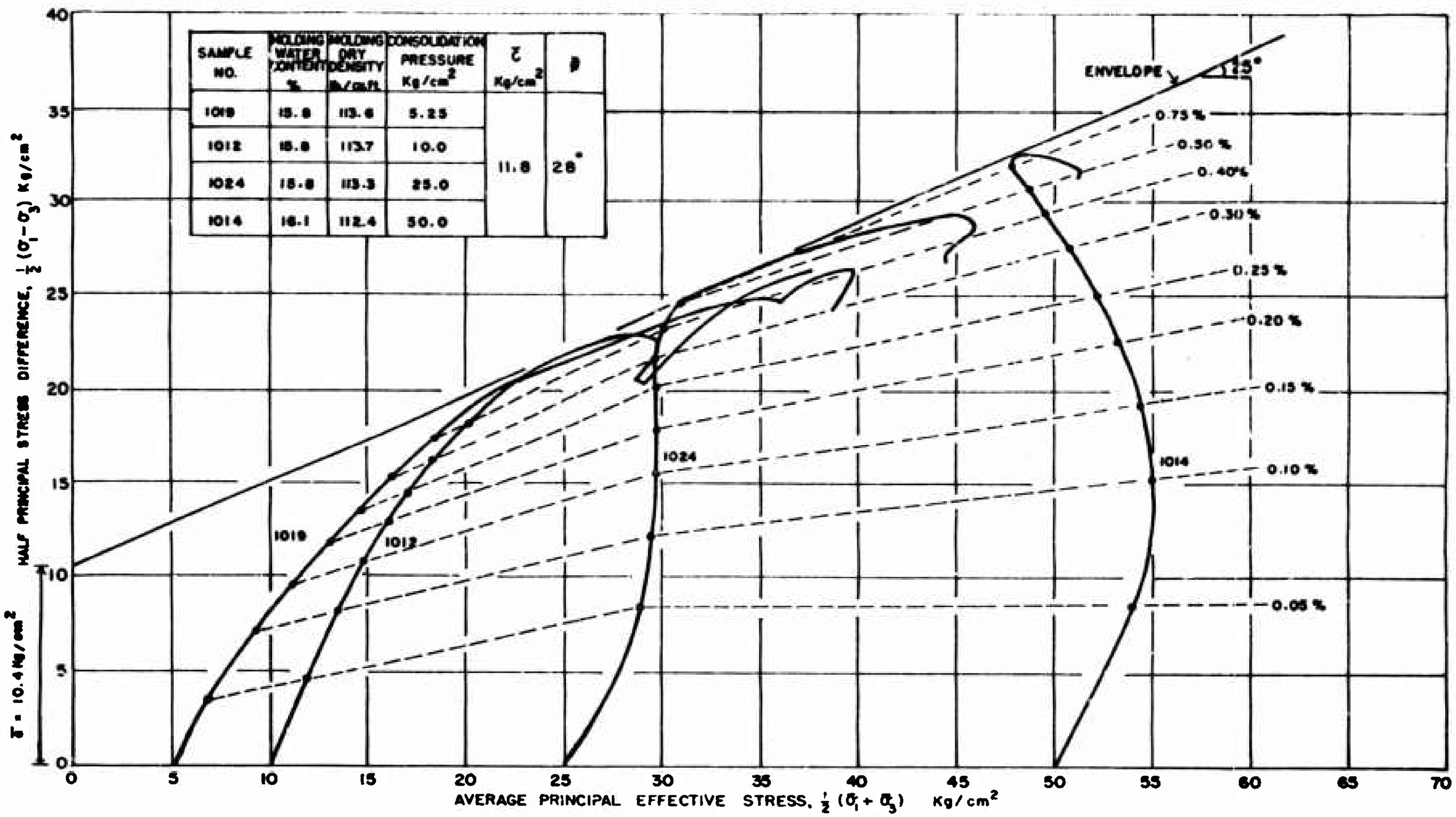

FIGURE 3.10 EFFECTIVE STRESS–STRENGTH BEHAVIOR OF M-21 + 5 % LIME COMPACTED AT OPTIMUM

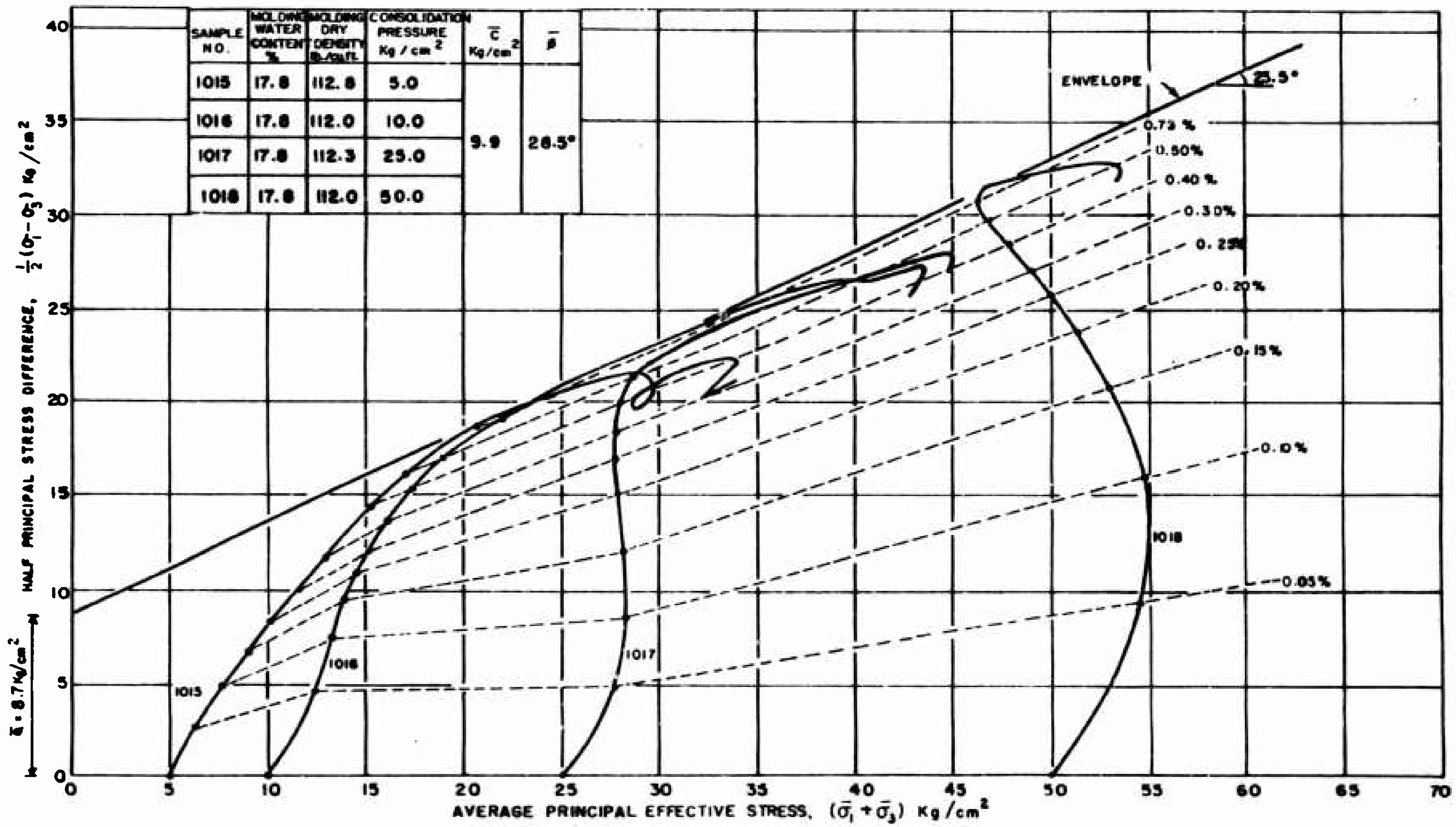

FIGURE 3.11 EFFECTIVE STRESS—STRENGTH BEHAVIOR OF M-21 + 5% LIME COMPACTED WET OF OPTIMUM

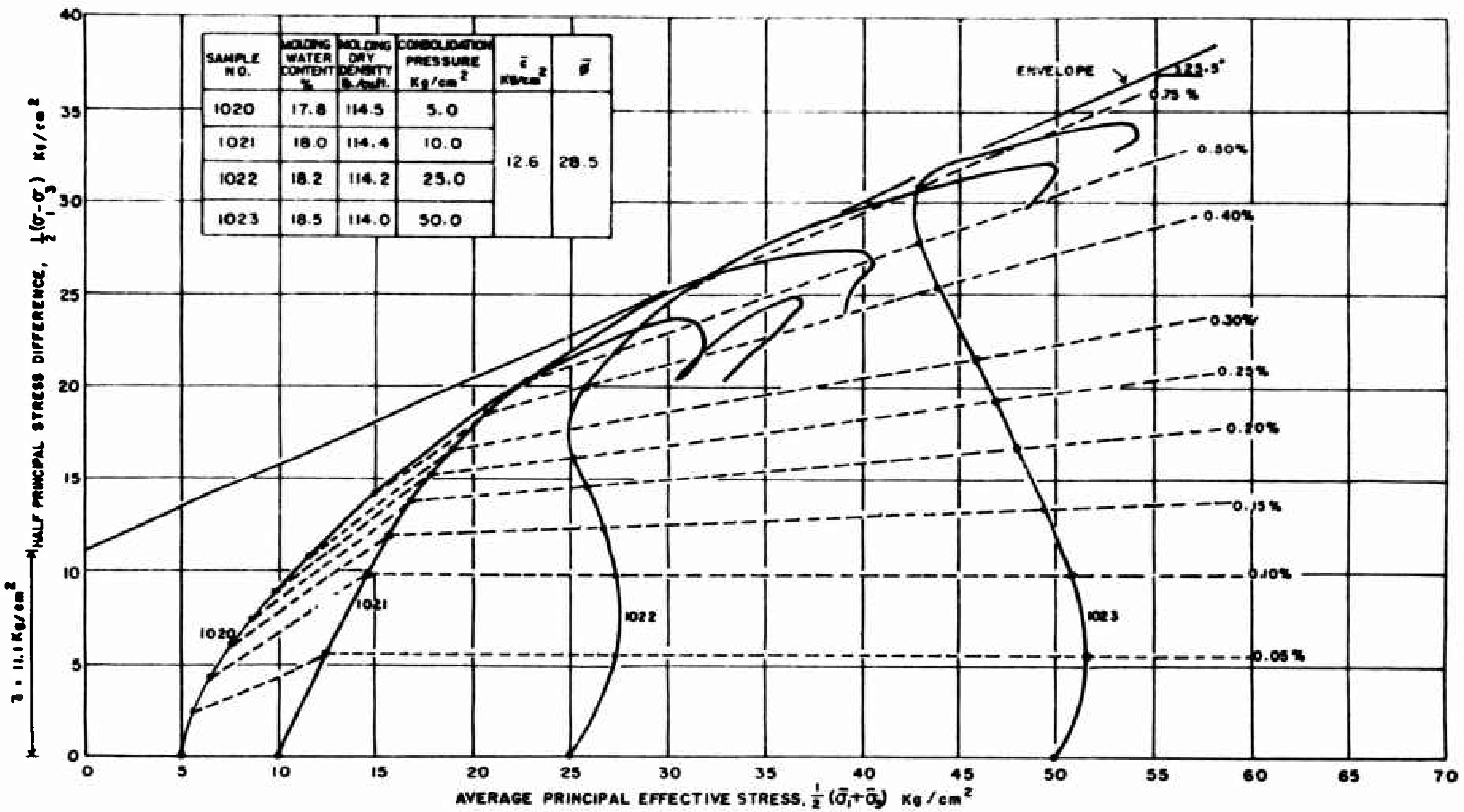

SAMPLE NO.	MOLDING WATER CONTENT %	MOLDING DRY DENSITY lb./cu.ft.	CONSOLIDATION PRESSURE Kg/cm^2	$\bar{c}$ Kg/cm^2	$\bar{\phi}$
1020	17.8	114.5	5.0	12.6	28.5
1021	18.0	114.4	10.0		
1022	18.2	114.2	25.0		
1023	18.5	114.0	50.0		

FIGURE 3.12 EFFECTIVE STRESS-STRENGTH BEHAVIOR OF M-21 + 5% LIME COMPACTED TO HIGH DENSITY

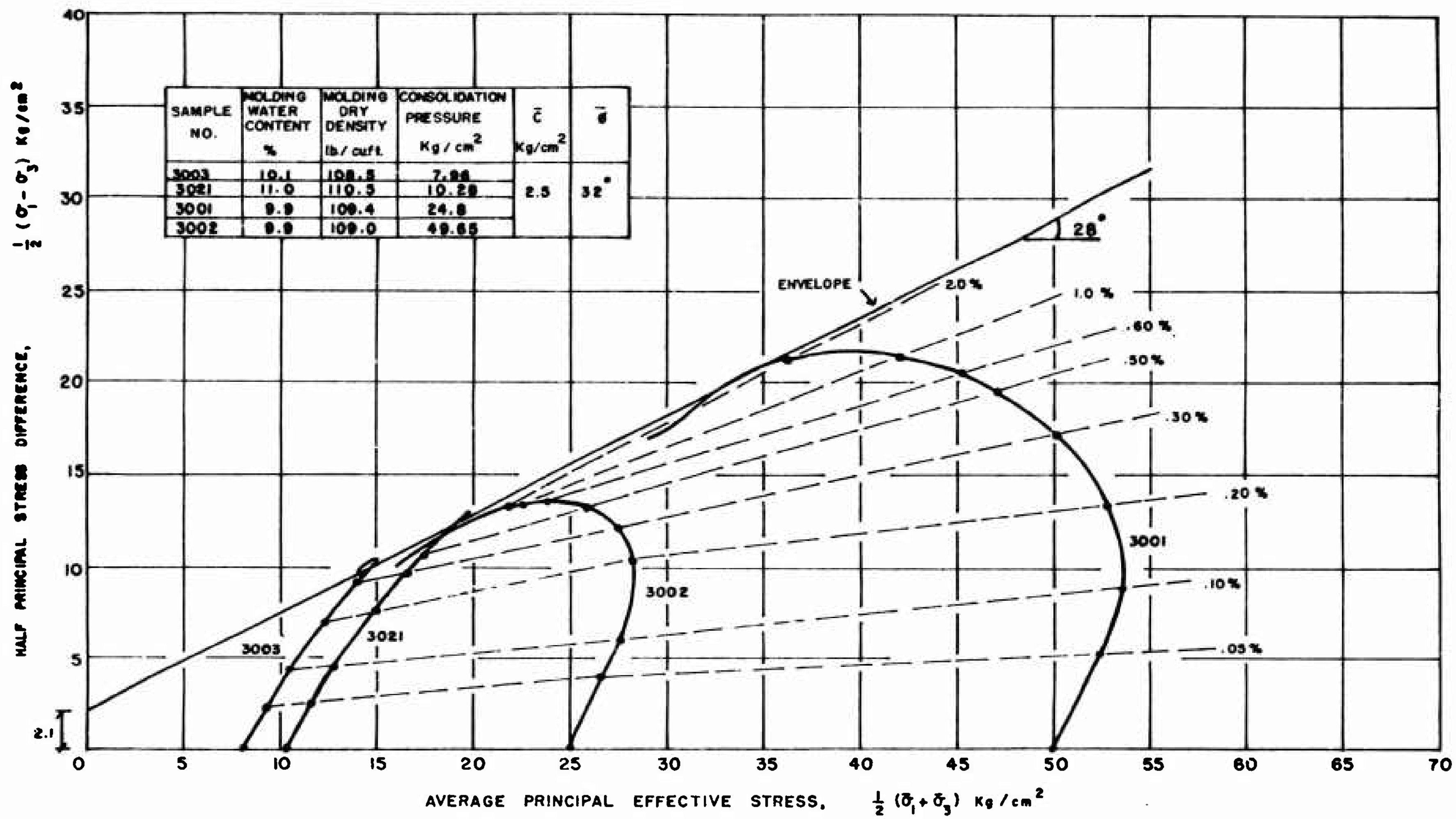

SAMPLE NO.	MOLDING WATER CONTENT %	MOLDING DRY DENSITY lb/cu.ft.	CONSOLIDATION PRESSURE Kg/cm^2	$\bar{c}$ Kg/cm^2	$\bar{\phi}$
3003	10.1	108.5	7.96	2.5	32°
3021	11.0	110.5	10.28		
3001	9.9	109.4	24.8		
3002	9.9	109.0	49.65		

FIGURE 3.13 EFFECTIVE STRESS – STRENGTH BEHAVIOR M-21 + 5 % CEMENT COMPACTED DRY OF OPTIMUM

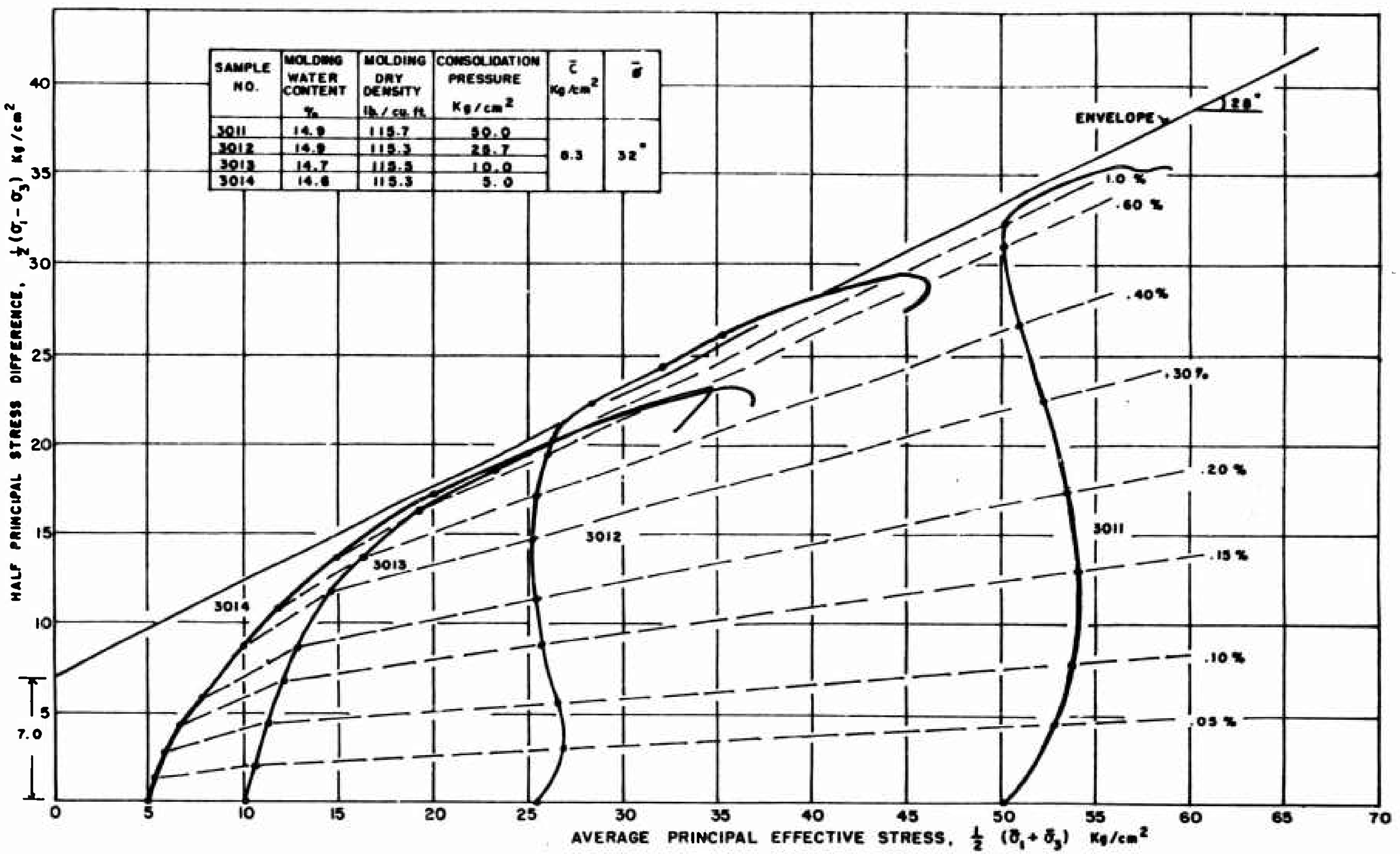

SAMPLE NO.	MOLDING WATER CONTENT %	MOLDING DRY DENSITY lb./cu.ft.	CONSOLIDATION PRESSURE Kg/cm²	$\bar{c}$ Kg/cm²	$\bar{\phi}$
3011	14.9	115.7	50.0	8.3	32°
3012	14.9	115.3	28.7		
3013	14.7	115.5	10.0		
3014	14.8	115.3	5.0		

FIGURE 3.14 EFFECTIVE STRESS-STRENGTH BEHAVIOR OF M-21 + 5% CEMENT COMPACTED AT OPTIMUM

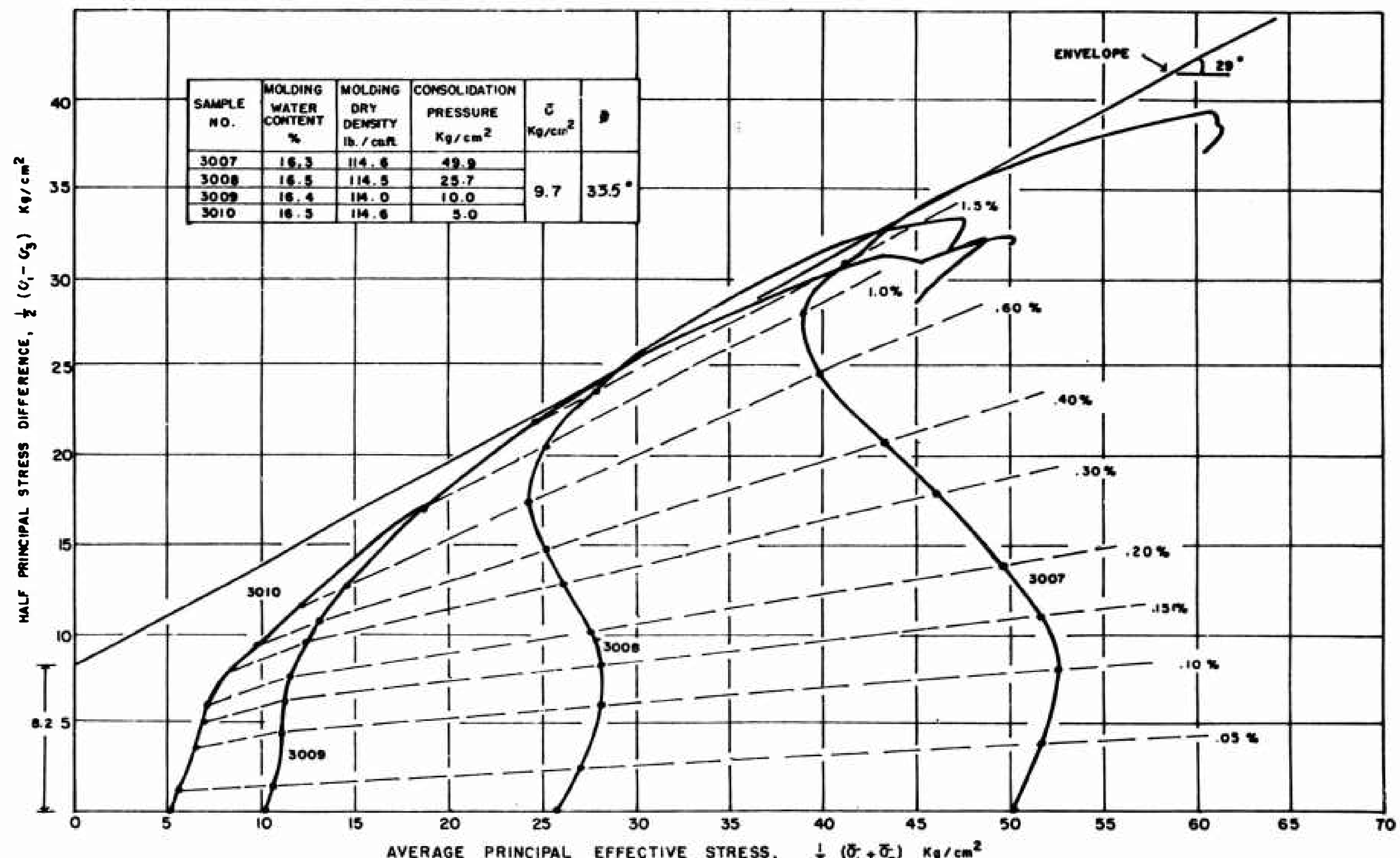

SAMPLE NO.	MOLDING WATER CONTENT %	MOLDING DRY DENSITY lb./cu.ft.	CONSOLIDATION PRESSURE Kg/cm^2	$\bar{c}$ Kg/cm^2	$\bar{\phi}$
3007	16.3	114.6	49.9	9.7	33.5°
3008	16.5	114.5	25.7		
3009	16.4	114.0	10.0		
3010	16.5	114.6	5.0		

FIGURE 3.15 EFFECTIVE STRESS – STRENGTH BEHAVIOR OF M-21 + 5 % CEMENT COMPACTED WET OF OPTIMUM

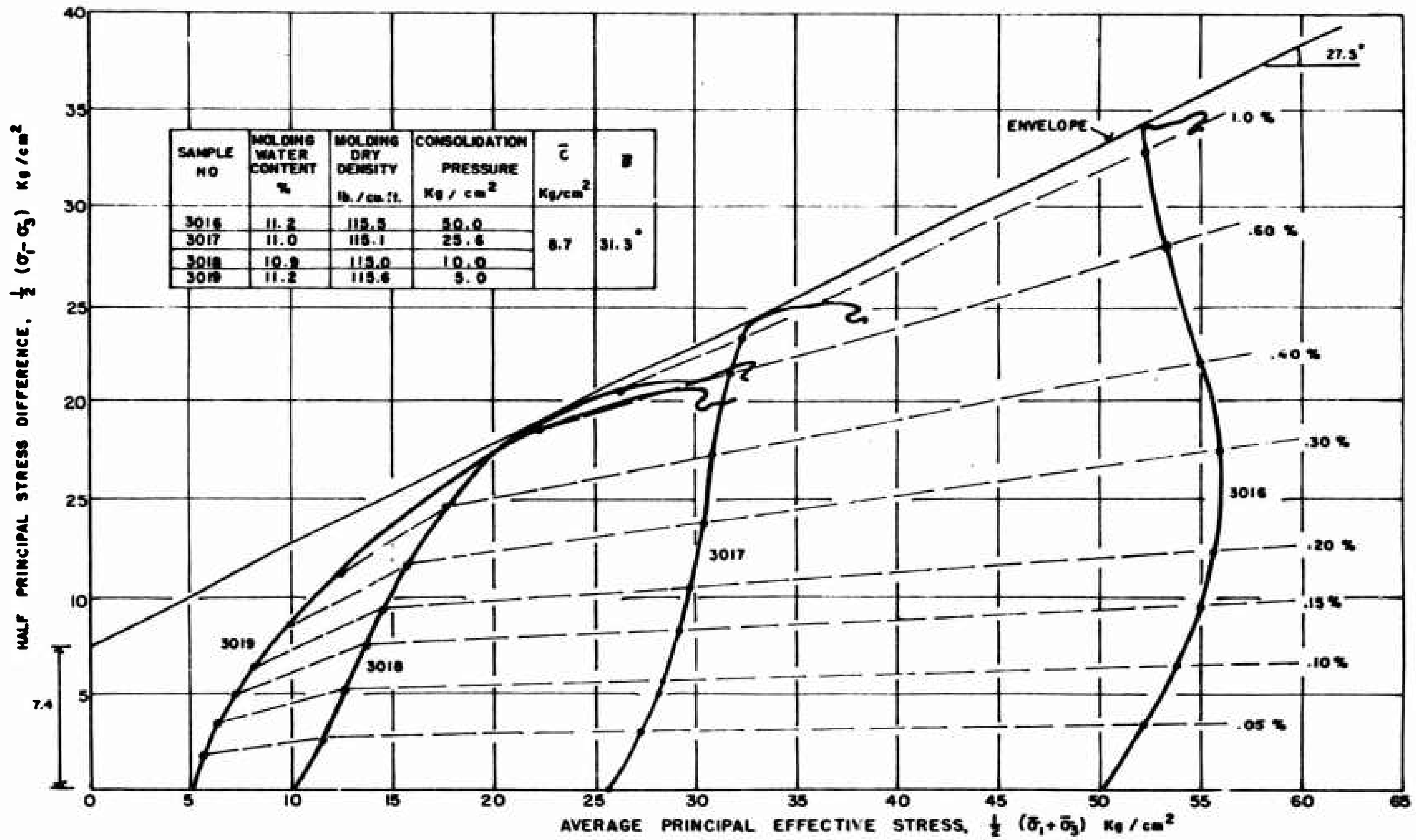

FIGURE 3.16 EFFECTIVE STRESS – STRENGTH BEHAVIOR OF M-21 + 5 % CEMENT COMPACTED AT HIGH DENSITY

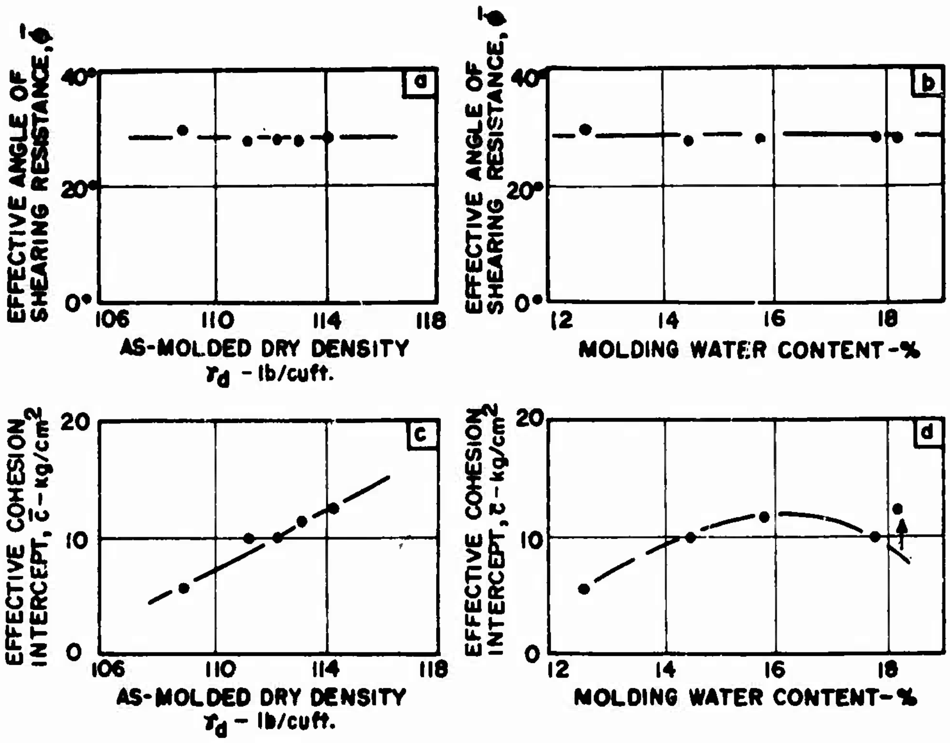

FIG.3.17 INFLUENCE OF MOLDING CONDITIONS ON THE MOHR-COULOMB EFFECTIVE STRESS-STRENGTH PARAMETERS OF M-21 STABILIZED WITH 5% LIME

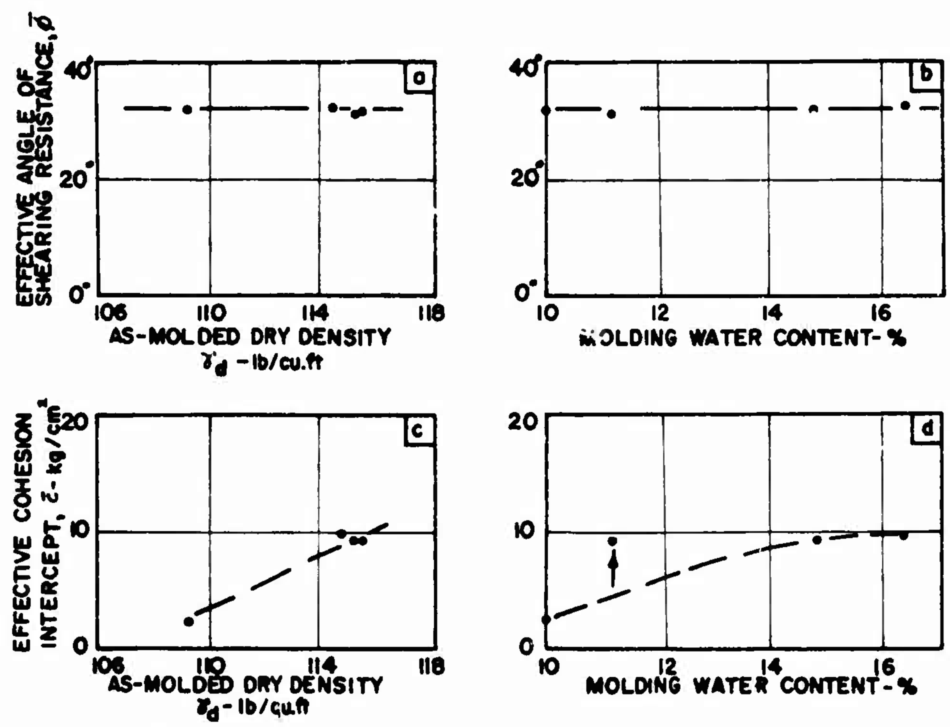

FIG. 3.18 INFLUENCE OF MOLDING CONDITIONS ON THE MOHR-COULOMB EFFECTIVE STRESS-STRENGTH PARAMETERS OF M-21 STABILIZED WITH 5% CEMENT

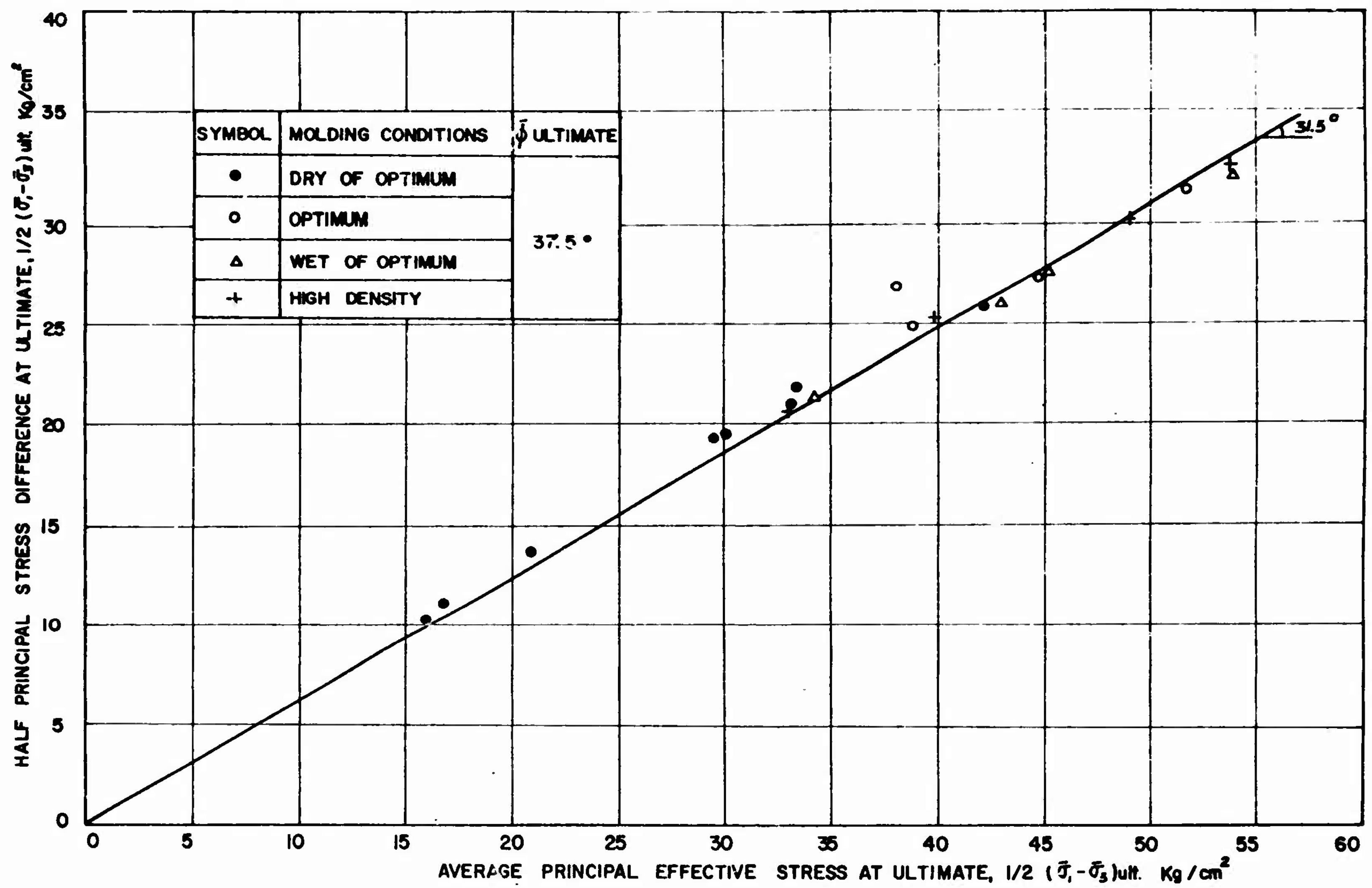

FIGURE 3.19 EFFECTIVE STRESS-STRENGTH RELATION AT ULTIMATE FOR M-21 + 5% LIME

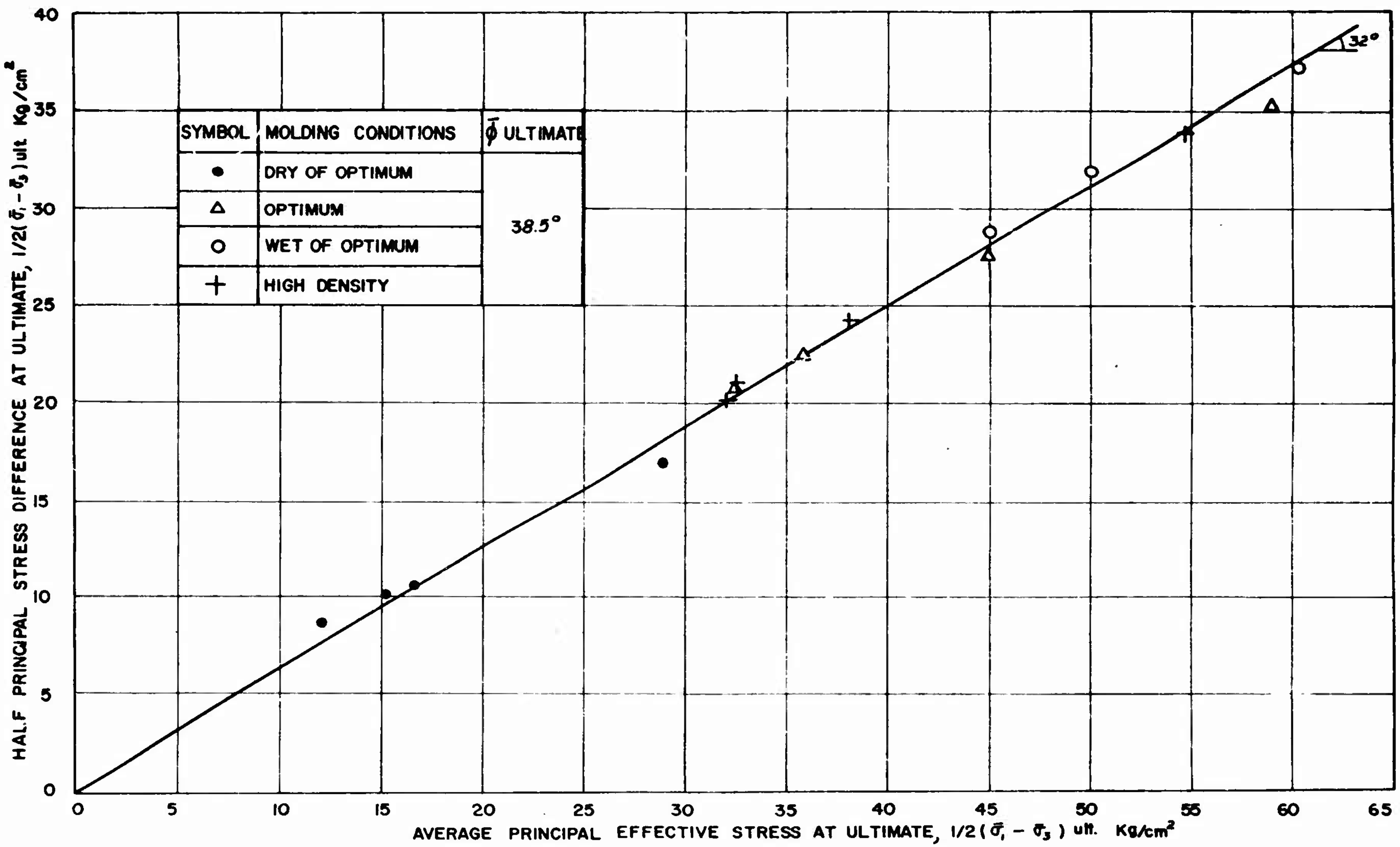

FIGURE 3.20 EFFECTIVE STRESS-STRENGTH RELATION AT ULTIMATE FOR M-21 + 5% CEMENT

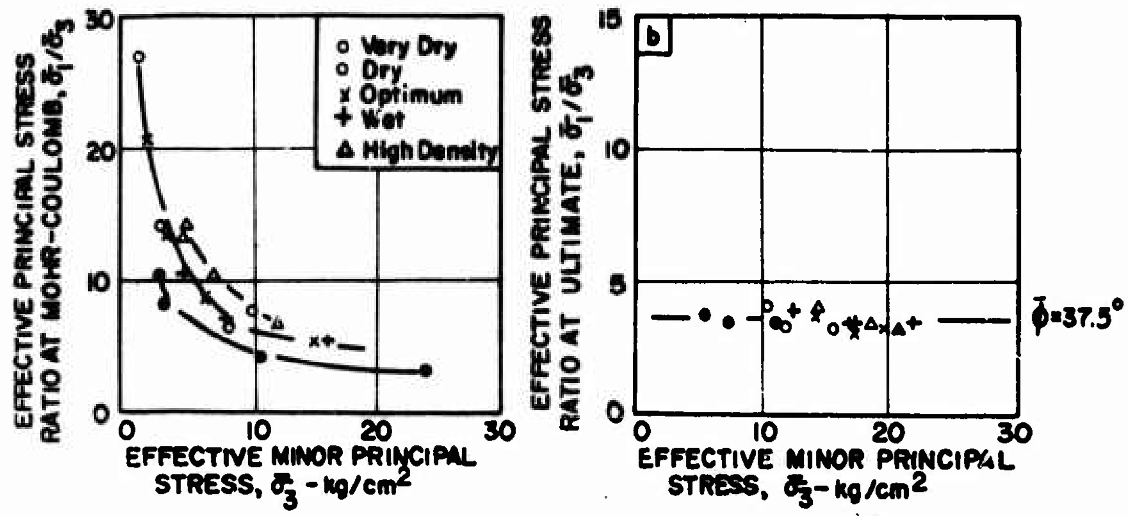

FIG.3.21 COMPARISON OF EFFECTIVE PRINCIPAL STRESS RATIO FOR M-21 WITH 5% LIME AT MOHR-COULOMB AND ULTIMATE AS A FUNCTION OF MOLDING CONDITIONS

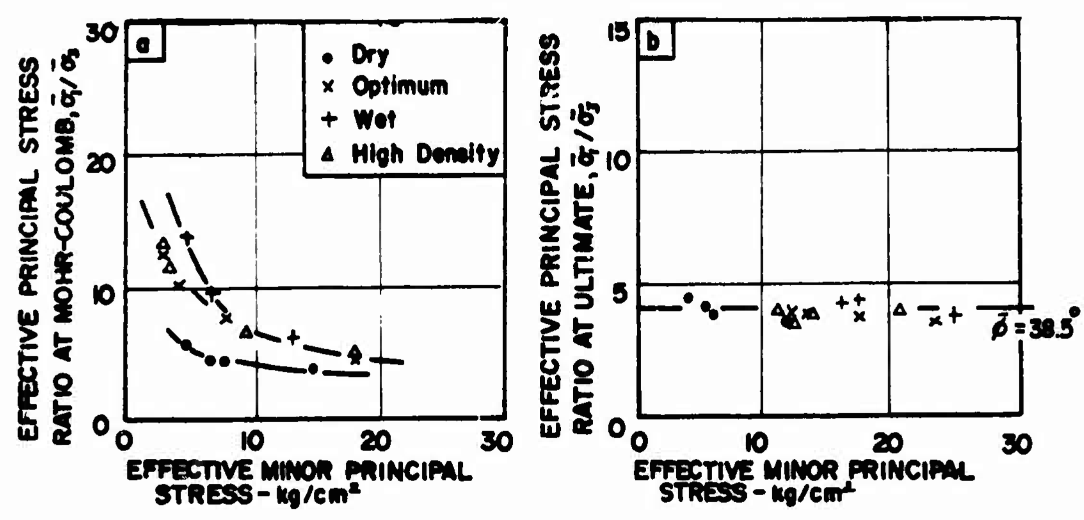

FIG. 3.22 COMPARISON OF EFFECTIVE PRINCIPAL STRESS RATIO FOR M-21 WITH 5% CEMENT AT MOHR-COULOMB AND ULTIMATE AS A FUNCTION OF MOLDING CONDITIONS

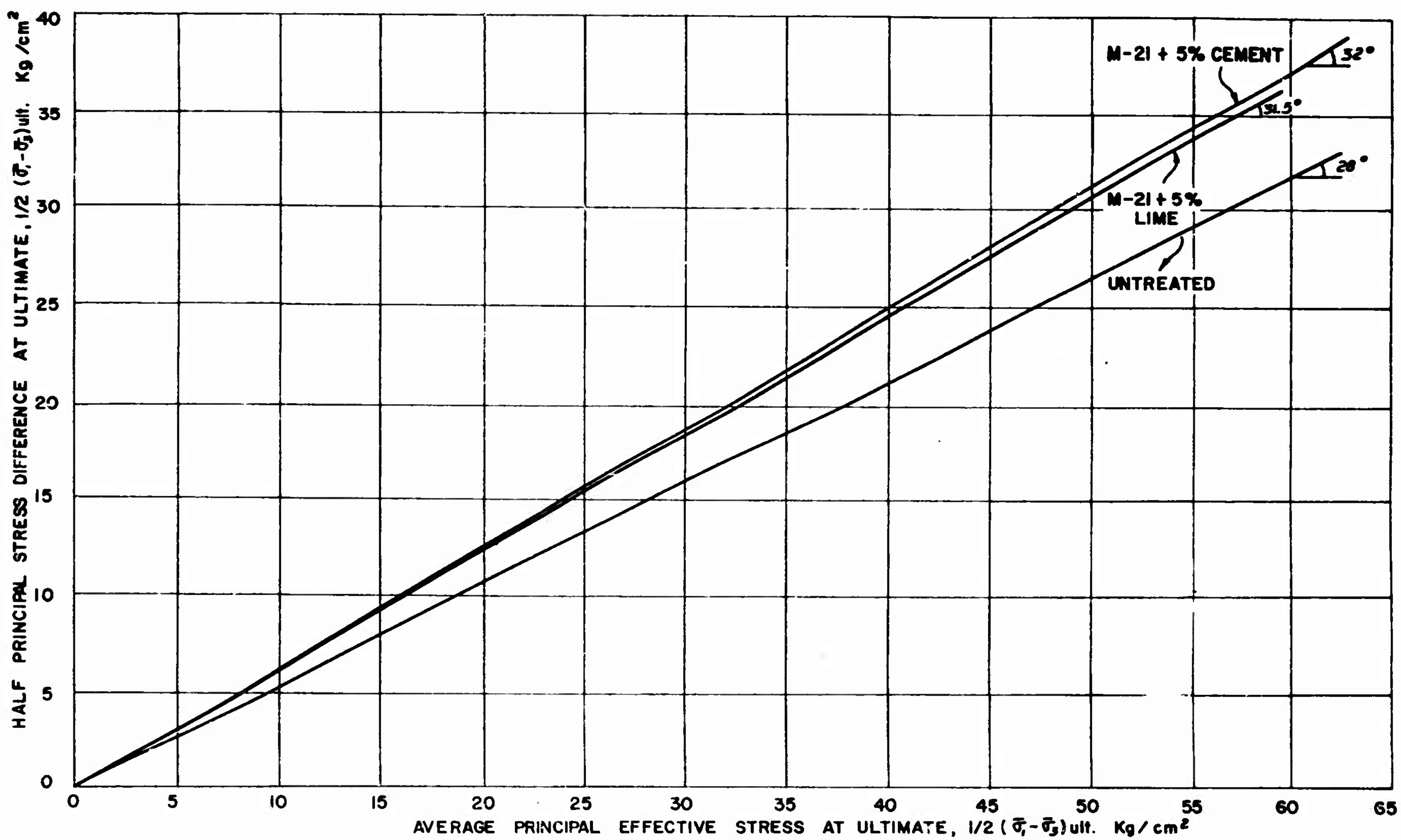

FIGURE 3.23 EFFECTIVE STRESS-STRENGTH RELATION AT ULTIMATE FOR THE M-21 SYSTEMS

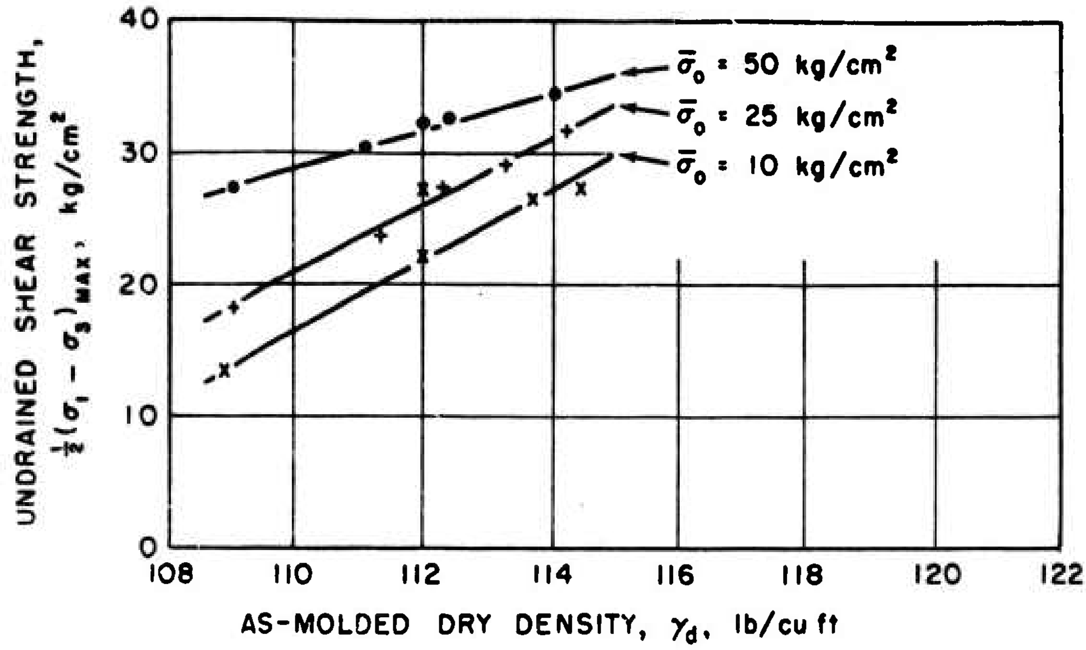

FIG.3.24 INFLUENCE OF MOLDING DRY DENSITY ON THE UNDRAINED STRENGTH OF M-21 STABILIZED WITH 5% LIME.

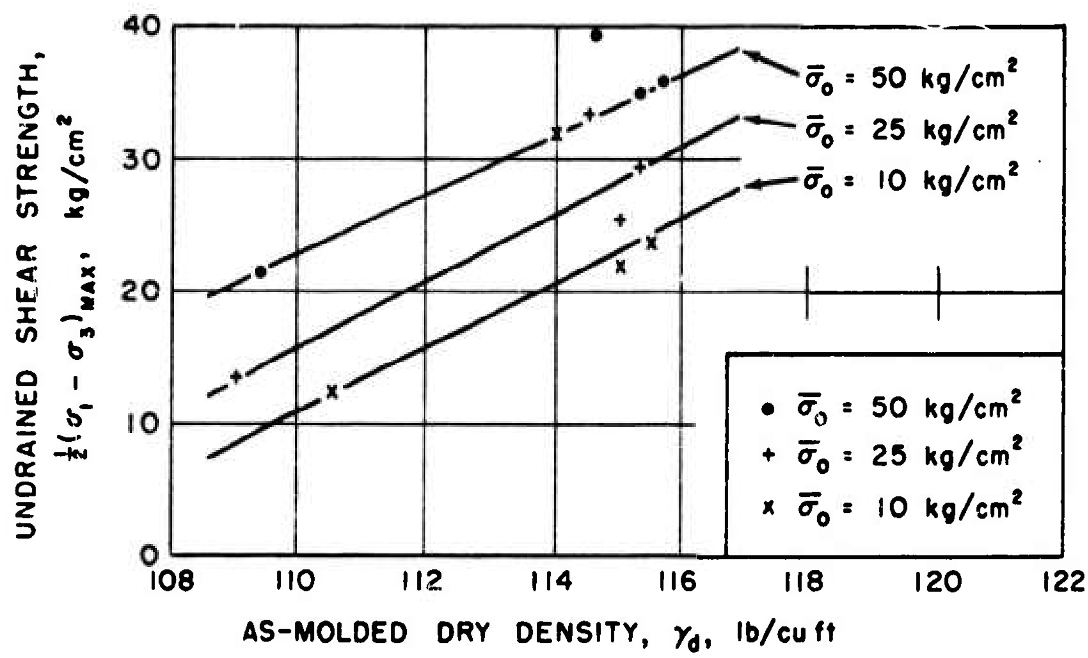

FIG.3.25 INFLUENCE OF MOLDING DRY DENSITY ON THE UNDRAINED STRENGTH OF M-21 STABILIZED WITH 5% CEMENT.

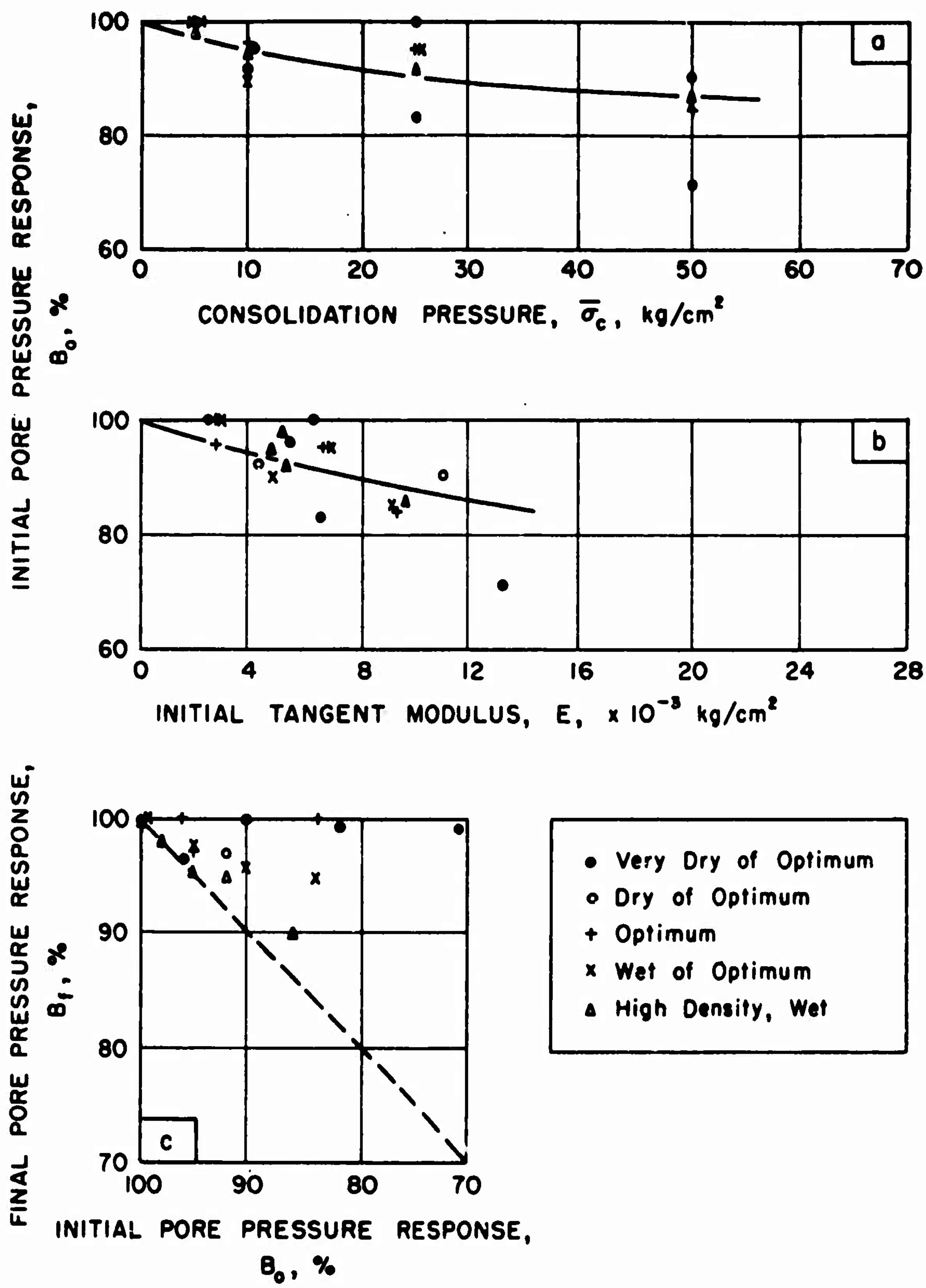

FIG.3.26 PORE PRESSURE RESPONSE OF UNTREATED MASSACHUSETTS CLAYEY SILT.

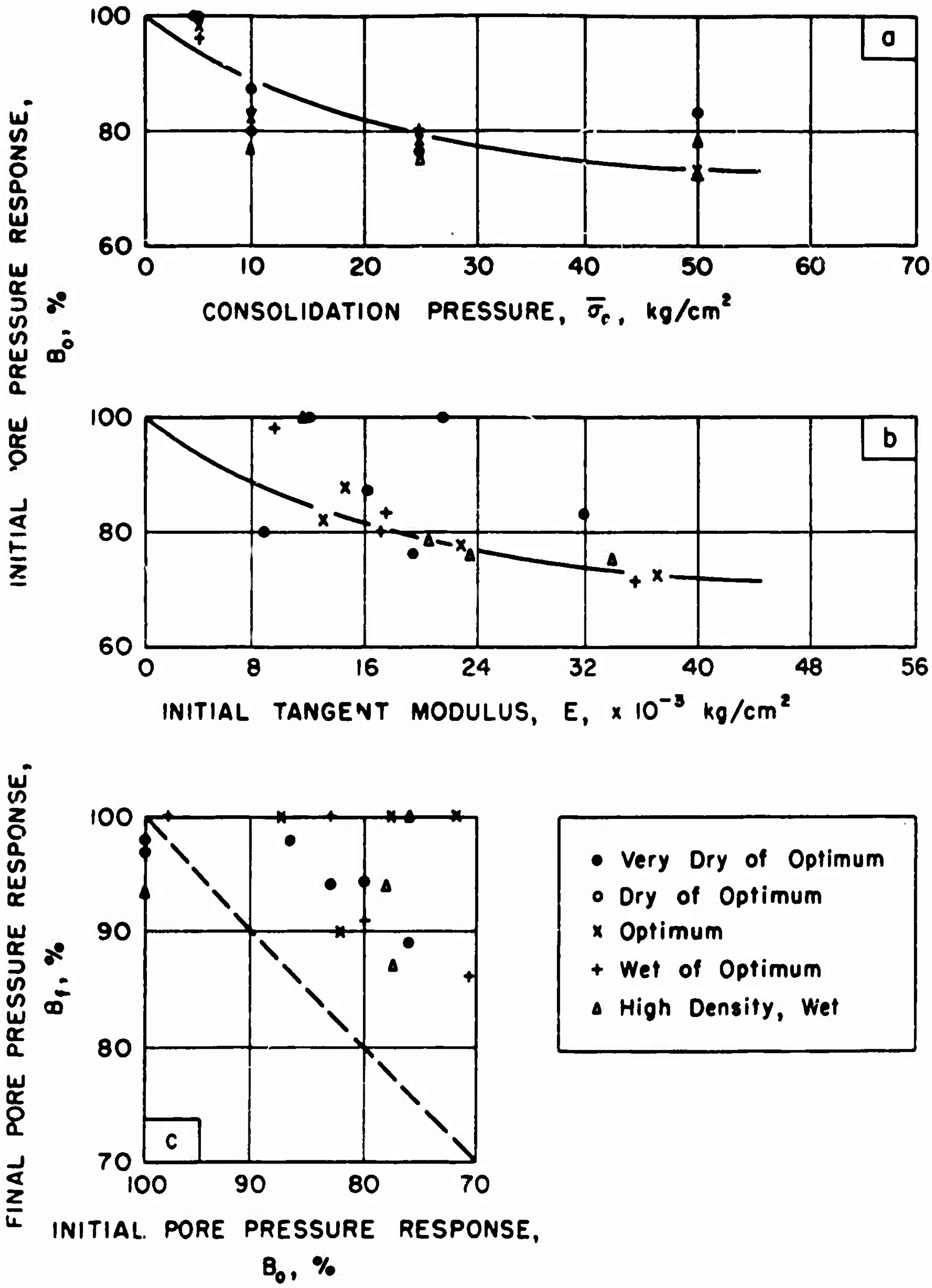

FIG. 3.27 PORE PRESSURE RESPONSE OF LIME STABILIZED MASSACHUSETTS CLAYEY SILT.

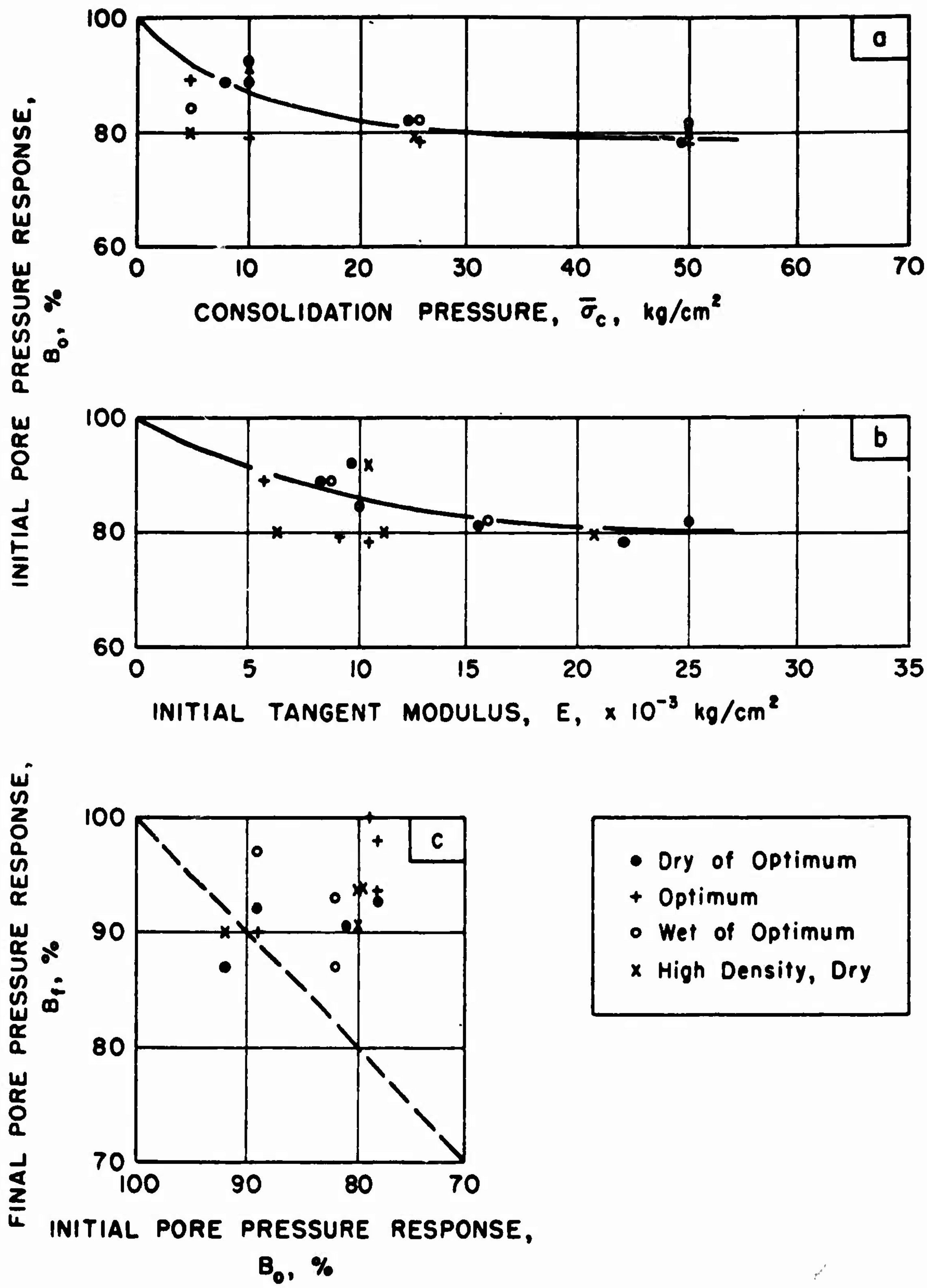

FIG. 3.28 PORE PRESSURE RESPONSE OF CEMENT STABILIZED MASSACHUSETTS CLAYEY SILT.

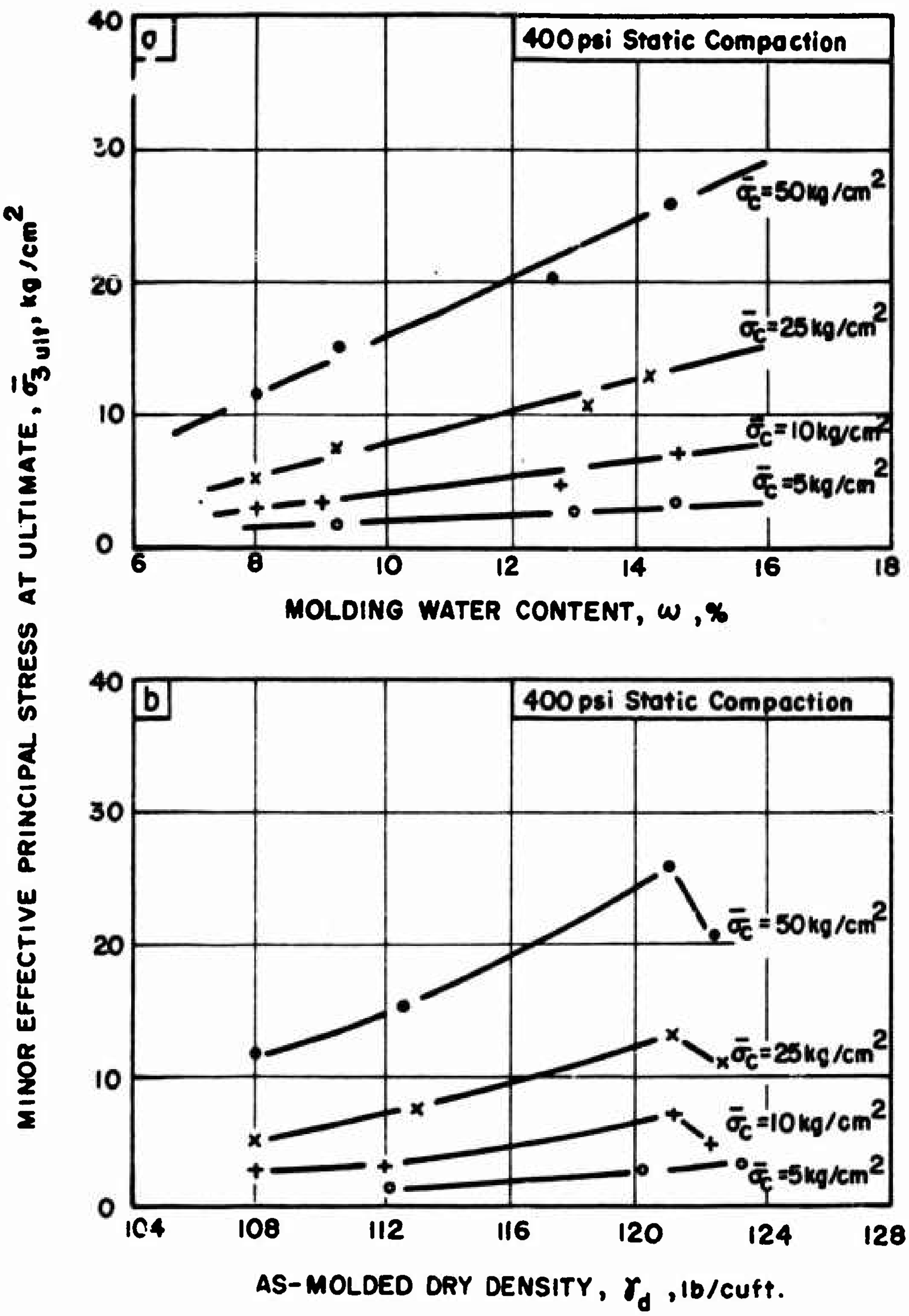

FIG. 3.29 INFLUENCE OF MOLDING CONDITIONS ON THE EFFECTIVE MINOR PRINCIPAL STRESS OF UNTREATED MASSACHUSETTS CLAYEY SILT AT ULTIMATE

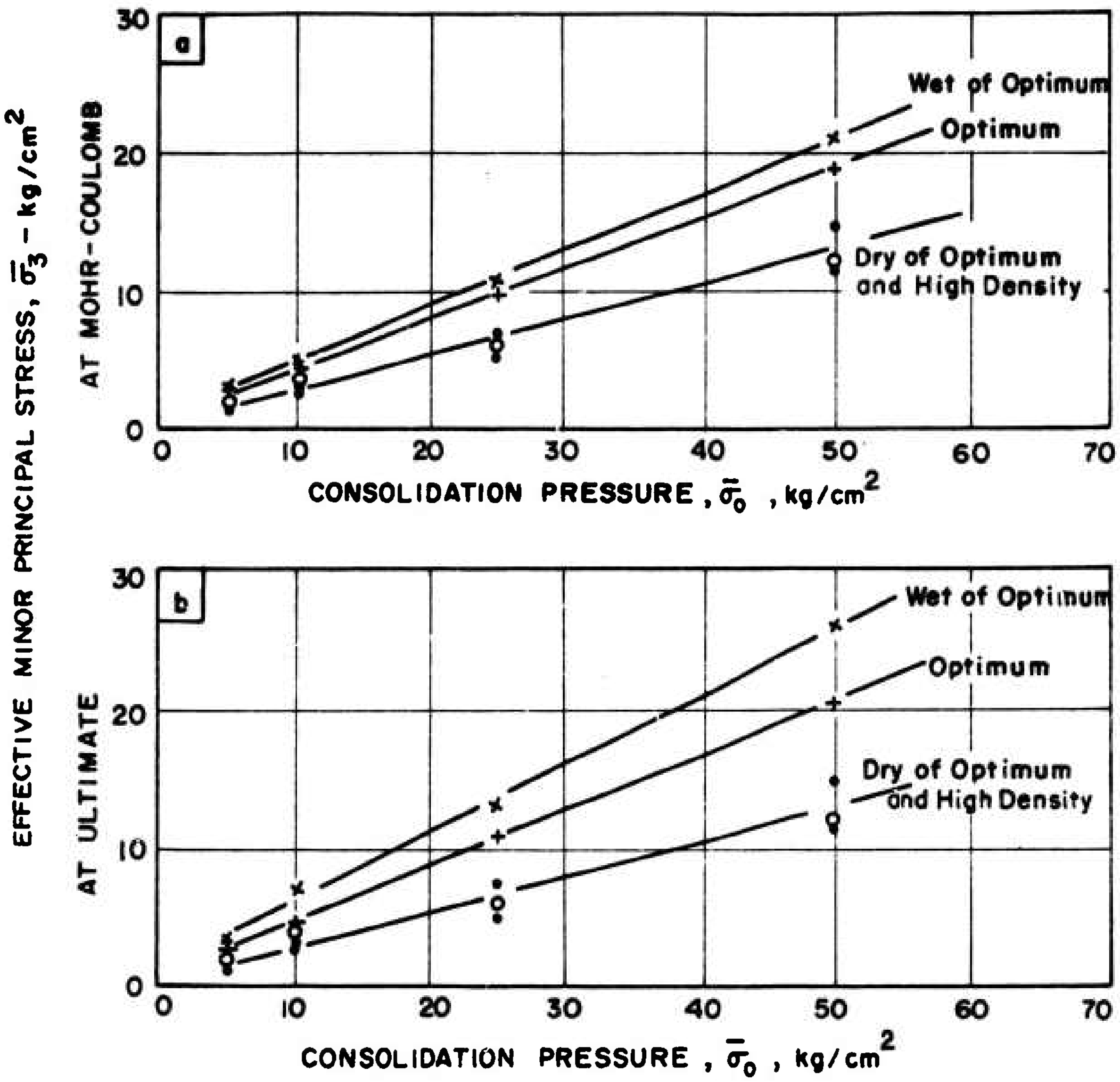

FIG. 3.30 INFLUENCE OF MOLDING CONDITIONS ON THE EFFECTIVE MINOR PRINCIPAL STRESS OF UNTREATED MASSACHUSETTS CLAYEY SILT DURING UNDRAINED SHEAR

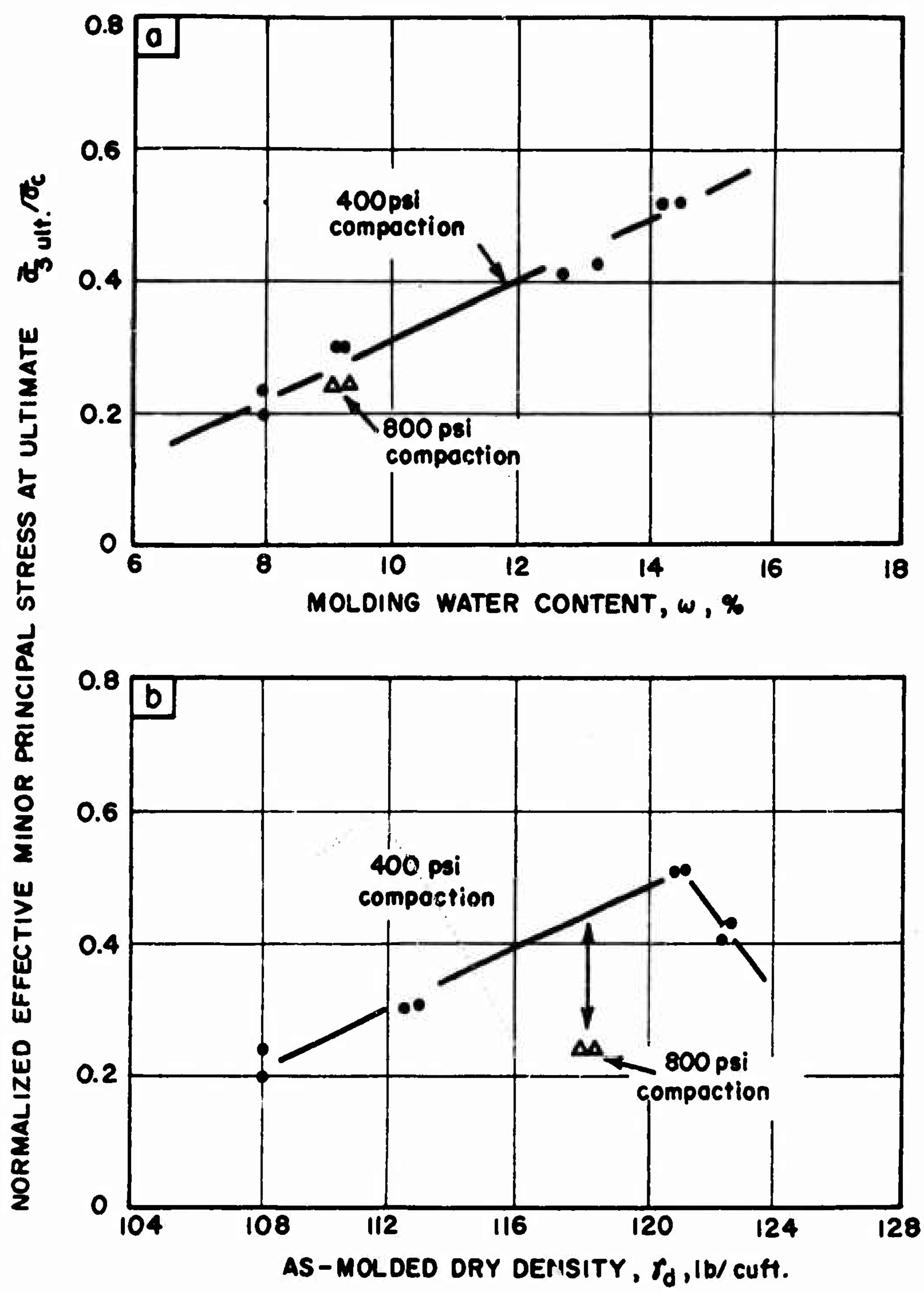

FIG.3.31 INFLUENCE OF STATIC COMPACTION EFFORT ON THE NORMALIZED EFFECTIVE MINOR PRINCIPAL STRESS OF UNTREATED MASSACHUSETTS SILT AT ULTIMATE

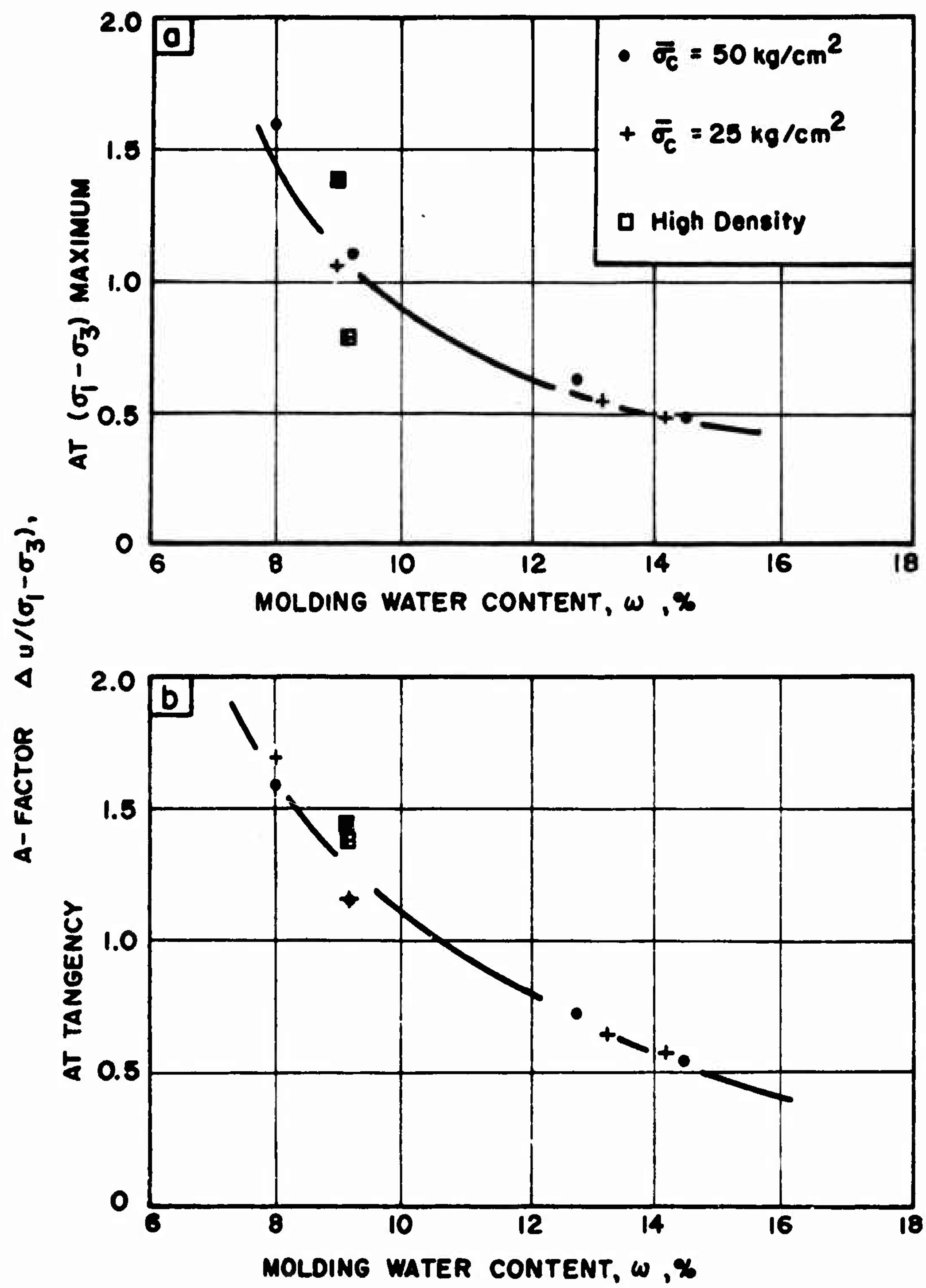

FIG.3.32 INFLUENCE OF MOLDING WATER CONTENT ON THE A-FACTOR OF UNTREATED MASSACHUSETTS CLAYEY SILT

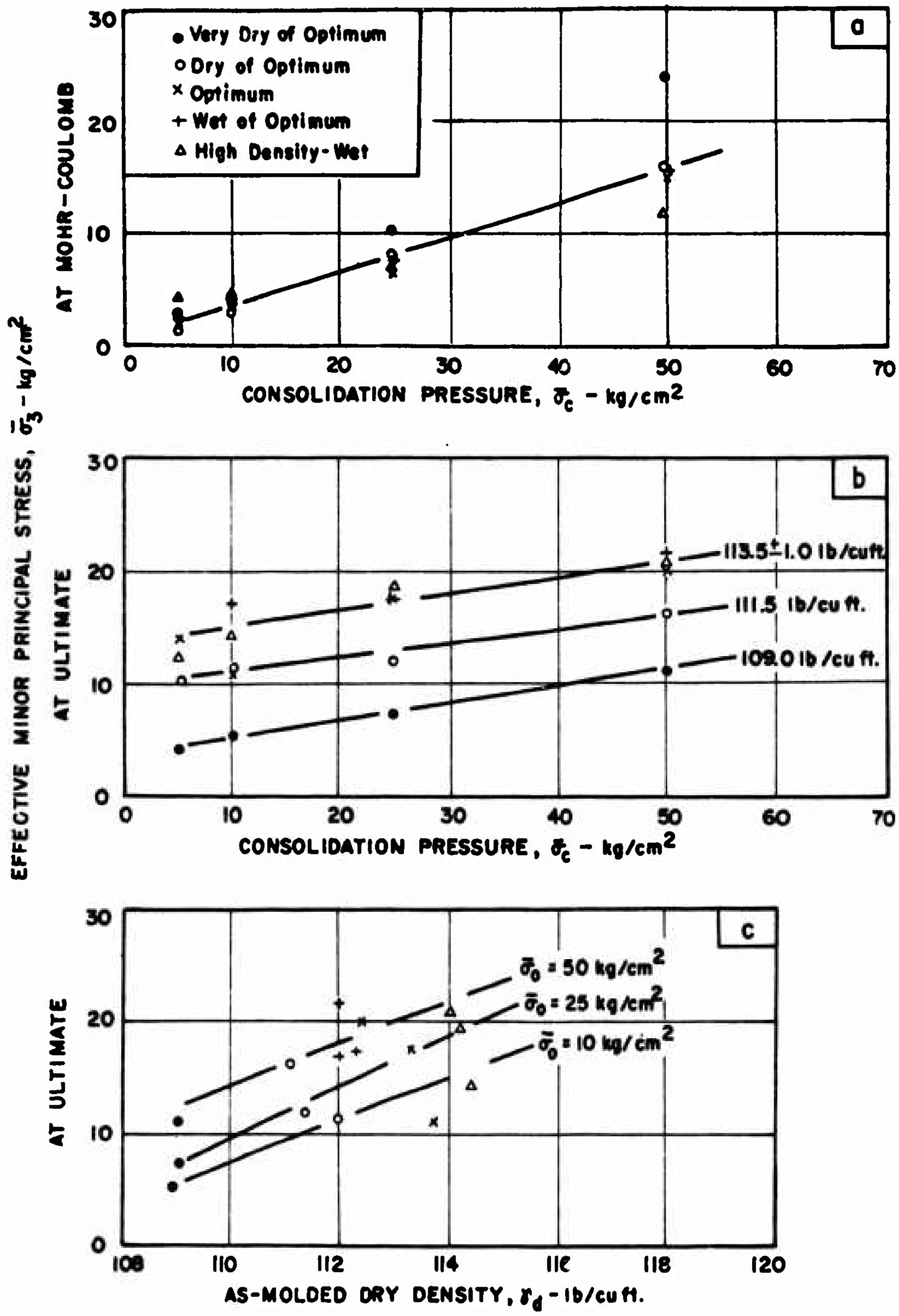

FIG. 3.33 INFLUENCE OF MOLDING CONDITIONS ON THE EFFECTIVE MINOR PRINCIPAL STRESS OF M-21 STABILIZED WITH 5% LIME

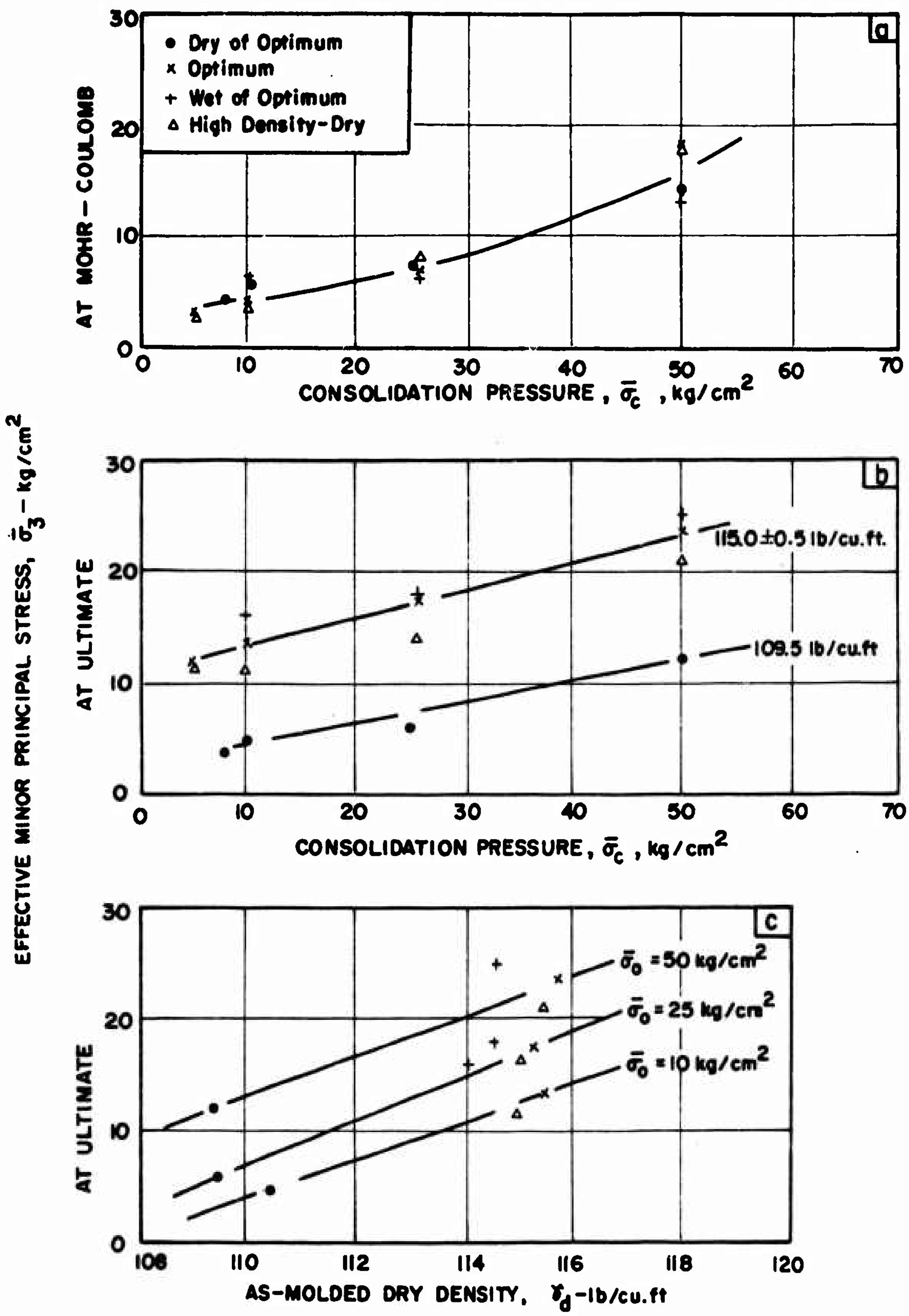

FIG. 3.34 INFLUENCE OF MOLDING CONDITIONS ON THE EFFECTIVE MINOR PRINCIPAL STRESS OF M-21 STABILIZED WITH 5% CEMENT

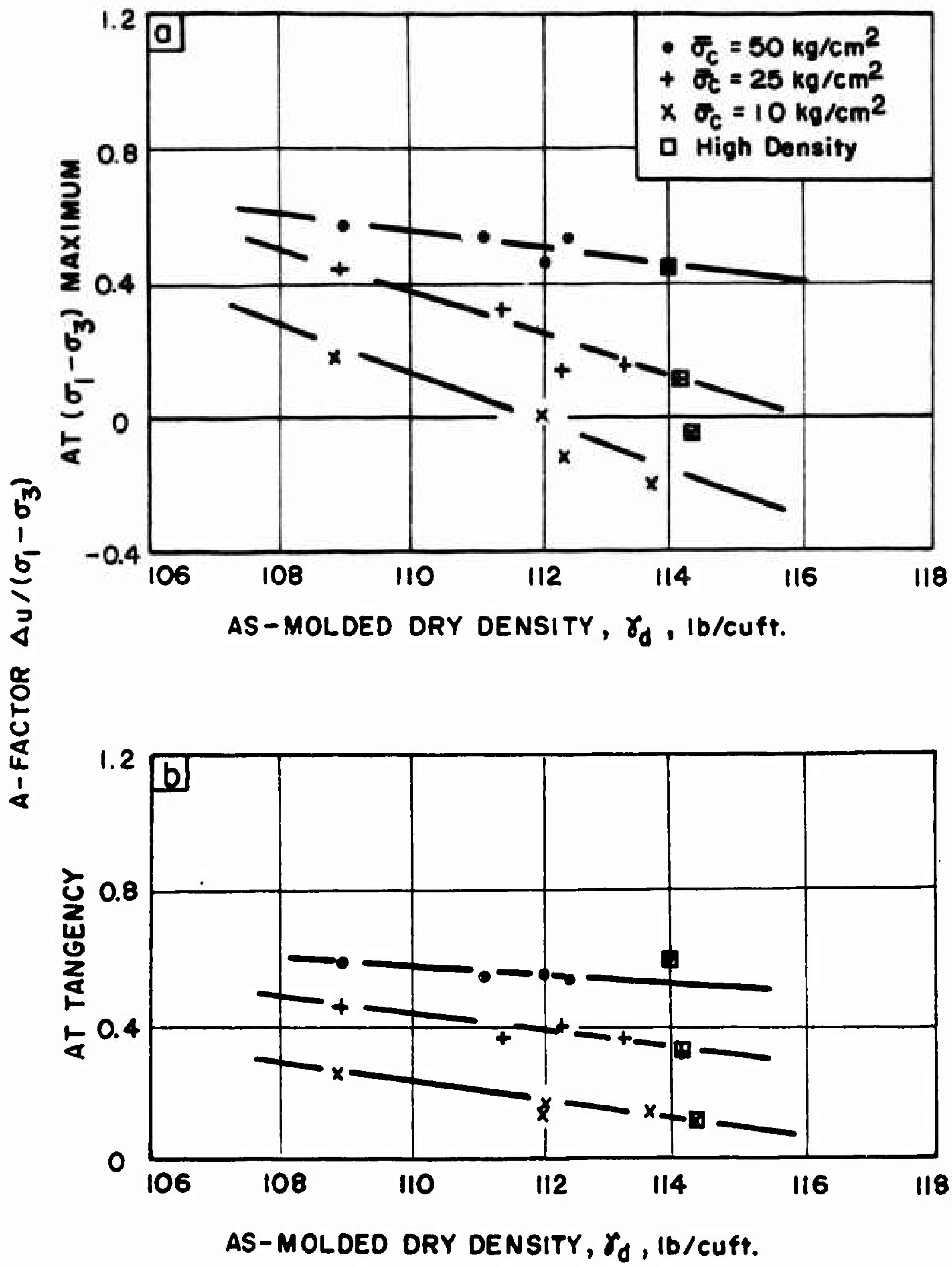

FIG.3.35 INFLUENCE OF AS-MOLDED DRY DENSITY ON THE A-FACTOR OF MASSACHUSETTS CLAYEY SILT STABILIZED WITH 5% LIME

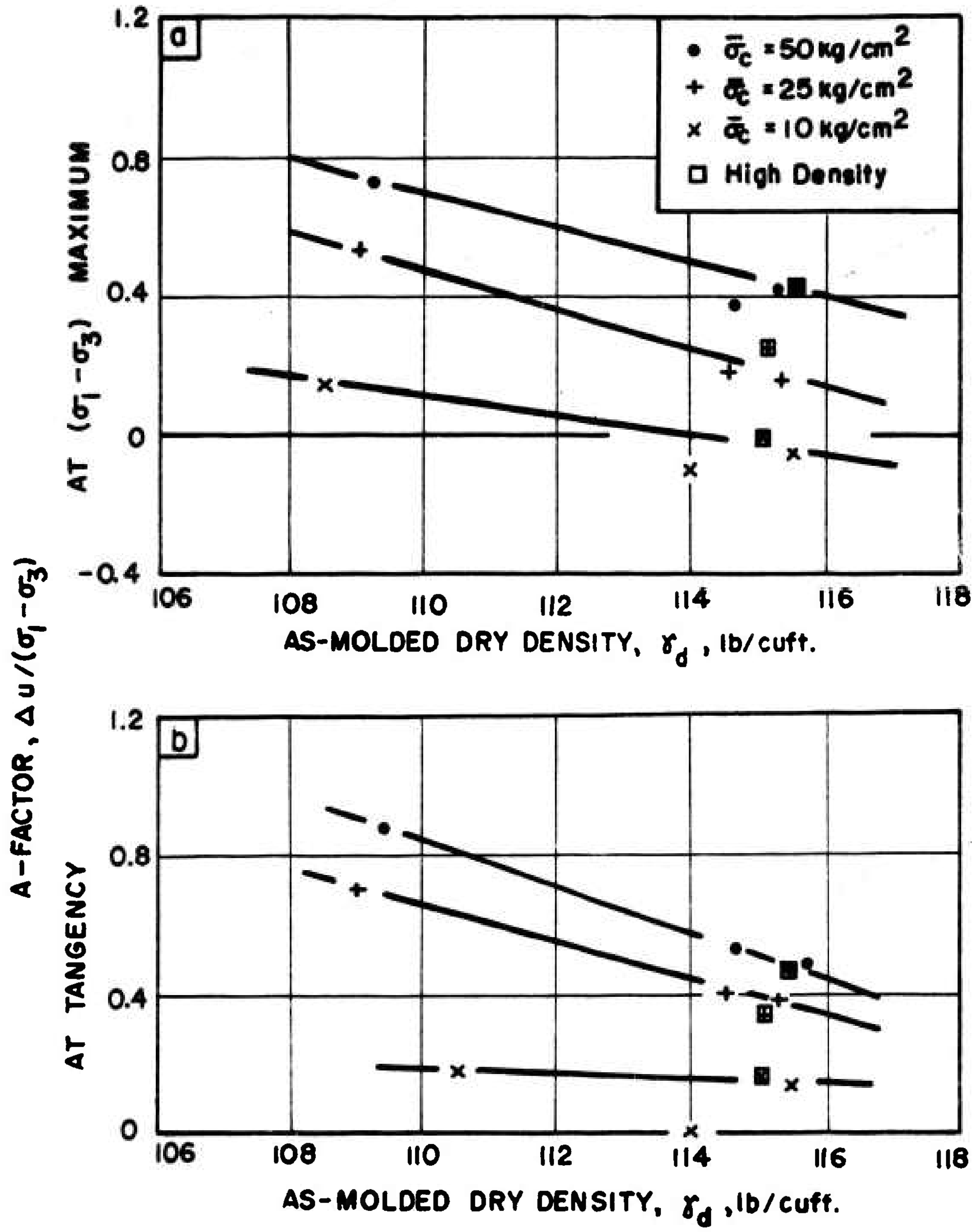

FIG.3.36 INFLUENCE OF AS-MOLDED DRY DENSITY ON THE A-FACTOR OF MASSACHUSETTS CLAYEY SILT STABILIZED WITH 5% CEMENT

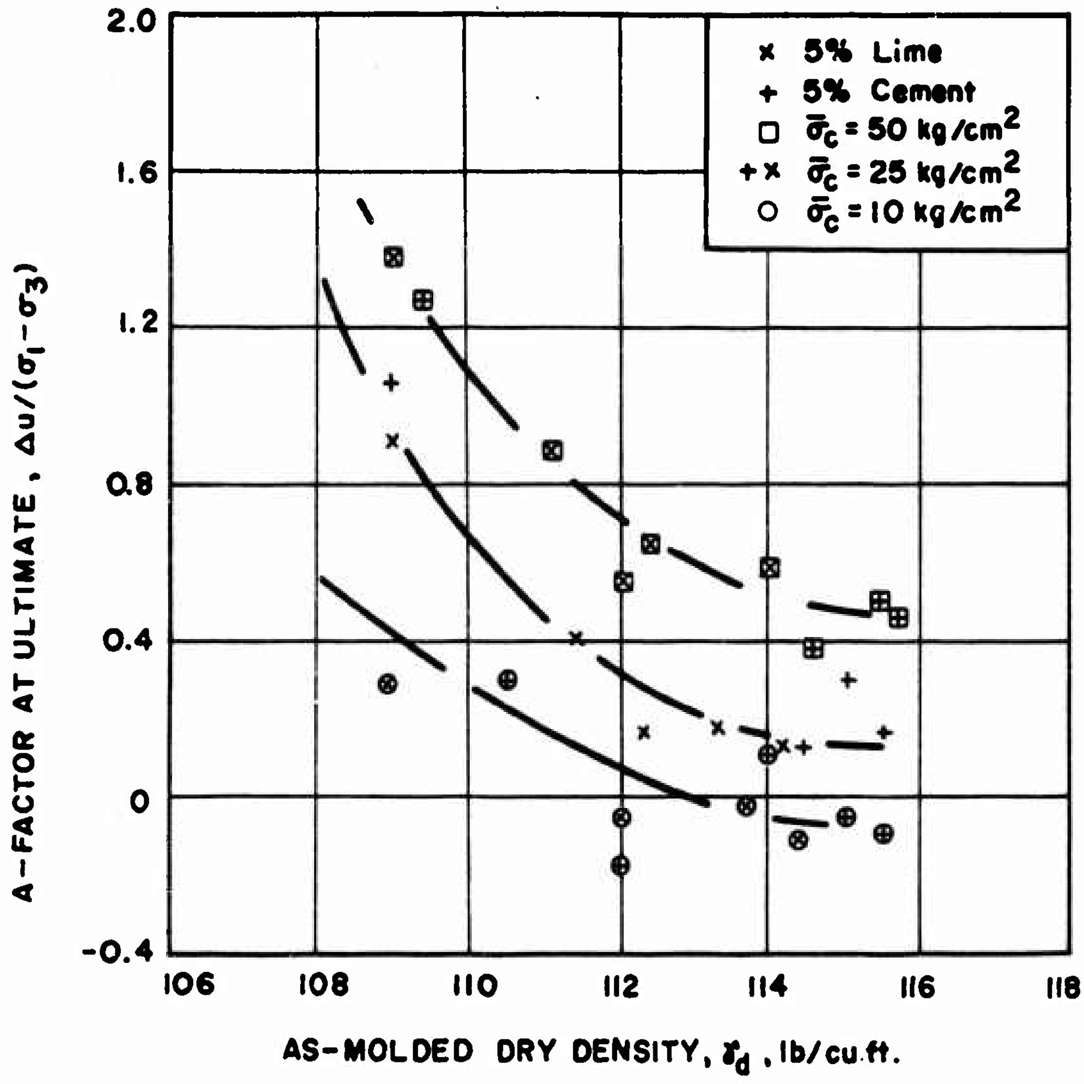

FIG.3.37 INFLUENCE OF AS-MOLDED DRY DENSITY ON THE ULTIMATE A-FACTOR OF M-21+5% LIME AND M-21+5% CEMENT

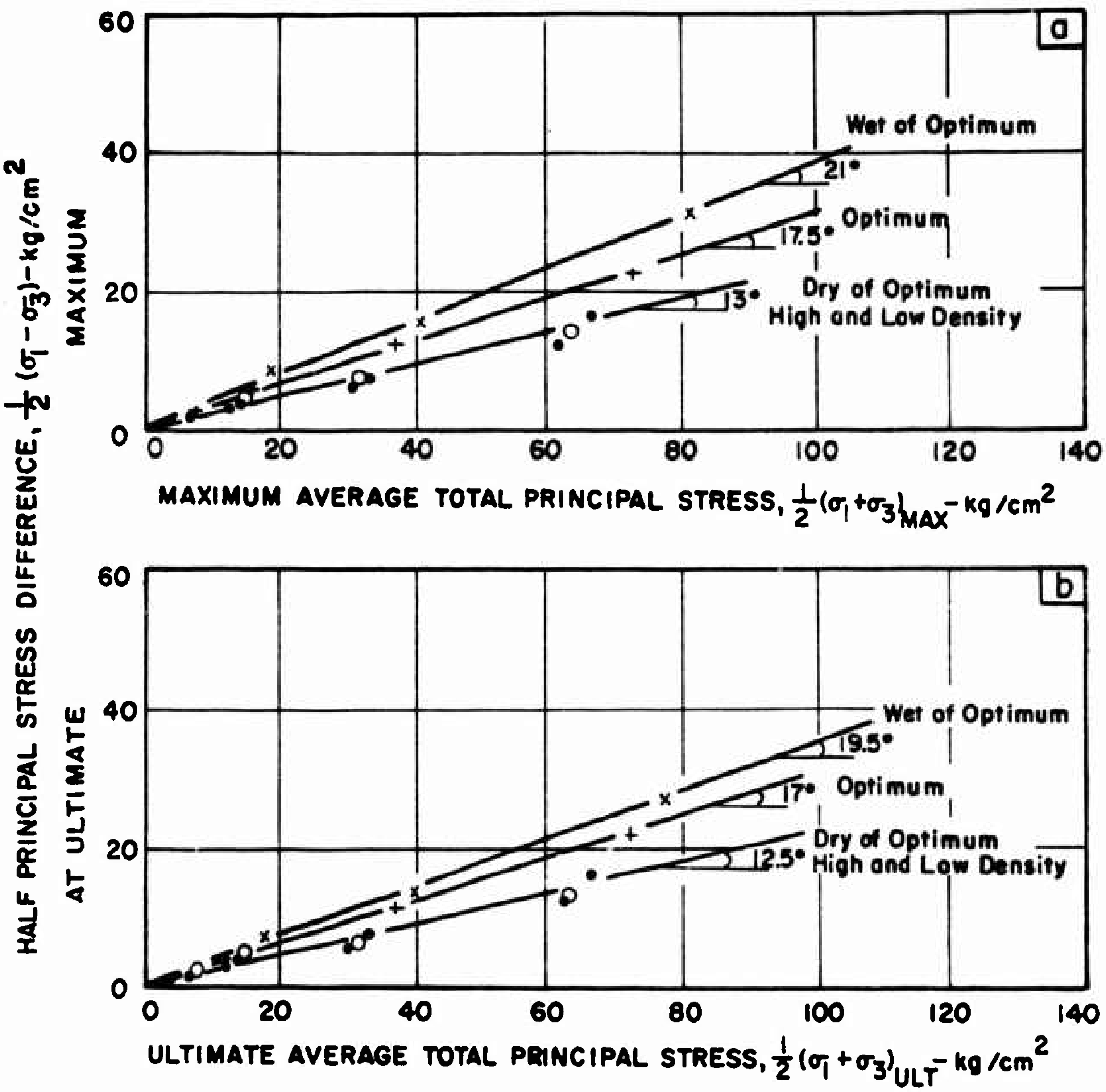

FIG.3.38 INFLUENCE OF MOLDING CONDITIONS ON THE STRESS-STRENGTH BEHAVIOR OF UNTREATED MASSACHUSETTS CLAYEY SILT

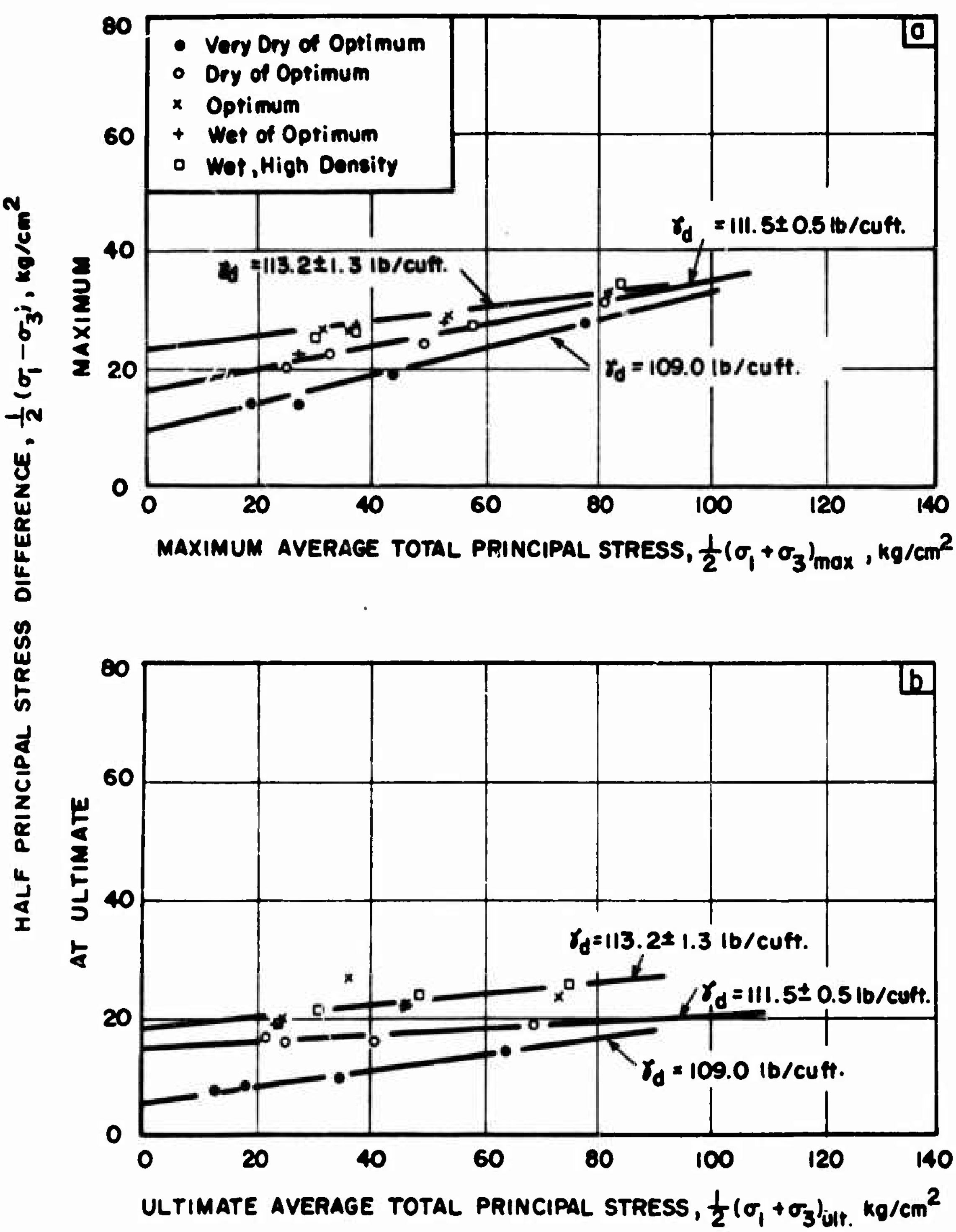

FIG.3.39 INFLUENCE OF MOLDING CONDITIONS ON THE TOTAL STRESS-STRENGTH BEHAVIOR OF MASSACHUSETTS CLAYEY SILT STABILIZED WITH 5% LIME

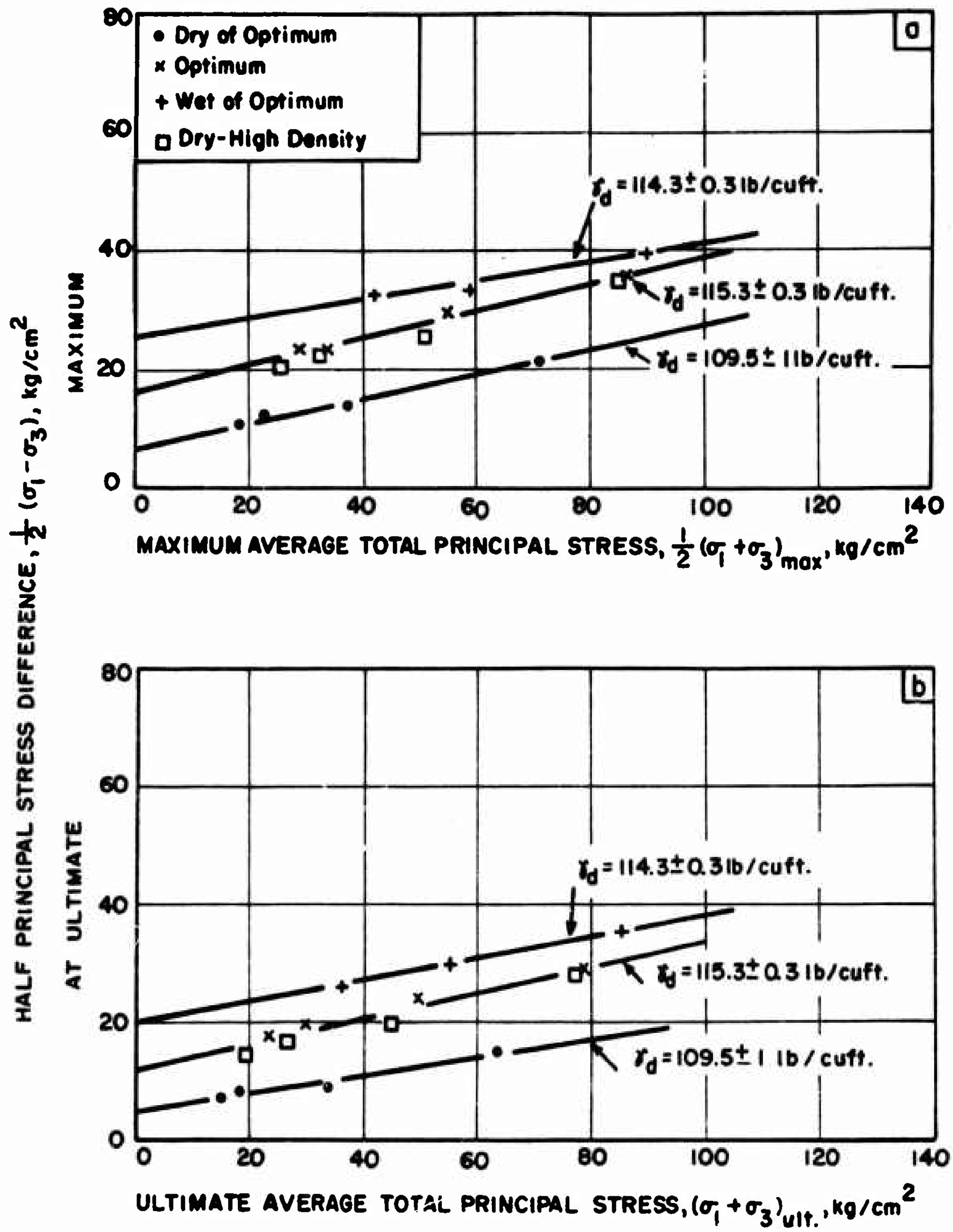

FIG. 3.40 INFLUENCE OF MOLDING CONDITIONS ON THE TOTAL STRESS-STRENGTH BEHAVIOR OF MASSACHUSETTS CLAYEY SILT STABILIZED WITH 5% CEMENT

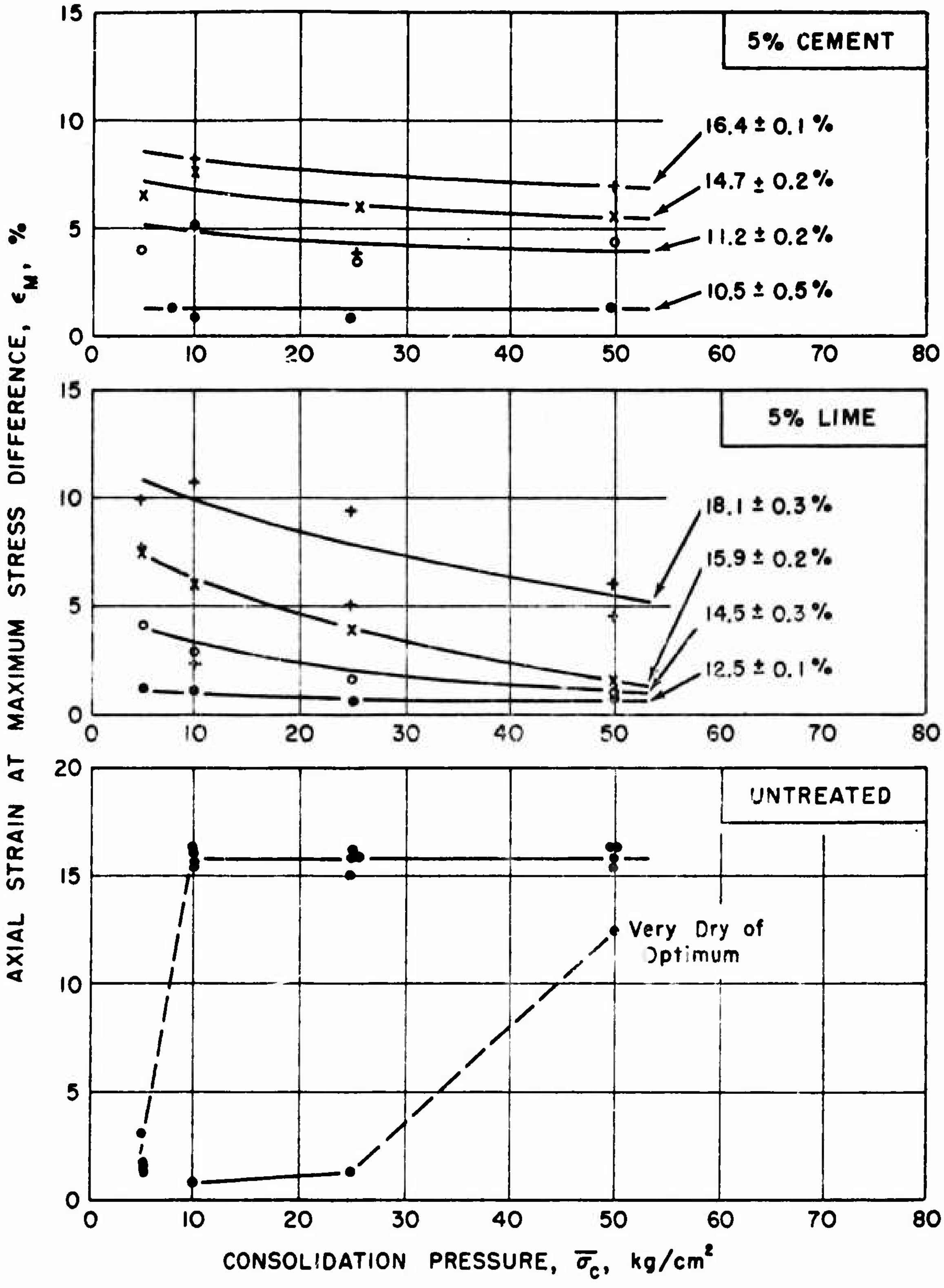

FIG.3.4/ INFLUENCE OF MOLDING CONDITIONS ON THE AXIAL STRAIN REQUIRED TO REACH MAXIMUM STRESS DIF-

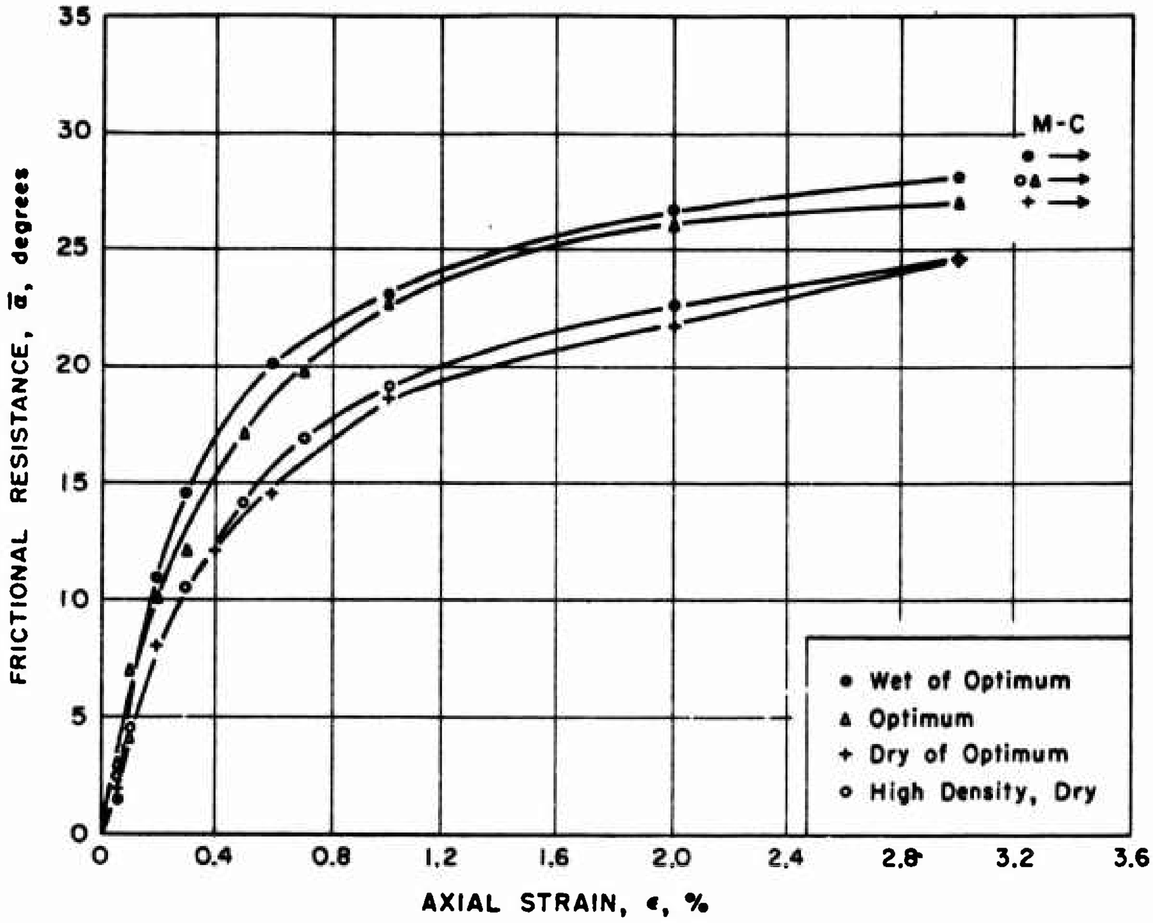

FIG. 3.42 DEVELOPMENT OF FRICTIONAL RESISTANCE AS A FUNCTION OF AXIAL STRAIN FOR UNTREATED MASSACHUSETTS CLAYEY SILT.

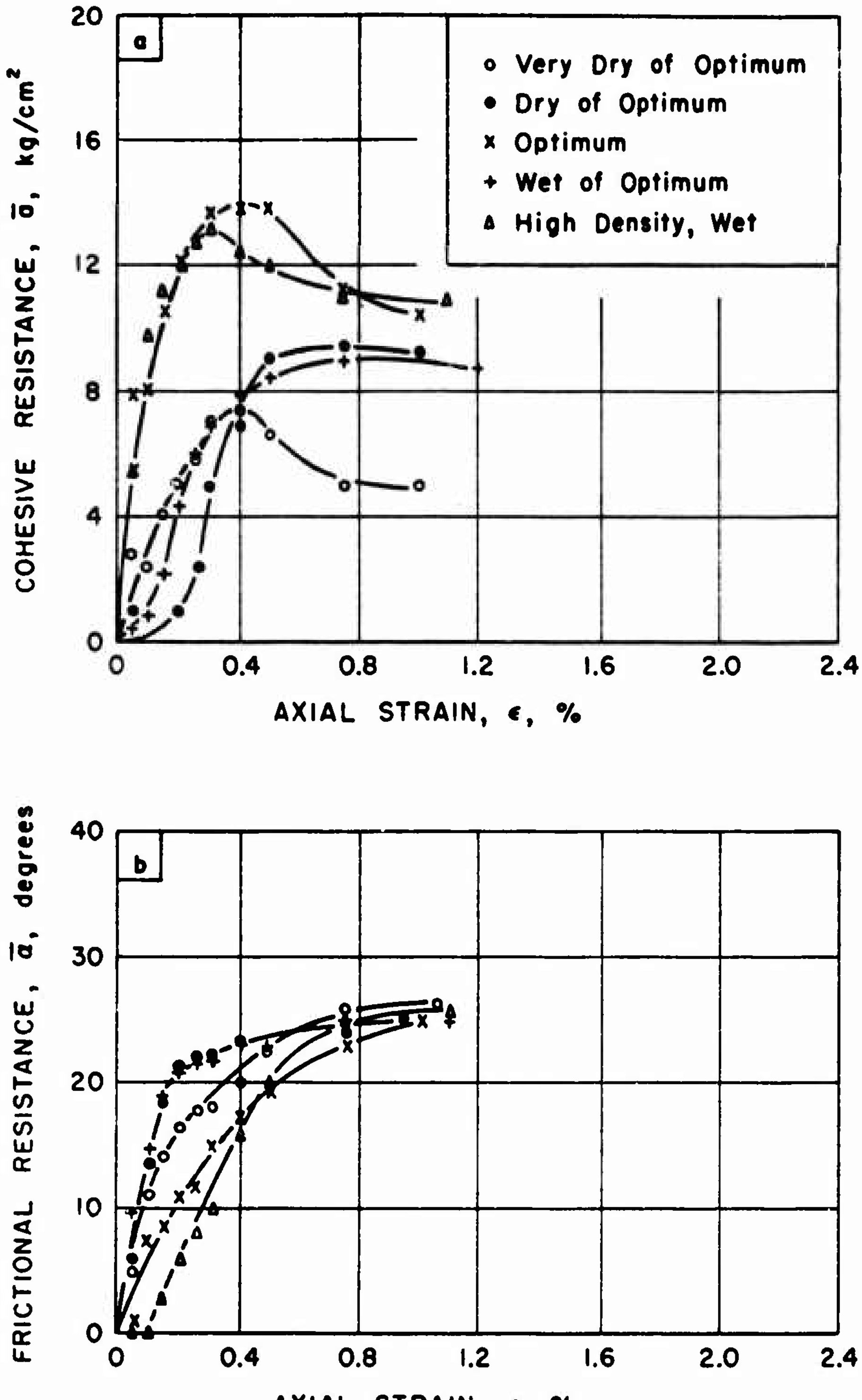

FIG.3.43 DEVELOPMENT OF FRICTIONAL AND COHESIVE RESISTANCE OF MASSACHUSETTS CLAYEY SILT WITH 5% LIME AS A FUNCTION OF AXIAL STRAIN.

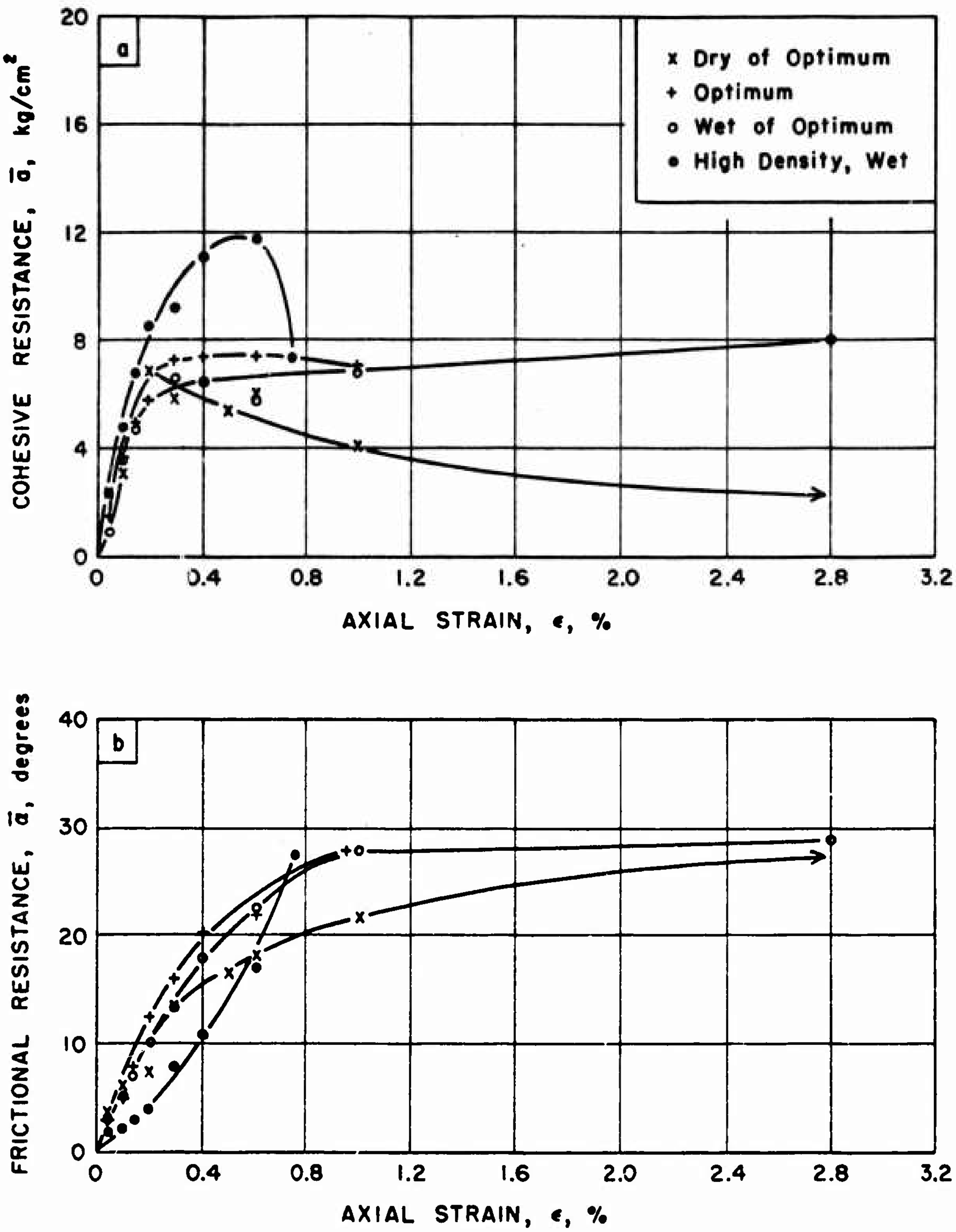

FIG.3.44 DEVELOPMENT OF FRICTIONAL AND COHESIVE RESISTANCE OF MASSACHUSETTS CLAYEY SILT WITH 5% CEMENT AS A FUNCTION OF AXIAL STRAIN.

Chapter 4

INFLUENCE OF DELAY TIME PRIOR TO COMPACTION

4.1 DELAY TIME COMPACTION

In order to investigate the effect of delaying the time of compaction after mixing on the stress-strength behavior of M-21 + 5 per cent cement, three sets of samples were prepared using two-end static compaction. Samples of the set named DTO were compacted at an effort of 400 psi immediately after mixing. Samples of the set DT1 were compacted at the same effort as the DTO set after 5 hours delay following mixing in of the molding water. Samples of the set DT2 were compacted to a dry density equal to that of the DTO set after 5 hours delay following mixing in of the molding water, by increasing the compaction effort to about 800 psi in order to obtain the same density as the DTO set.

All the samples of the three sets were compacted at an average molding water content of 13.4 per cent (see summary data in Table 4.1).

4.2 EFFECTIVE STRESS-STRENGTH BEHAVIOR

The Mohr-Coulomb effective stress-strength envelopes of the three sets tested (sets DTO, DT1, and DT2) are shown

in Figs. 4.1 through 4.3. Over the range of consolidation pressures used, the envelopes for the three conditions investigated were straight lines.

As shown in Figs. 4.1 and 4.3, delay time of compaction, per se, had no effect on either the effective Mohr-Coulomb angle of shearing resistance or the effective cohesion intercept since these two sets of samples, which had the same as-molded dry density (a higher compactive effort was needed for the delay time set), have the same envelope.

In Fig. 4.2 samples of the DT1 set showed a slightly lower cohesion intercept and a much lower angle of shearing resistance than series DTO and DT2. This reflects the effect of the much lower as-molded dry density obtained in the DT1 samples, which had a delay time prior to compaction of 5 hours and were compacted at a constant effort of 400 psi. The drop in density with delay time has been observed by other investigators (Armen et al, 1965).

In summary, it can be said that delay time prior to compaction causes a significant drop in the as-molded dry density for a given compactive effort and this in turn is reflected as a much lower effective Mohr-Coulomb angle of shearing resistance. Nevertheless, if delay time mixes

are compacted to the same as-molded dry density as the non-delay time mixes, there is no difference in the effective stress-strength parameters for a given molding water content. This may not be practical to achieve in the field since it requires a considerable increase in the applied compaction effort.

By the time ultimate conditions are reached at large strains, the soil behaves like a granular material having zero effective cohesion intercept and a high effective angle of shearing resistance ($\bar{\Phi}_{ult}$) which is not only independent of molding conditions but also is independent of delay time prior to compaction (see Fig. 4.4).

Fig. 4.5 shows the influence of delay time on the effective principal stress ratio of the cemented soil at Mohr-Coulomb and ultimate conditions as a function of effective minor principal stress. At Mohr-Coulomb (Fig. 4.5a), the data of sets DTO and DT2 show that the effective principal stress ratio is not influenced by delay time of compaction, per se, although it is a function of $\bar{\sigma}_3$ for the same reasons as given in Art. 3.1.2 for molding conditions. At ultimate conditions $\bar{\sigma}_1/\bar{\sigma}_3$ is independent of $\bar{\sigma}_3$, as shown in Fig. 4.5b, since $\bar{c}$ is zero and $\bar{\Phi}_{ult}$ is independent of delay time prior to compaction, and of molding conditions.

4.3 PORE PRESSURE RESPONSE

4.3.1 Prior to Shear

The pore pressure response was determined after consolidation and saturation, but prior to shear for the reasons stated in Art. 3.2.1. In addition, leak checks were run after each pore pressure response determination by closing the drainage valve and measuring the change in pore pressure as a function of time. Leaks in the system proved to be the cause for the low B factors initially obtained (not reported herein). Once the leaks were corrected, the pore pressure response went up to its normal values for the soil-cement system at the different consolidation pressures as shown in Fig. 4.6a.

No correlation appears to exist between delay time prior to compaction and B factor as can be seen in Fig. 4.6a. In general the pore pressure response prior to shear, B_o, decreased with increasing rigidity of the soil skeleton as expected. Fig. 4.7b is a plot of initial tangent modulus versus consolidation pressure. The data points show significant scatter but an important observation can be made. Sample DT2-1 shows a significantly higher modulus than sample DT2-2, both being at approximately the same consolidation pressure. Sample DT2-1 was brought up to the effective

consolidation pressure in four increments, allowing for consolidation after each increment, while sample DT2-2 was brought up to the final value of consolidation pressure in one step. This same procedure was used with samples DT1-3 and DT1-4. Also, samples DT2-1 and DT1-3 showed a higher strength than samples DT2-2 and DT1-4, respectively (see Figs. 4.2 and 4.3). This seems to indicate that applying the consolidation stress in one increment, especially at the higher consolidation pressures, produces some premature cracking that weakens the samples and lowers its rigidity. Keeping this in mind, one can conclude that the general trend is for an increase in rigidity with increase in consolidation pressure if the samples do not crack prematurely during consolidation, the increase being smaller for the more strongly cemented (stiffer) test sets.

4.3.2 After Shearing

Pore pressure response after shearing was determined as explained in Section 3.2.2. The results are plotted in Fig. 4.6b. This shows that B_f was greater than B_o, since the results plotted above the 45° line shown in the figure.

4.4 PORE PRESSURE DURING SHEAR

Since the total minor principal stress was kept constant

during consolidation and shear, the excess pore pressure developed during undrained shear is equal to the consolidation pressure minus the effective minor principal stress. Therefore from Figs. 4.8a and 4.8b, which are plots of $\bar{\sigma}_3$ at maximum stress difference and at tangency versus consolidation pressure, respectively, it is seen that the excess pore pressure during undrained shear is not influenced by delay time. Even though the delay samples at constant compactive effort (DT1 set) had a much lower as-molded dry density, their excess pore pressures at Mohr-Coulomb tangency, for a given consolidation pressure, were the same as for the higher as-molded dry density samples of the sets DTO and DT2 (Fig. 4.8b). This is in agreement with the results reported in Section 3.3.2, which showed that molding conditions had no significant influence on the excess pore pressures of the stabilized soil at Mohr-Coulomb failure.

From Fig. 4.8a it is also seen that delay time, per se, and as-molded dry density does not influence the excess pore pressure at maximum stress difference. At ultimate failure (Fig. 4.8c), the excess pore pressure at any given consolidation pressure is independent of delay time, per se, since the DTO and DT2 sets had the same pore water pressures; however, the delay time DT1 set, which had a lower as-molded dry density than the other two sets, developed higher excess

pore water pressures. This is also in agreement with the results presented in Section 3.3.2.

Apparently, at Mohr-Coulomb and tangency conditions, the cementation between the soil-cement aggregates containing high cement concentrations has not yet been appreciably destroyed; therefore, the differences in dry density are not reflected as a difference in excess pore pressure. This is reinforced by the fact that at Mohr-Coulomb, the three sets of samples had about the same effective cohesion intercept. This does not necessarily mean that the maximum cohesive resistance in the low density delay time samples is as large as for the higher density samples. Based on the fact that at Mohr-Coulomb $\bar{\Phi}$ for the low density delay time samples was lower than for the high density samples, whereas at ultimate all the sets had the same $\bar{\Phi}_{ult}$, it appears that in the low density set, more of the shearing resistance at Mohr-Coulomb was due to cohesion and less due to friction than for the high density sets. As will be shown later in Section 4.6.2, the axial strains needed to reach maximum stress difference were lower for the low density delay time set (DT1) than for the high density sets (DTO and DT2). Therefore, less friction is mobilized and less cohesion (cementation between aggregates) is destroyed in the low density delay set at Mohr-Coulomb failure than in the high density sets.

At ultimate failure the excess pore water pressures in the low density delay time set were higher than for the high density sets at the same consolidation pressure, because the cementation between aggregates has now been destroyed and the soil behaves like uncemented sands, which show an increase in excess pore pressure during undrained shear with a decrease in dry density.

4.5 TOTAL STRESS-STRENGTH BEHAVIOR

Fig. 4.9 shows plots of average principal stress difference, $1/2(\sigma_1 - \sigma_3)$, versus average total principal stress, $1/2(\sigma_1 + \sigma_3)$, at maximum stress difference and at ultimate. The data in Fig. 4.9a show that delay time has little effect on the total strength parameters at maximum stress difference. However, as seen from Fig. 4.9b, at ultimate conditions the low density delay time samples DT1 have a lower cohesion intercept in terms of total stresses than the high density samples DTO and DT2, whereas there is no difference between the DTO and DT2 sets of samples, meaning that delay time, per se, has no effect on the strength parameters in terms of total stresses. This solely is a reflection of the influence of the excess pore water pressures on the ultimate shear resistance of the soil, since $\bar{c}$ at ultimate was zero and $\bar{\Phi}_{ult}$ was independent of delay time and molding conditions.

4.6 STRESS-STRAIN BEHAVIOR

4.61 Initial Tangent Modulus

Although seating corrections had to be made to the stress-strain curves of all these tests, the initial tangent modulus was computed from the straight line portion of the curves (see Table 4.2). A plot of initial tangent modulus versus consolidation pressure was presented in Fig. 4.7b and discussed in Section 4.3.1.

4.6.2 Axial Strain to Reach Maximum Stress Difference

Fig. 4.10 is a plot of axial strain at maximum stress difference, ε_m, versus consolidation pressure. By comparing ε_m for the DT0 and DT2 sets (which had the same as-molded dry density) at a given consolidation pressure, it is seen that delay time, per se, has no effect on the axial strains required to reach maximum stress difference. However, at the lower consolidation pressures, the DT1 set, which had a lower as-molded dry density than the other two sets, DT0 and DT2, reached maximum stress difference at lower axial strains. This is probably due to the more open packing of the DT1 set, which causes, at these relatively small strains, more of the shearing stress to be carried by the cementation between cemented soil aggregates and less by inter-aggregate friction.

Stress-strain curves, as well as change in pore pressure and A-factor versus percentage of axial strain, are presented in Appendix A.

TABLE 4.1

PRESHEAR DATA FOR M-21 + 5% CEMENT

SAMPLE No.	COMPACTIVE EFFORT PSI	AS-MOLDED ω %	AS-MOLDED γ_d lb./ft^3	CONSOLIDATION PRESS. $\bar{\sigma}_o$ kg/cm^3	FINAL WATER CONTENT %	PORE PRESS. RESPONSE B %
DTO-1	400	13.4	112	49.2	18.0	—
DTO-2	400	13.4	112	10.0	19.0	—
DTO-3	400	13.3	112	25.0	18.9	—
DTO-4	400	13.6	112	50.0	—	93.2
DT1-1	400	13.2	104	25.0	22.7	—
DT1-2	400	13.4	104	10.1	22.5	—
DT1-3	400	13.4	103	50.1	21.6	85.1
DT1-4	400	13.4	103	50.0	20.3	—
DT2-1	400	13.3	112	50.1	18.3	90.7
DT2-2	~800	13.3	112	50.0	—	86.6
DT2-3	~800	13.5	112	10.0	18.8	91.4
DT2-5	~800	13.5	112	25.0	18.0	86.9

TABLE 4.2 SUMMARY OF STRESS - STRAIN CHARACTERISTICS FOR M - 21 + 5% CEMENT

SAMPLE NO.	Consolidation Press. $\bar{\sigma}$ Kg/cm²	Init. Tang. Mod. E Kg/cm²	AT MAXIMUM DIFFERENCE $(\bar{\sigma}_1 - \bar{\sigma}_3)_{m}$							AT FIRST TANGENCY WITH ENVELOPE							AT ULTIMATE				FINAL B FACTOR %	REMARKS
			Axial Strain %	$\bar{\sigma}_3$ Kg/cm²	$\bar{\sigma}_1 - \bar{\sigma}_3$ Kg/cm²	Δu Kg/cm²	$\bar{A}$ Kg/cm²	q Kg/cm²	$\bar{p}$ Kg/cm²	Axial Strain %	$\bar{\sigma}_3$ Kg/cm²	$\bar{\sigma}_1 - \bar{\sigma}_3$ Kg/cm²	Δu Kg/cm²	$\bar{A}$ Kg/cm²	q Kg/cm²	$\bar{p}$ Kg/cm²	q Kg/cm²	Δu Kg/cm²	$\bar{p}$ Kg/cm²	$\bar{A}$ Kg/cm²		
DTO-2	9.98	11,400	0.8	4.4	33.0	5.7	0.17	16.6	20.9	0.6	2.9	30.4	7.2	0.24	15.2	18.1	13.9	1.5	22.5	0.05	—	Seating Correction
DTO-3	24.96	18,900	1.2	7.2	38.3	17.6	0.46	19.1	26.3	0.9	7.0	38.0	17.8	0.47	19.0	26.0	15.6	15.8	24.6	0.60	—	"
DTO-4	49.92	23,000	0.8	15.4	57.0	34.5	0.61	28.5	43.9	1.5	13.9	55.8	36.1	0.65	27.9	41.8	30.6	34.9	45.6	0.57	93.2	"
DT1-1	24.96	26,800	0.6	4.1	33.6	14.1	0.42	16.8	25.9	0.8	8.1	32.5	15.1	0.47	16.3	24.3	9.2	17.8	14.6	0.97	—	"
DT1-2	10.05	9,200	0.7	4.3	26.7	6.0	0.23	13.3	17.7	2.0	5.1	23.5	5.2	0.22	11.8	16.9	8.9	5.4	13.8	0.30	—	"
DT1-3	50.00	25,700	0.6	19.8	46.9	30.2	0.64	23.4	43.3	1.8	12.7	41.3	37.3	0.90	20.7	33.4	12.0	40.2	21.8	1.68	100.76	"
DT1-4	49.92	16,000	0.7	17.8	43.1	28.5	0.66	21.5	39.4	2.3	11.4	38.1	35.0	0.92	19.1	30.4	14.1	37.1	23.4	1.31	—	"
DT2-1	50,00	—	0.8	14.9	60.8	34.5	0.57	30.4	45.3	1.1	13.3	59.1	36.1	0.61	29.6	42.9	21.0	34.8	35.7	0.83	103.01	"
DT2-2	49.92	11,500	1.3	16.4	58.7	28.9	0.49	29.3	45.7	1.6	15.6	57.6	29.7	0.52	28.8	44.4	19.9	28.7	36.5	0.72	90.17	"
DT2-3	9.98	17,142	1.3	6.3	36.4	3.3	0.09	18.2	24.5	0.4	3.0	31.8	6.6	0.21	15.9	18.9	14.8	0.1	24.3	0.00	94.10	"
DT2-5	25.03	12,500	1.2	12.1	49.7	12.5	0.25	24.9	36.9	1.8	11.9	49.3	12.6	0.26	24.6	36.6	18.7	10.9	32.3	0.29	89.05	"

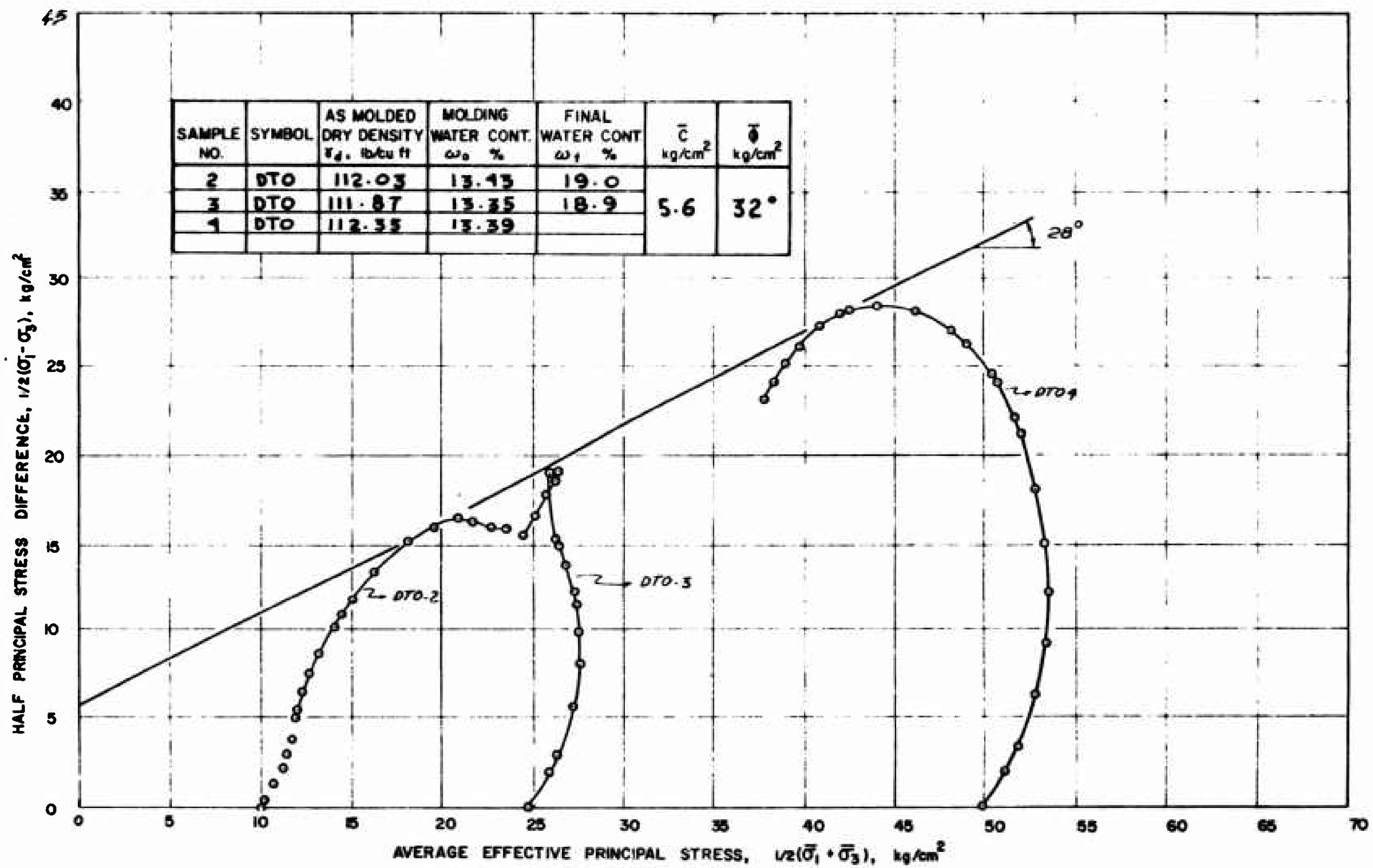

SAMPLE NO.	SYMBOL	AS MOLDED DRY DENSITY γ_d, lb/cu ft	MOLDING WATER CONT. ω_o %	FINAL WATER CONT ω_f %	$\bar{c}$ kg/cm²	$\bar{\phi}$ kg/cm²
2	DTO	112.03	13.43	19.0	5.6	32°
3	DTO	111.87	13.35	18.9		
4	DTO	112.35	13.39			

FIGURE 4.1 EFFECTIVE STRESS-STRENGTH BEHAVIOR IN UNDRAINED SHEAR OF M-21+5% CEMENT NO DELAY TIME PRIOR TO COMPACTION AT CONSTANT EFFORT

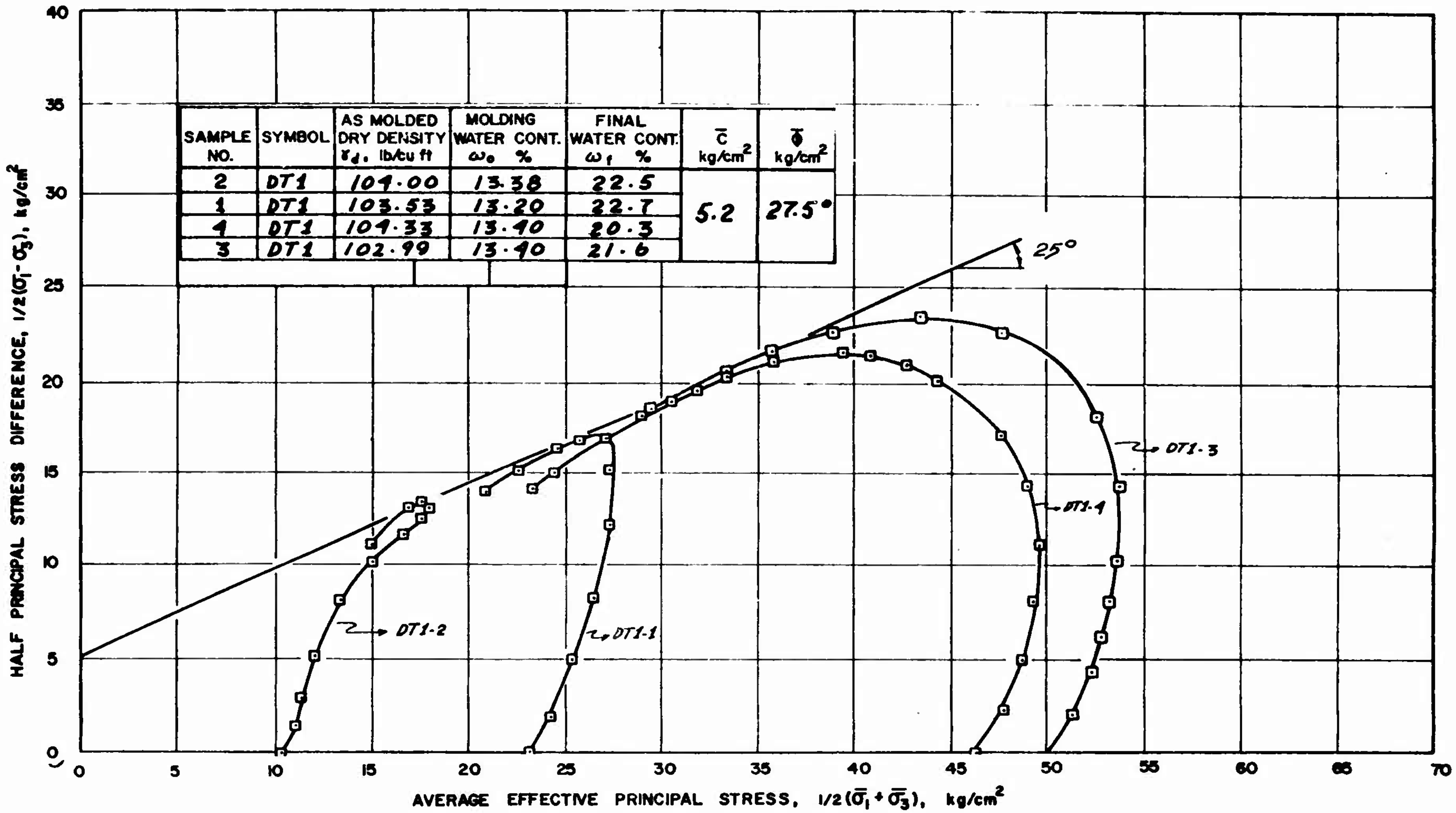

SAMPLE NO.	SYMBOL	AS MOLDED DRY DENSITY γ_d, lb/cu ft	MOLDING WATER CONT. ω_o %	FINAL WATER CONT. ω_f %	$\bar{c}$ kg/cm²	$\bar{\phi}$ kg/cm²
2	DT1	104.00	13.38	22.5	5.2	27.5°
1	DT1	103.53	13.20	22.7		
4	DT1	104.33	13.40	20.3		
3	DT1	102.99	13.40	21.6		

FIGURE 4.2 EFFECTIVE STRESS-STRENGTH BEHAVIOR IN UNDRAINED SHEAR OF M-21 + 5% CEMENT 5 HOURS DELAY TIME PRIOR TO COMPACTION AT CONSTANT EFFORT

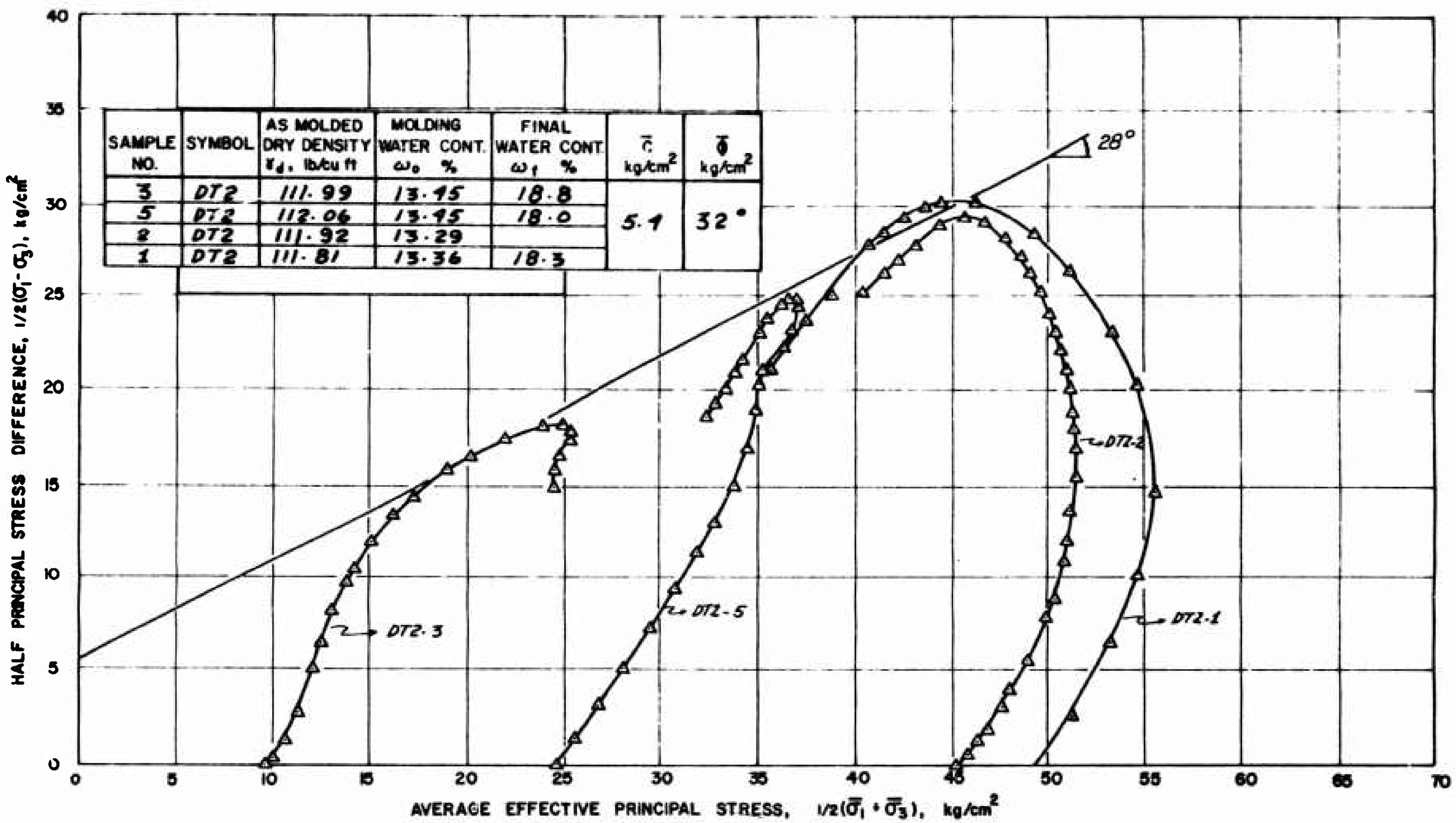

SAMPLE NO.	SYMBOL	AS MOLDED DRY DENSITY γ_d, lb/cu ft	MOLDING WATER CONT. ω_o %	FINAL WATER CONT. ω_f %	$\bar{c}$ kg/cm²	$\bar{\phi}$ kg/cm²
3	DT2	111.99	13.45	18.8	5.4	32°
5	DT2	112.06	13.45	18.0		
2	DT2	111.92	13.29			
1	DT2	111.81	13.36	18.3		

FIGURE 4.3 EFFECTIVE STRESS-STRENGTH BEHAVIOR IN UNDRAINED SHEAR OF M-21 + 5% CEMENT. 5 HOURS DELAY TIME PRIOR TO COMPACTION AT CONSTANT DENSITY

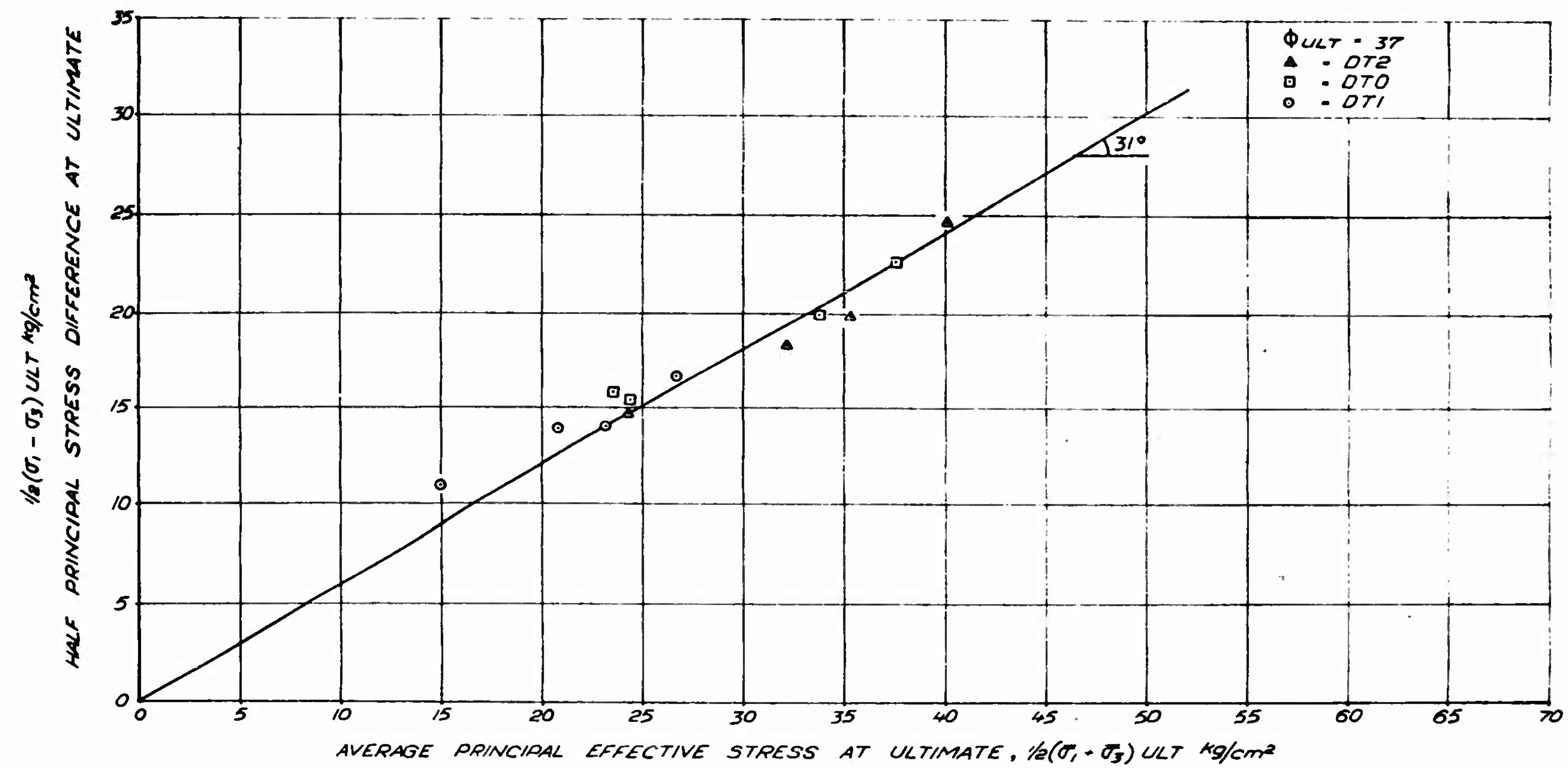

FIGURE 4.4 EFFECTIVE STRESS-STRENGTH BEHAVIOR OF M-21 + 5% CEMENT. AT ULTIMATE NO DELAY AND 5 HOURS DELAY TIME PRIOR TO COMPACTION

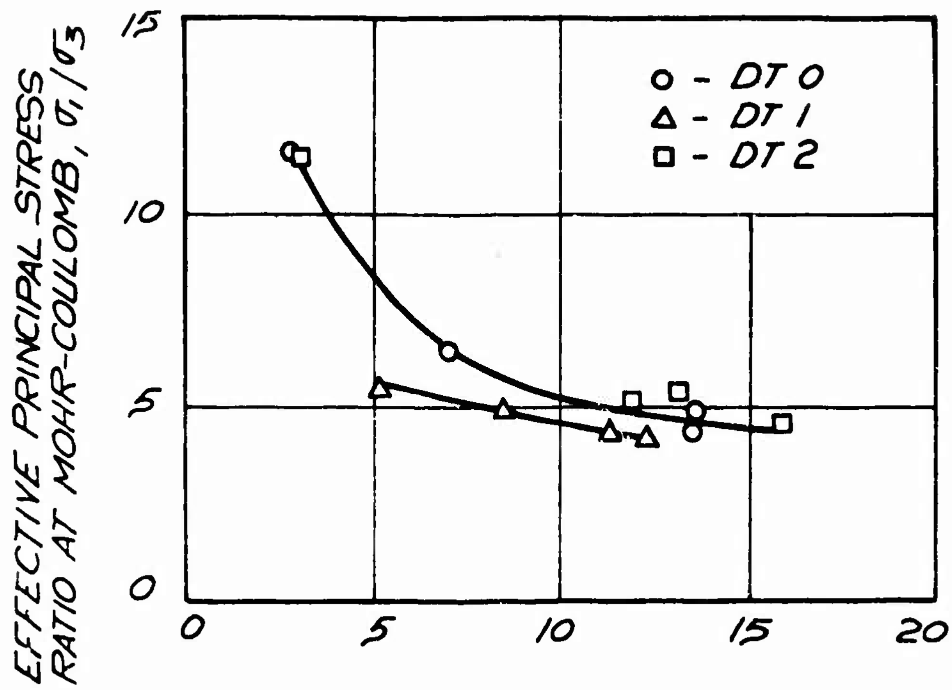
EFFECTIVE PRINCIPAL STRESS RATIO AT MOHR-COULOMB, σ_1/σ_3
o - DT 0
Δ - DT 1
□ - DT 2
15
10
5
0
0
5
10
15
20

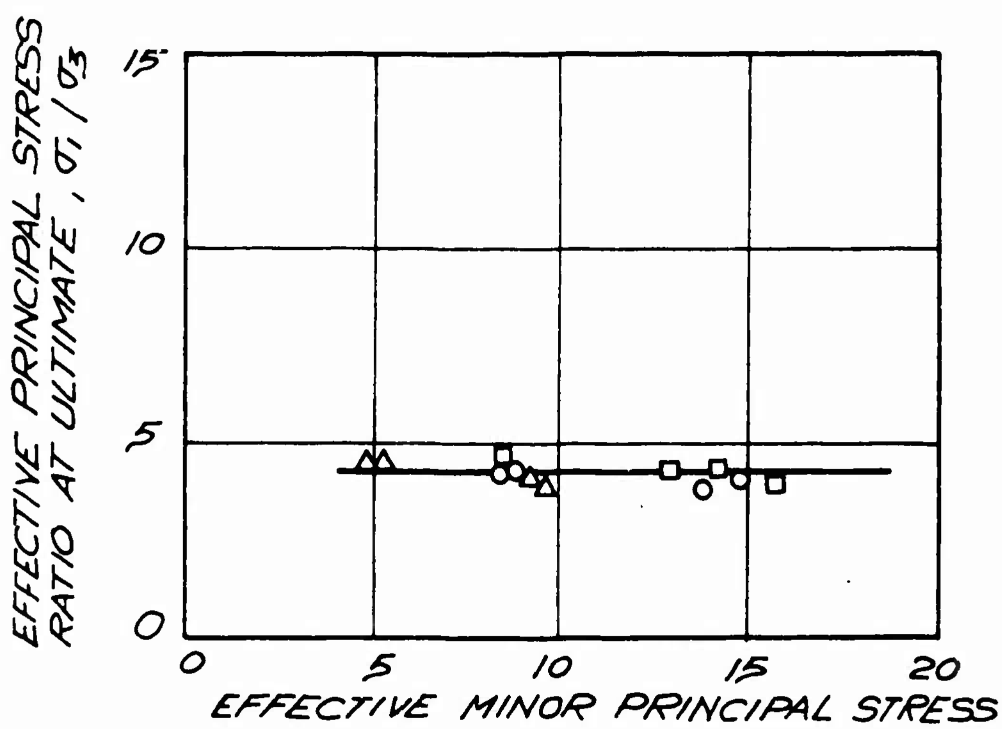
EFFECTIVE PRINCIPAL STRESS RATIO AT ULTIMATE, σ_1/σ_3
15
10
5
0
0
5
10
15
20
EFFECTIVE MINOR PRINCIPAL STRESS

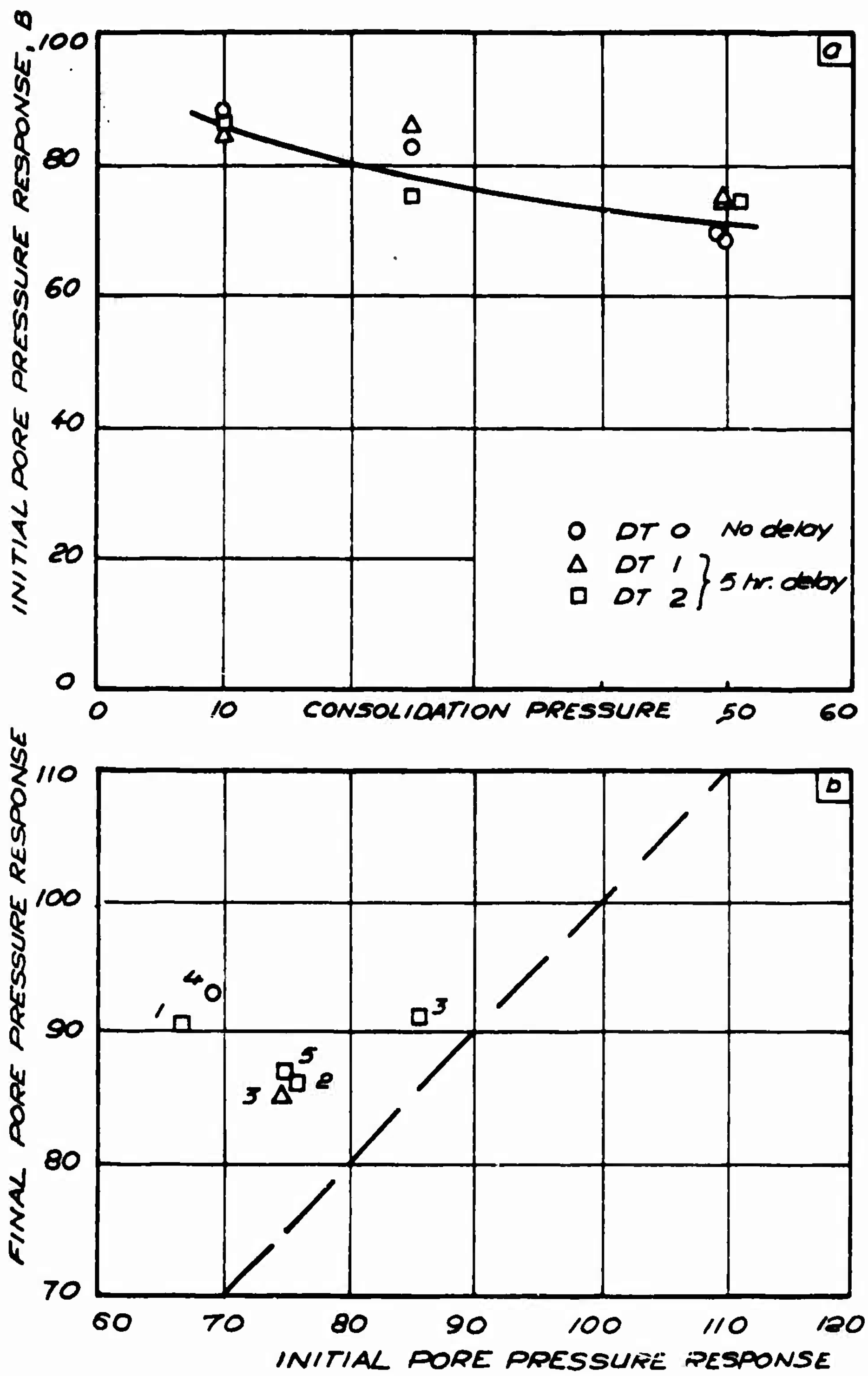

FIG. 4.6 PORE PRESSURE RESPONSE OF M-21 + 5% CEMENT

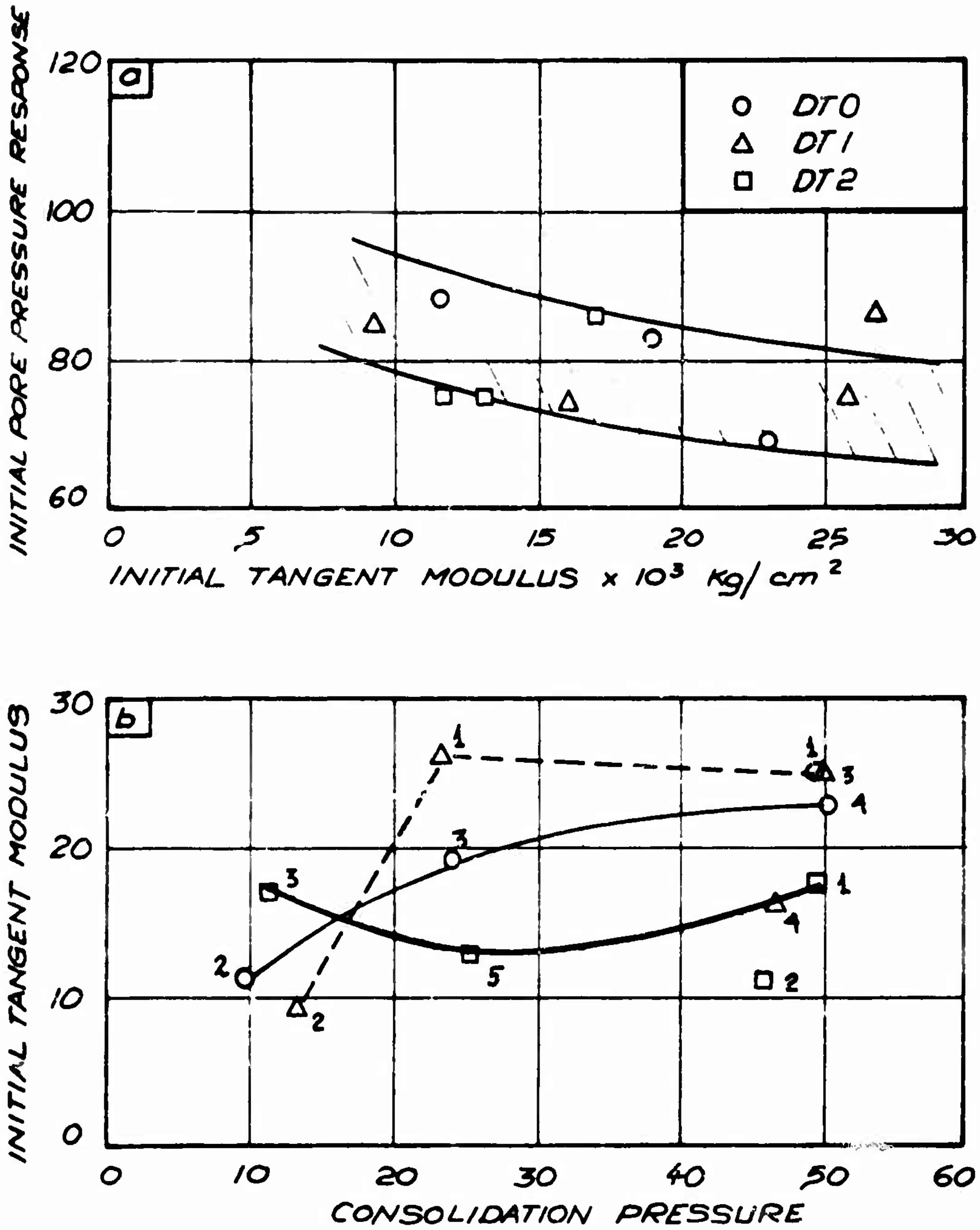

FIG. 4.7 PORE PRESSURE RESPONSE OF M-21 + 5 % CEMENT AND INITIAL TANGENT MODULUS

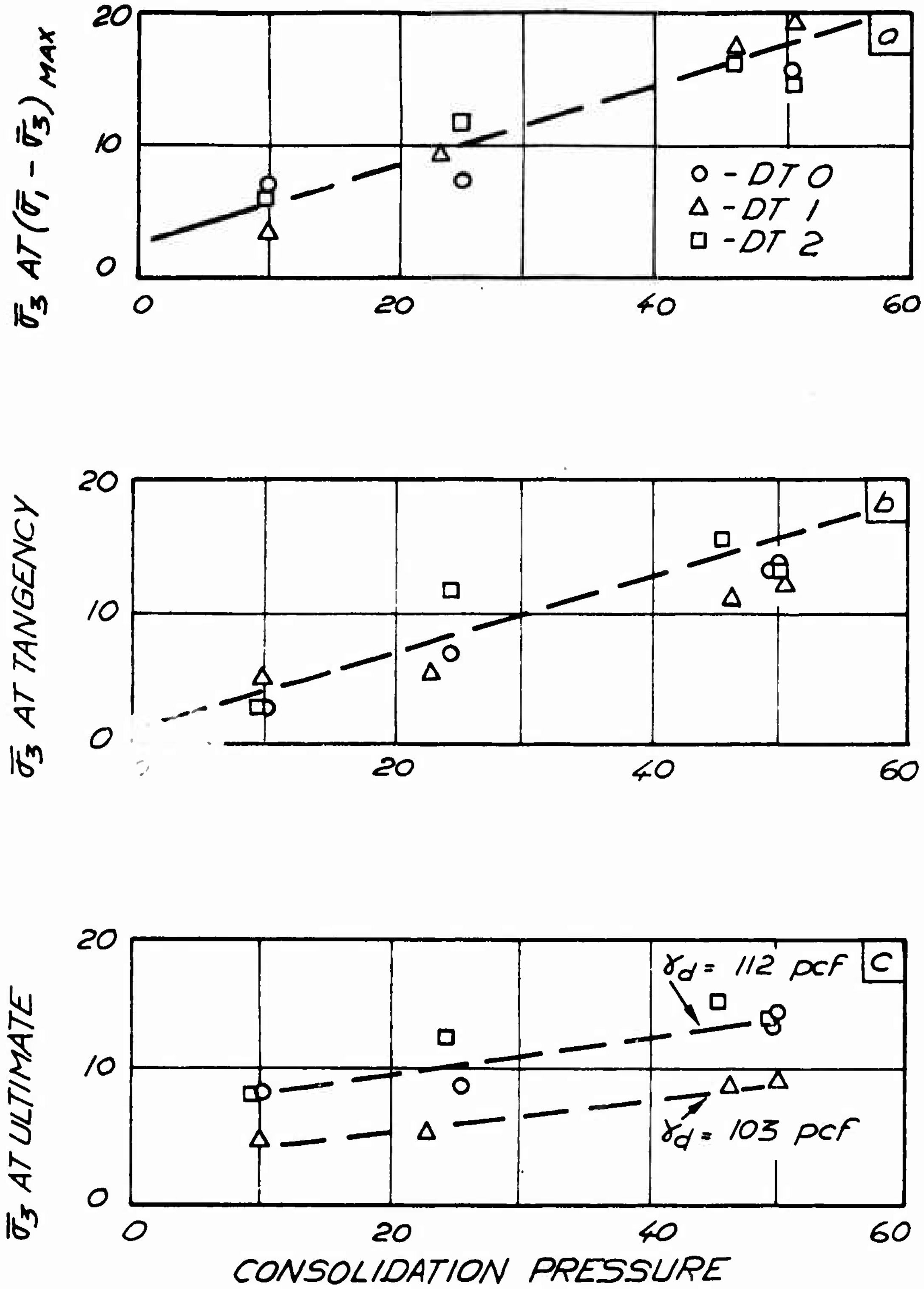

FIG. 4.8 INFLUENCE OF DELAY TIME OF COMPACTION ON THE EFFECTIVE MINOR PRINCIPAL STRESS

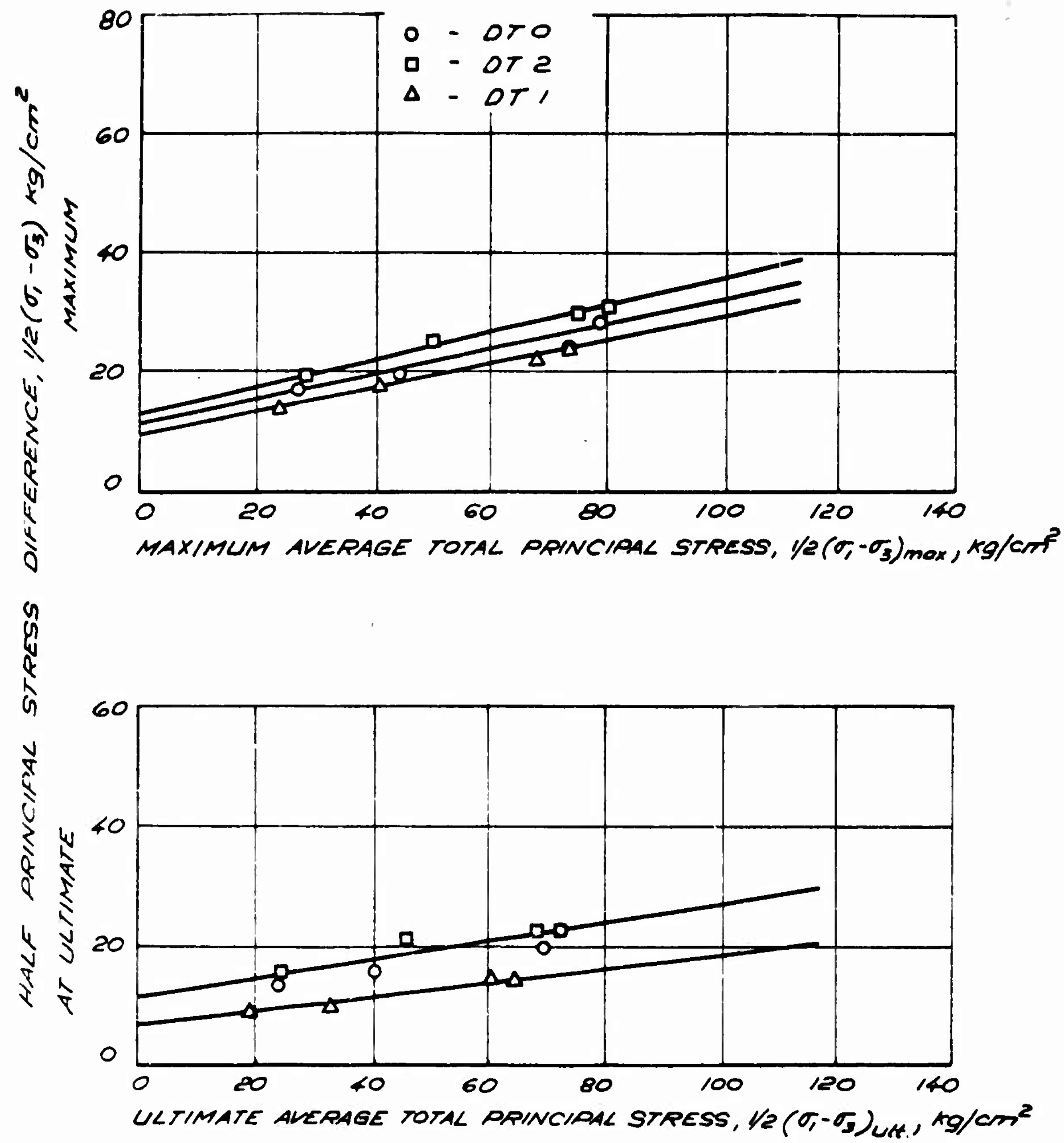

FIG. 4.9 INFLUENCE OF DELAY TIME OF COMPACTION ON THE TOTAL STRESS - STRENGTH BEHAVIOR OF M-21 + 5% CEMENT.

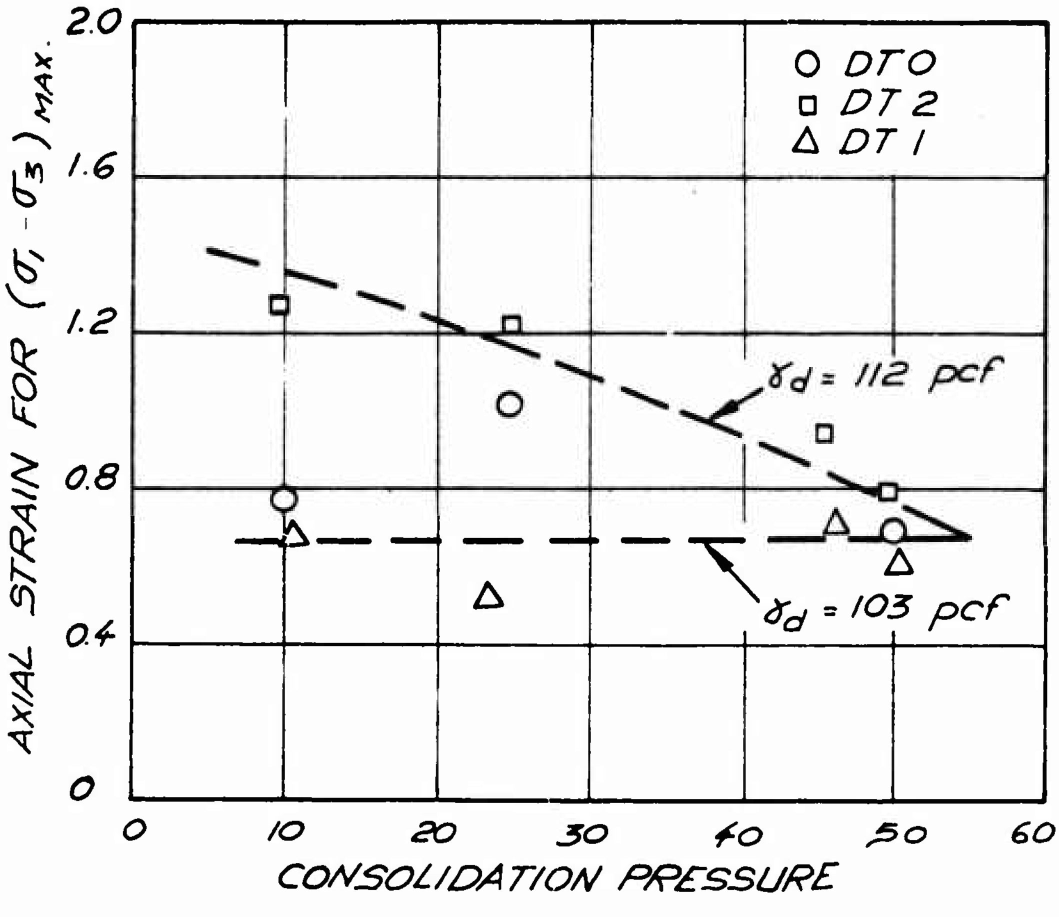

FIG. 4.10 INFLUENCE OF DELAY TIME OF COMPACTION ON THE AXIAL STRAIN REQUIRED TO REACH MAXIMUM STESS DIFFERENCE

Chapter 5

CONCLUSIONS

The following conclusions are drawn regarding the effects of molding conditions and delay time after mixing and prior to compaction, on the effective stress-strength and stress-strain behavior of a clayey silt both untreated and stabilized with 5 per cent hydrated lime and 5 per cent portland cement type 1.

1) Molding conditions have no significant effect on the strength parameters of the untreated compacted soil in terms of effective stresses but cause large changes in the total stress-strength parameters.

2) For both the lime-and the cement-stabilized soil, a significant increase in the Mohr-Coulomb effective cohesion intercept, $\bar{c}$, is produced by increasing as-molded dry density, but this does not cause any significant change in the effective angle of shearing resistance. Molding water content, per se, has no effect on the effective stress-strength parameters.

3) At ultimate conditions, the stabilized systems have no effective cohesion intercept and have an effective angle of shearing resistance that is independent of molding conditions. This is also the case for the untreated soil.

4) Molding water content rather than molding dry density controls the pore water pressure behavior of untreated fine-grained soils in undrained shear. Samples compacted dry of optimum develop the higher pore pressures during shear.

5) As-molded dry density, rather than molding water content, controls the pore water pressure behavior of cemented fine-grained soil in undrained shear. The higher the as-molded dry density, the lower the pore pressure induced during shear.

6) Delay time prior to compaction results in significantly lower as-molded dry density than non-delay compaction for the same compaction effort. This shows up in the effective stress-strength behavior primarily as a drop in the Mohr-Coulomb effective angle of shearing resistance. Nevertheless, if the delay time mixes are compacted to the same as-molded dry density as the non-delay mixes,

there is no difference in the effective stress-strength parameters. Delay time does not influence $\bar{\phi}_{ult}$ of this soil-cement system.

7) Delay time prior to compaction, per se, has no significant effect on the stress-strain behavior of this soil-cement system. However, the drop in as-molded dry density, which occurs due to delay time at constant compactive effort, causes the soil-cement system to reach maximum stress difference at lower axial strains. This is especially the case at low consolidation pressures and may be undesirable in the field.

LIST OF REFERENCES

Arman, A. and Saifan, F.S. (1965). "The Effect of Delayed Compaction on Stabilized Soil-Cement", Louisiana State University, Division of Eng. Research (Baton Rouge, La.), Bull. No. 88.

Lambe, T.W., (1958). "The Structure of Compacted Clay", and "The Engineering Behavior of Compacted Clay", Soil Mechanics and Foundations Division, ASCE, Vol. 84, No. SM2.

Seed, H.B., Mitchell, J.K. and Chan, C.K., (1960). "The Strength of Compacted Cohesive Soils", Amer. Soc. of Civil Engr., Research Conference on Shear Strength of Cohesive Soils, Boulder Colorado.

Skempton, A.W., (1954). "Pore Pressure Coefficients A and B", Geotechnique, 4:4:148.

Terzaghi, K., (1923). Die Berechnug der Durchlassigkeitsziffer des Tones aus dem Verlauf der Hydrodynamischen Spannungser-Scheinungen, Sitz. Akad. Wissen. Wien Mathnaturskl Abt. IIa, 132, 105-124.

Wissa, A.E.Z. and Ladd, C.C., (1964). "Effective Stress-Strength Behavior of Compacted Stabilized Soils", M.I.T. Soils Publication No. 164.

Wissa, A.E.Z. and Ladd, C.C., (1965). "Shear Strength Generation in Stabilized Soils", M.I.T. Soils Publication No. 173.

Wissa, A.E.Z. (1969). "Pore Pressure Measurements in Saturated Stiff Soils", Soil Mechanics and Foundation Division, ASCE, Vol. 95, No. SM4, July 1969.

Appendix A

STRESS-STRAIN BEHAVIOR

Preceding page blank

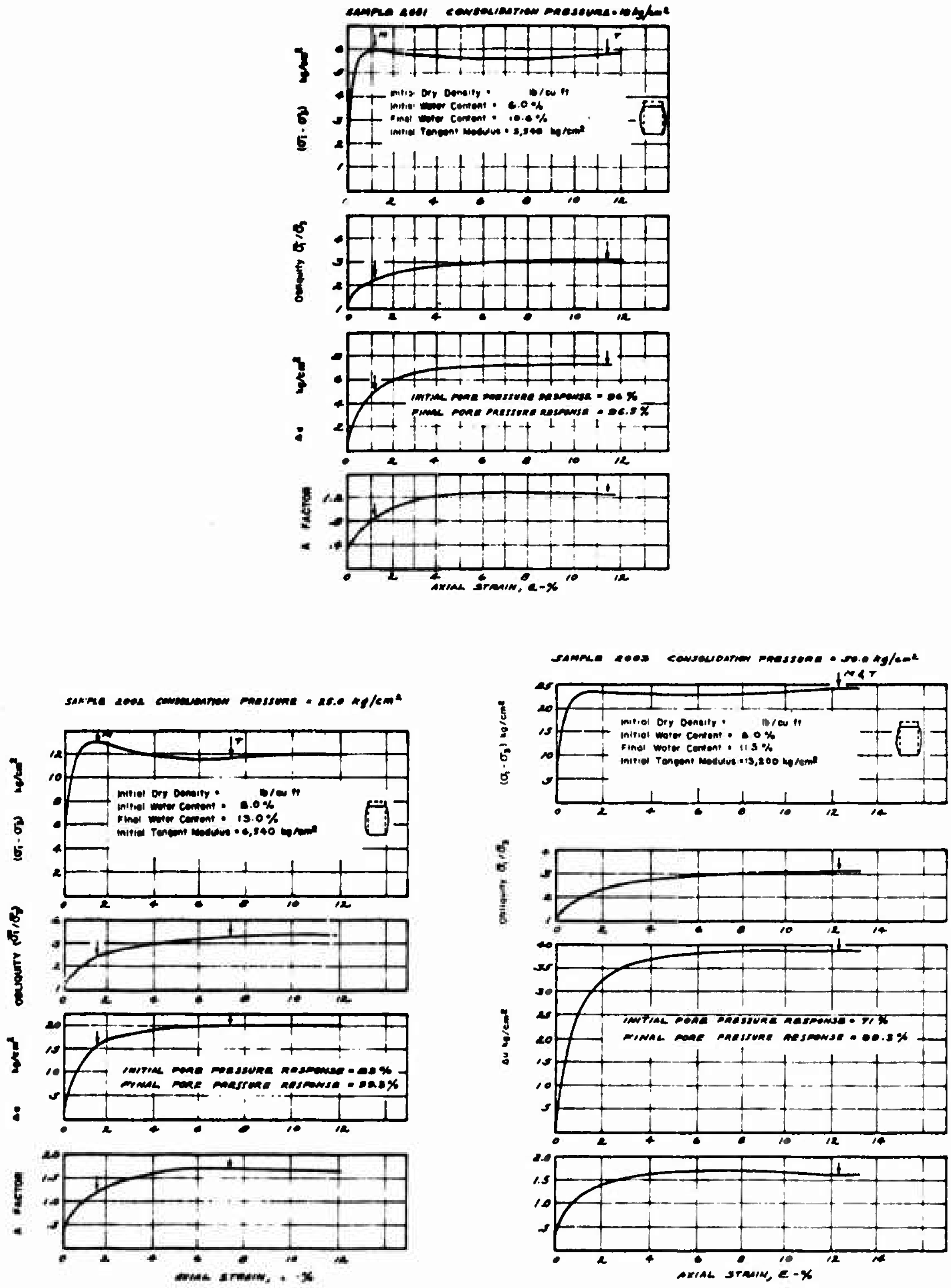

FIG. A-1 UNDRAINED STRESS-STRAIN BEHAVIOR OF UNTREATED M-21 SAMPLES COMPACTED DRY OF OPTIMUM

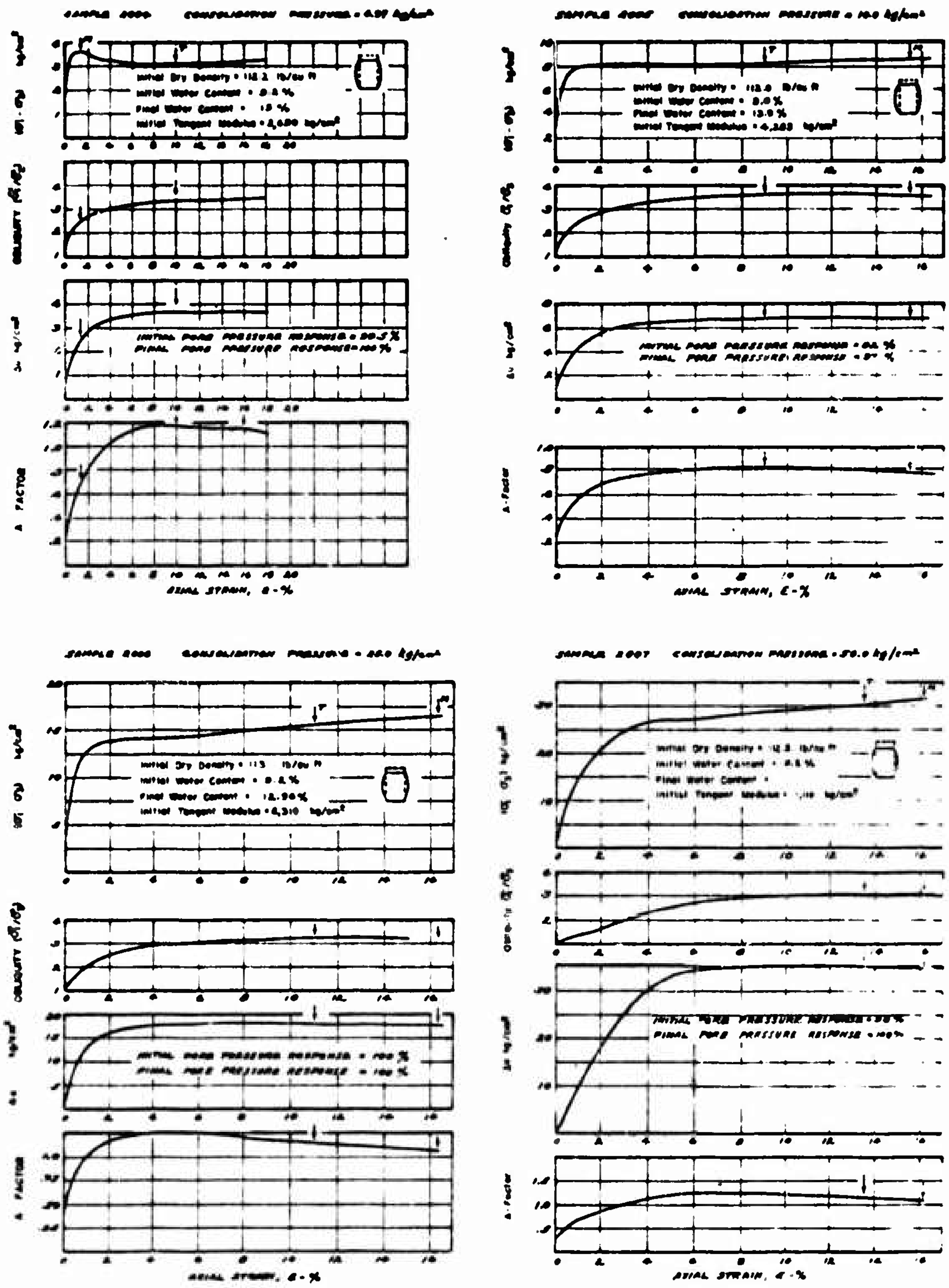

FIG. A-2 UNDRAINED STRESS-STRAIN BEHAVIOR OF UNTREATED M-21 SAMPLES COMPACTED DRY OF OPTIMUM

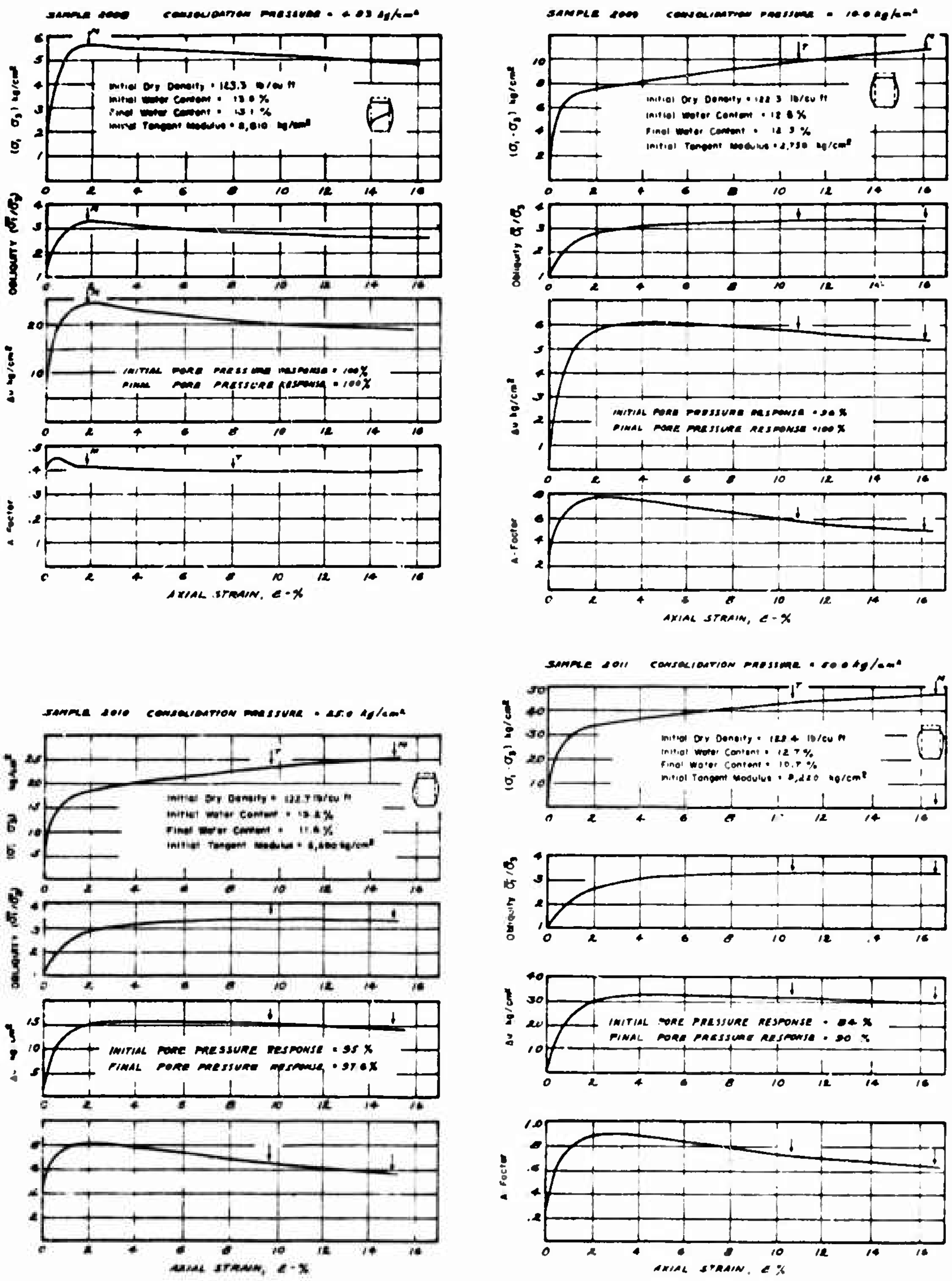

FIG. A-3 UNDRAINED STRESS-STRAIN BEHAVIOR OF UNTREATED M-21 SAMPLES COMPACTED AT OPTIMUM

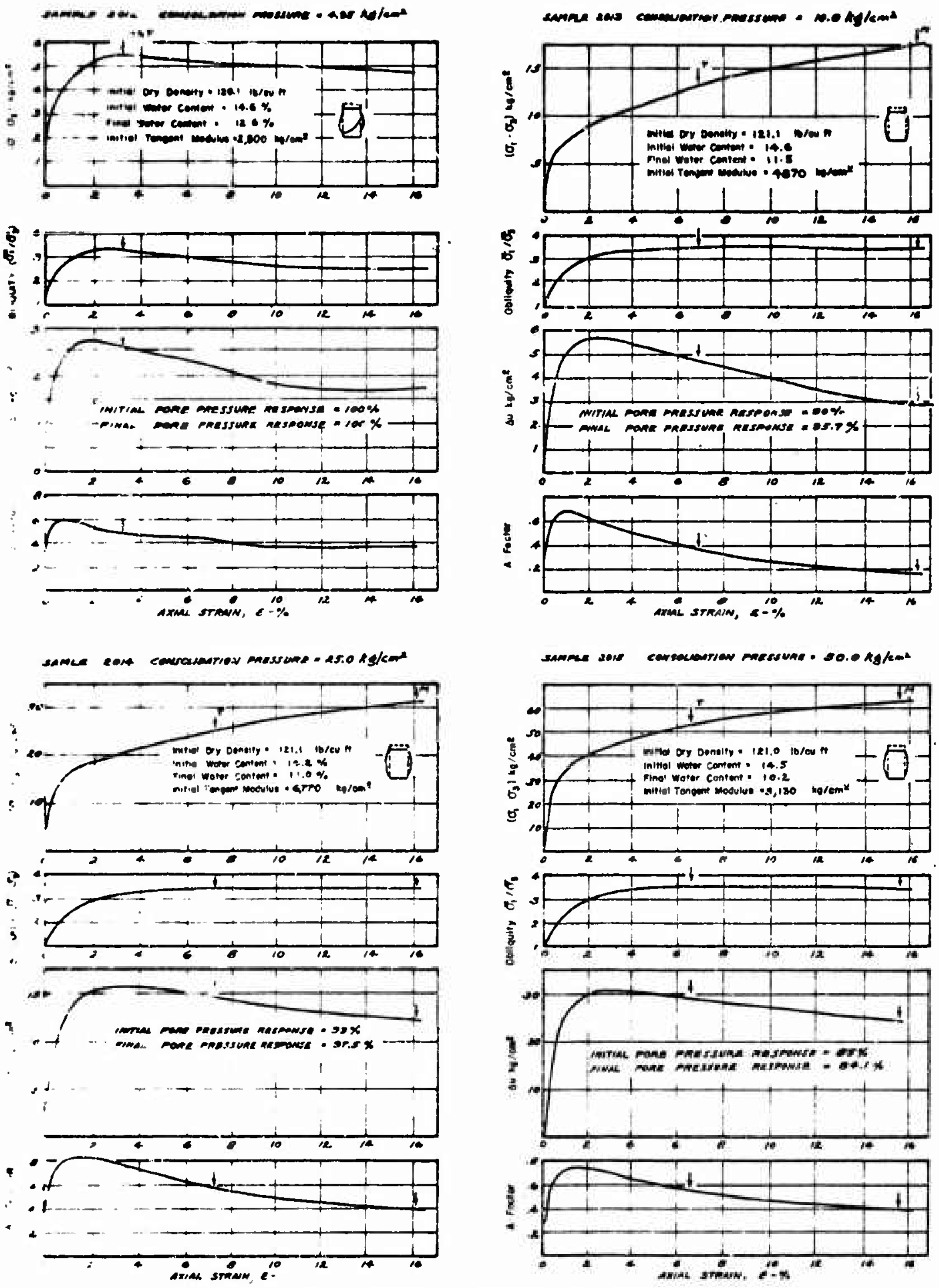

FIG A-4 UNDRAINED STRESS-STRAIN BEHAVIOR OF UNTREATED M-21 SAMPLES COMPACTED WET OF OPTIMUM

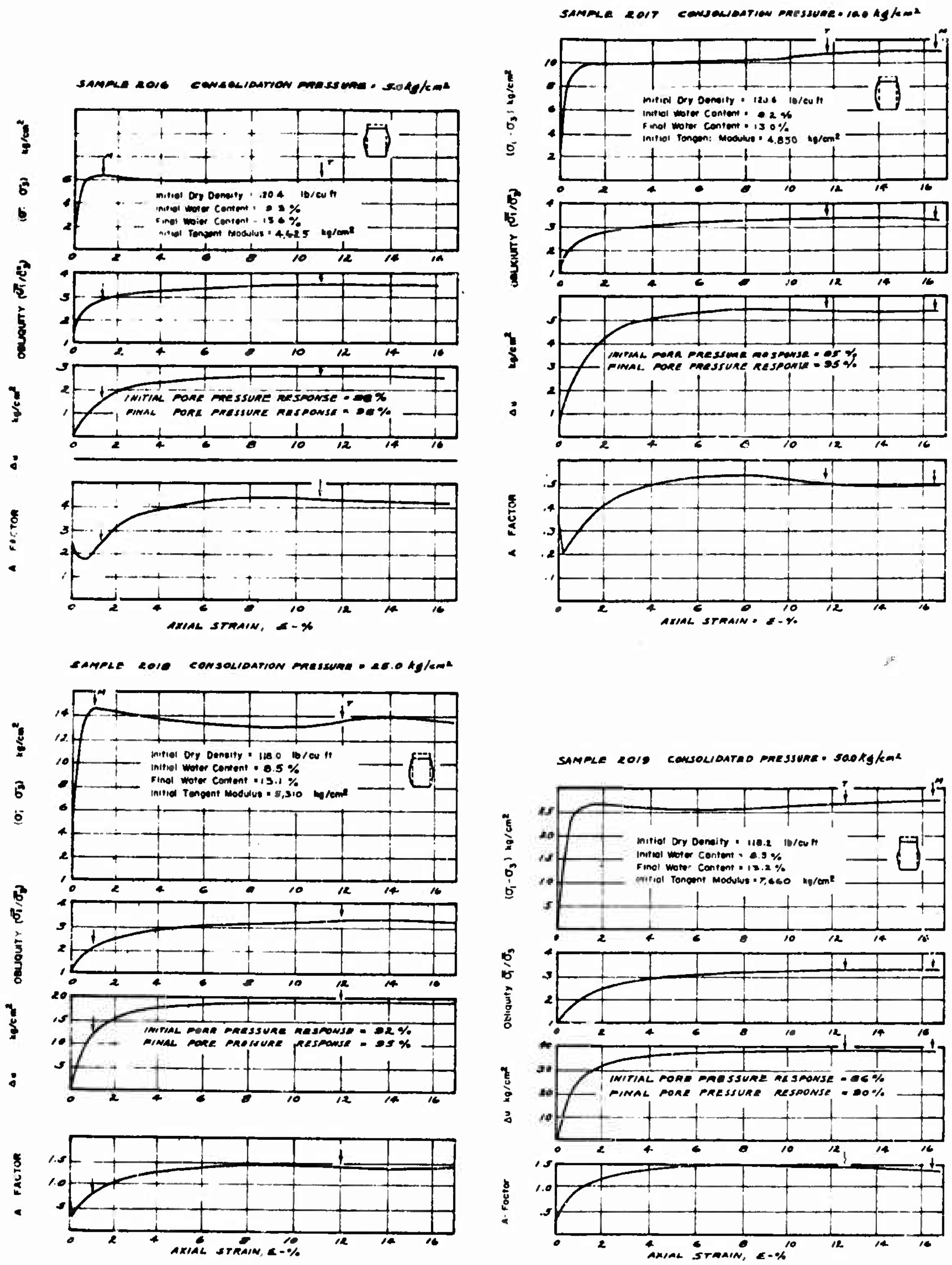

FIG. A-8 UNDRAINED STRESS-STRAIN BEHAVIOR OF UNTREATED M-21 SAMPLES COMPACTED TO HIGH DENSITY

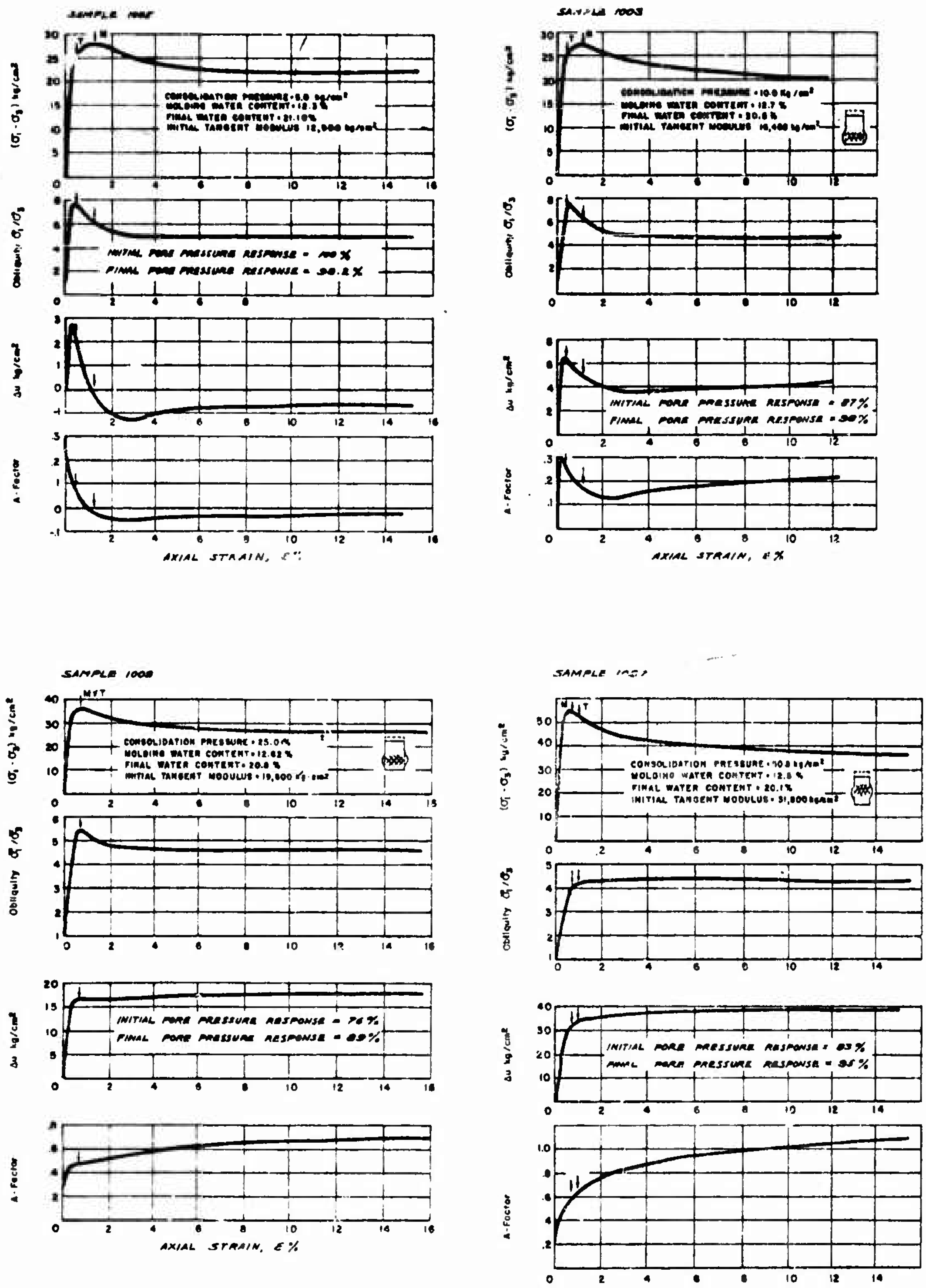

FIG. A-6 UNDRAINED STRESS STRAIN BEHAVIOR OF M-21 + 5% LIME SAMPLES COMPACTED DRY OF OPTIMUM

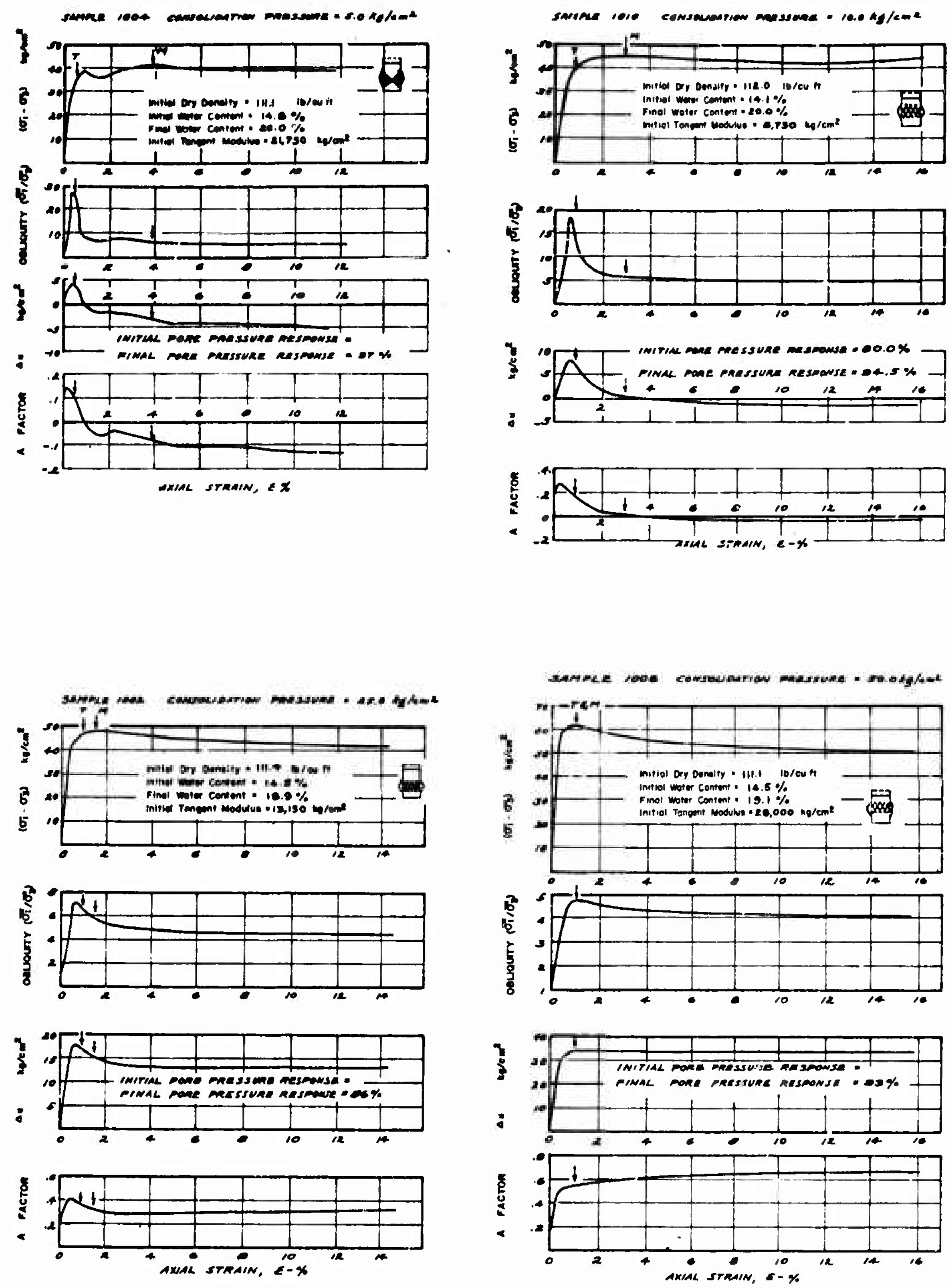

FIG. A-7 UNDRAINED STRESS-STRAIN BEHAVIOR OF M-21 + 5% LIME COMPACTED DRY OF OPTIMUM

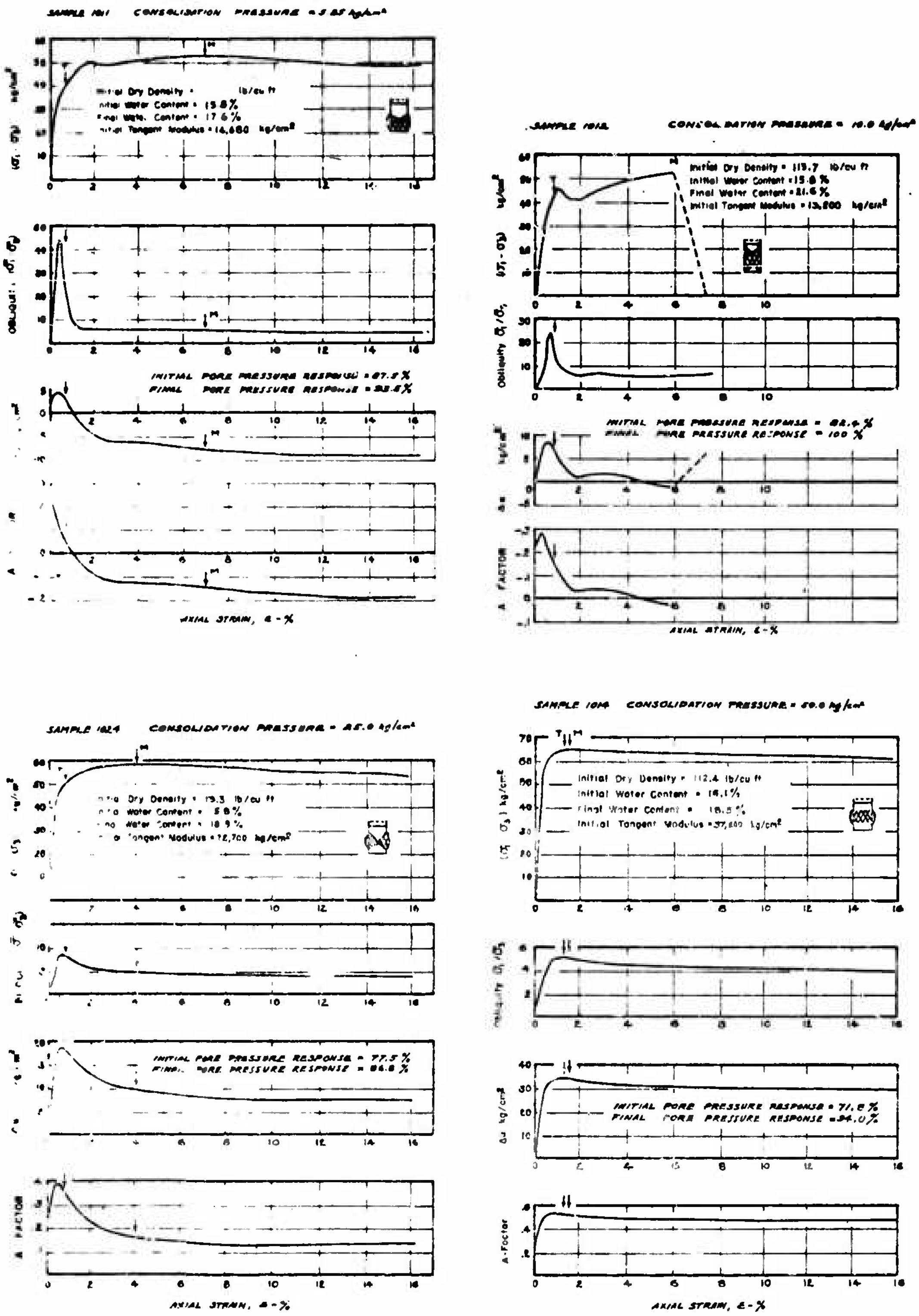

FIG. A-8 UNDRAINED STRESS-STRAIN BEHAVIOR OF M-21 + 5% LIME COMPACTED AT OPTIMUM

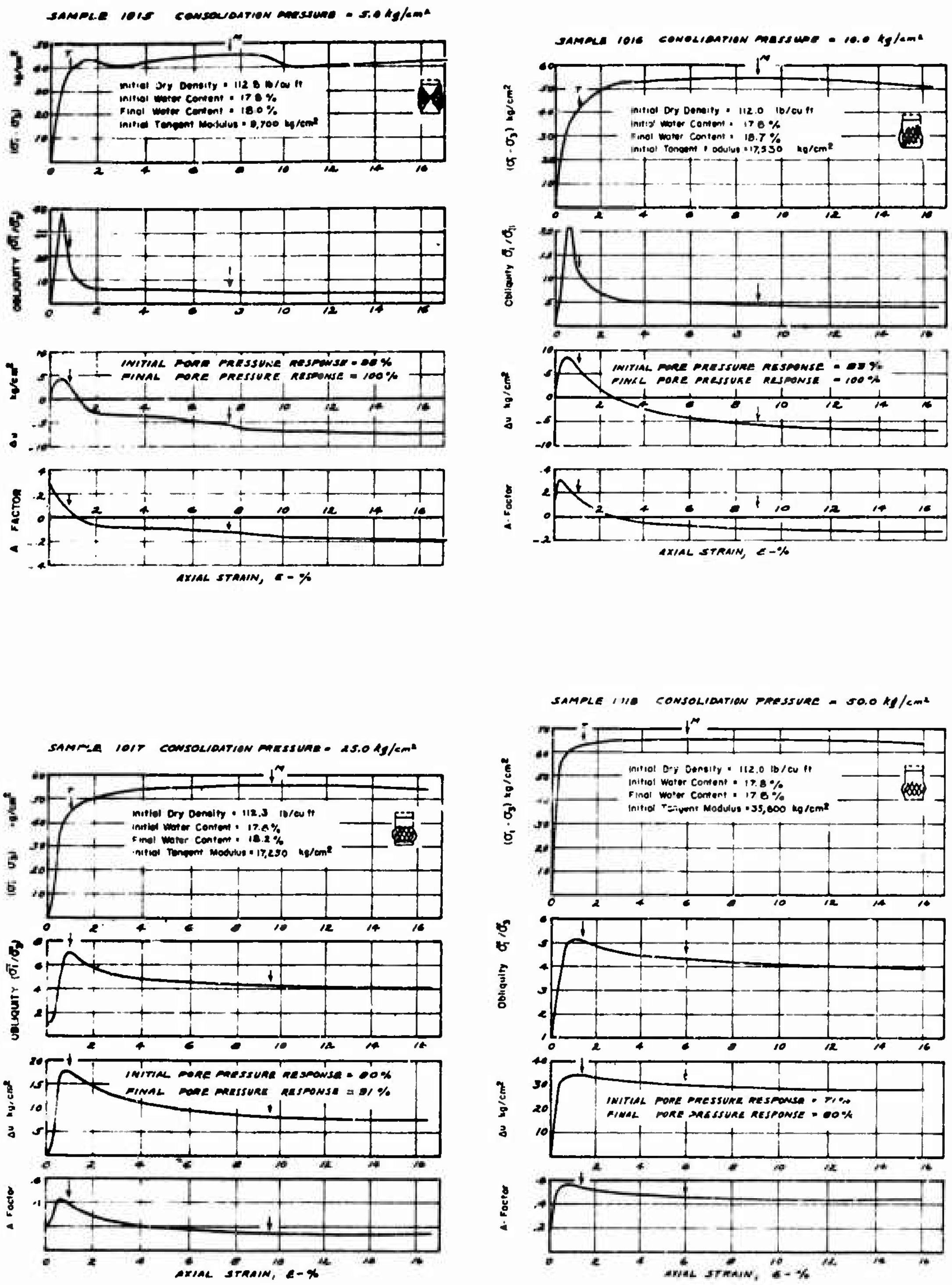

FIG. A-9 UNDRAINED STRESS-STRAIN BEHAVIOR OF M-21 + 5% LIME COMPACTED WET OF OPTIMUM

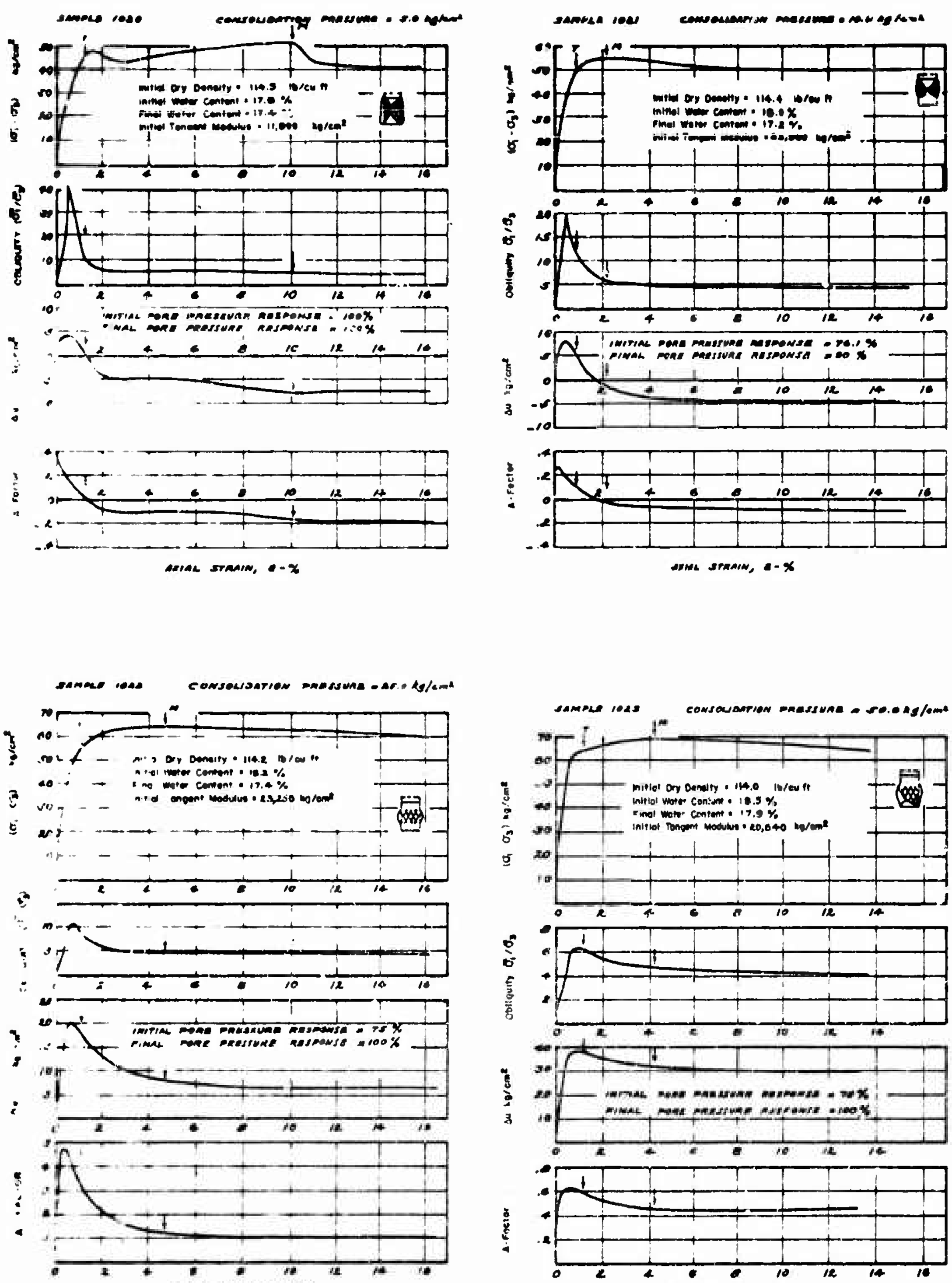

FIG A-10 UNDRAINED STRESS-STRAIN BEHAVIOR OF M-21 + 5% LIME COMPACTED TO HIGH DENSITY

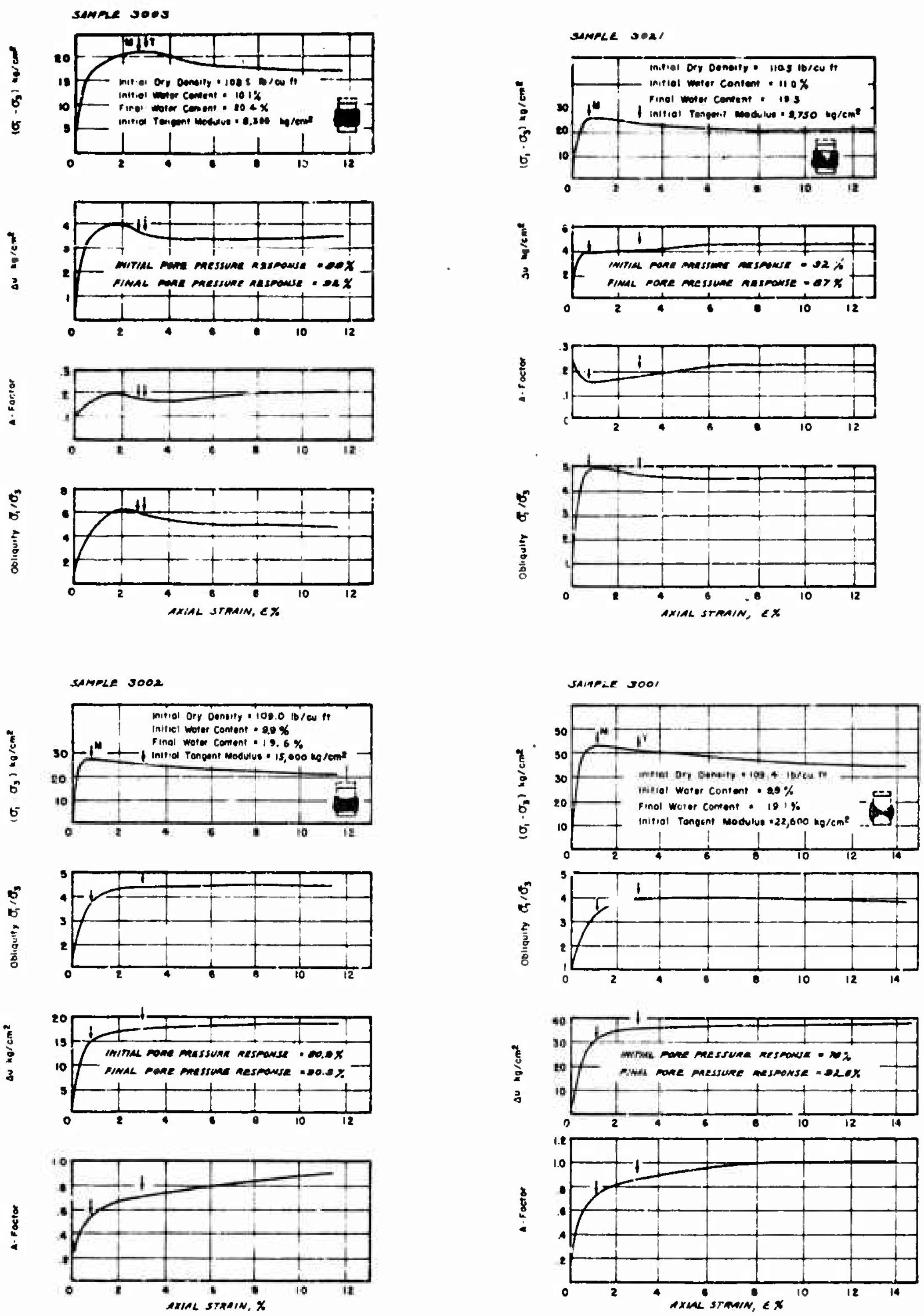

FIG. A-11 UNDRAINED STRESS-STRAIN BEHAVIOR OF M-21+5% CEMENT COMPACTED VERY DRY OF OPTIMUM

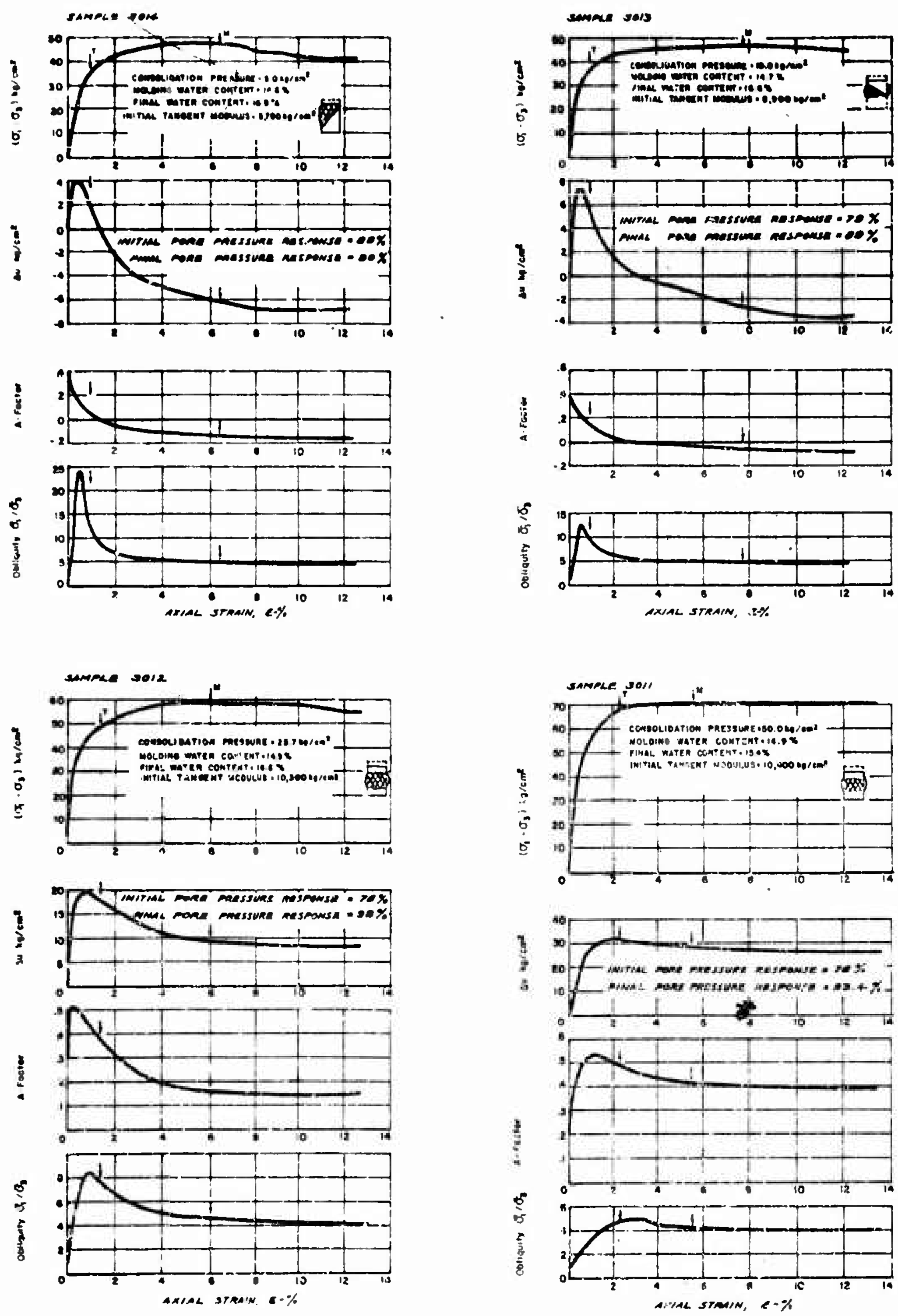

FIG. A-12 UNDRAINED STRESS STRAIN-BEHAVIOR OF M-21+5% CEMENT COMPACTED AT OPTIMUM

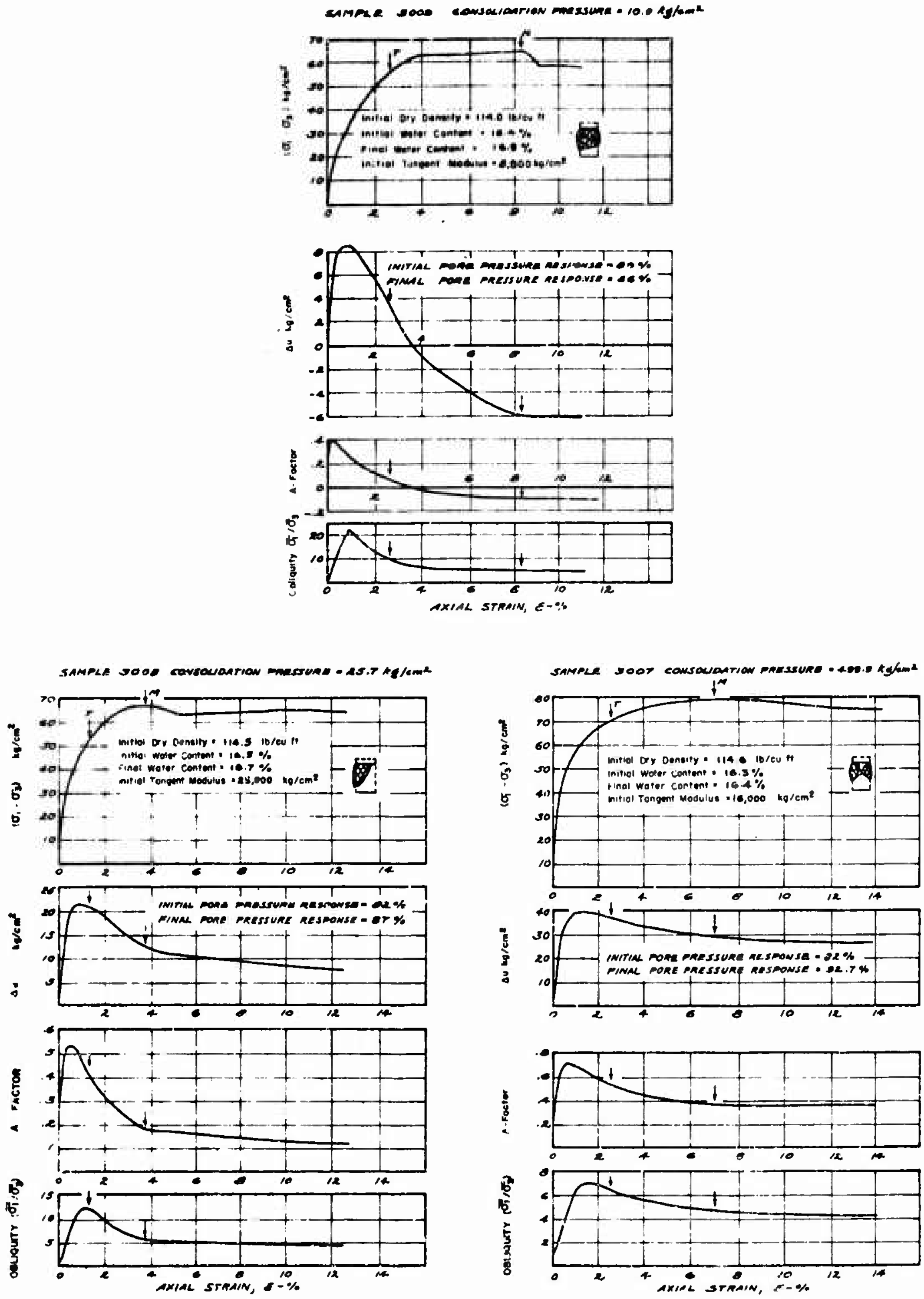

FIG. A-8 UNDRAINED STRESS-STRAIN BEHAVIOR OF M-21+5 % CEMENT COMPACTED WET OF OPTIMUM

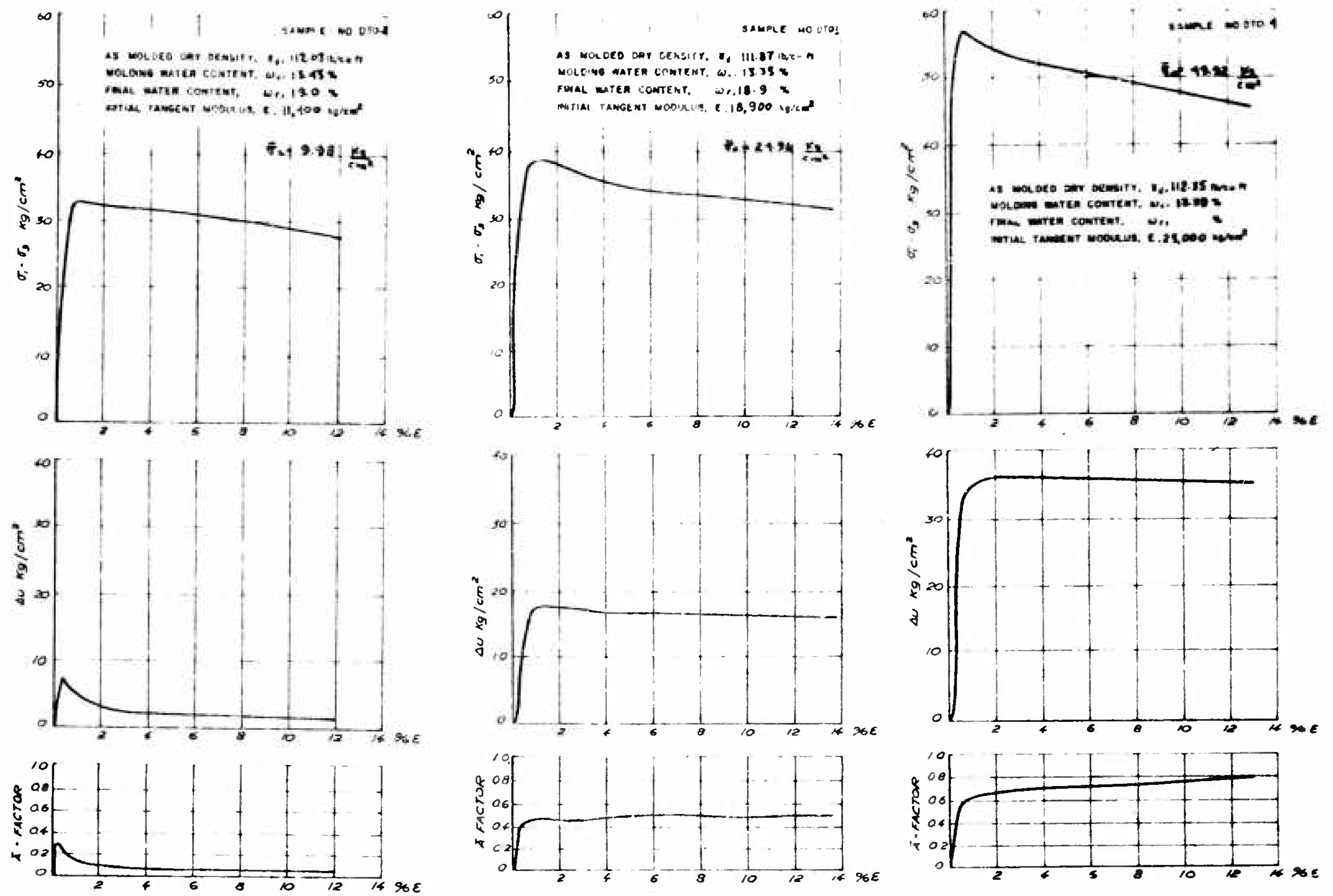

FIG. A-14 UNDRAINED STRESS-STRAIN BEHAVIOR OF M-21 + 5% CEMENT. NO DELAY TIME TO COMPACTION AT CONSTANT EFFORT

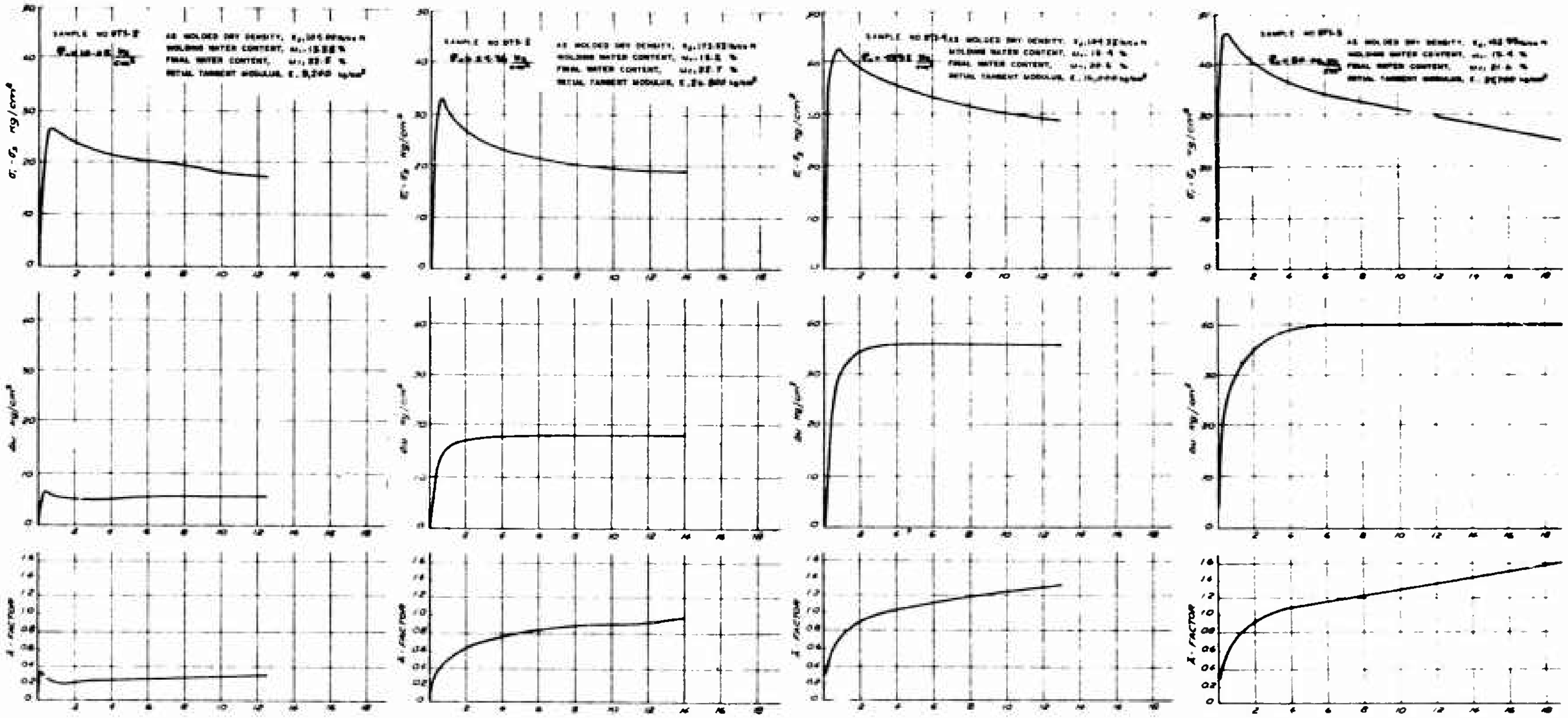

FIG A-15 UNDRAINED STRESS-STRAIN BEHAVIOR OF M-21 + 5% CEMENT. 5 HOURS DELAY TIME TO COMPACTION AT CONSTANT EFFORT

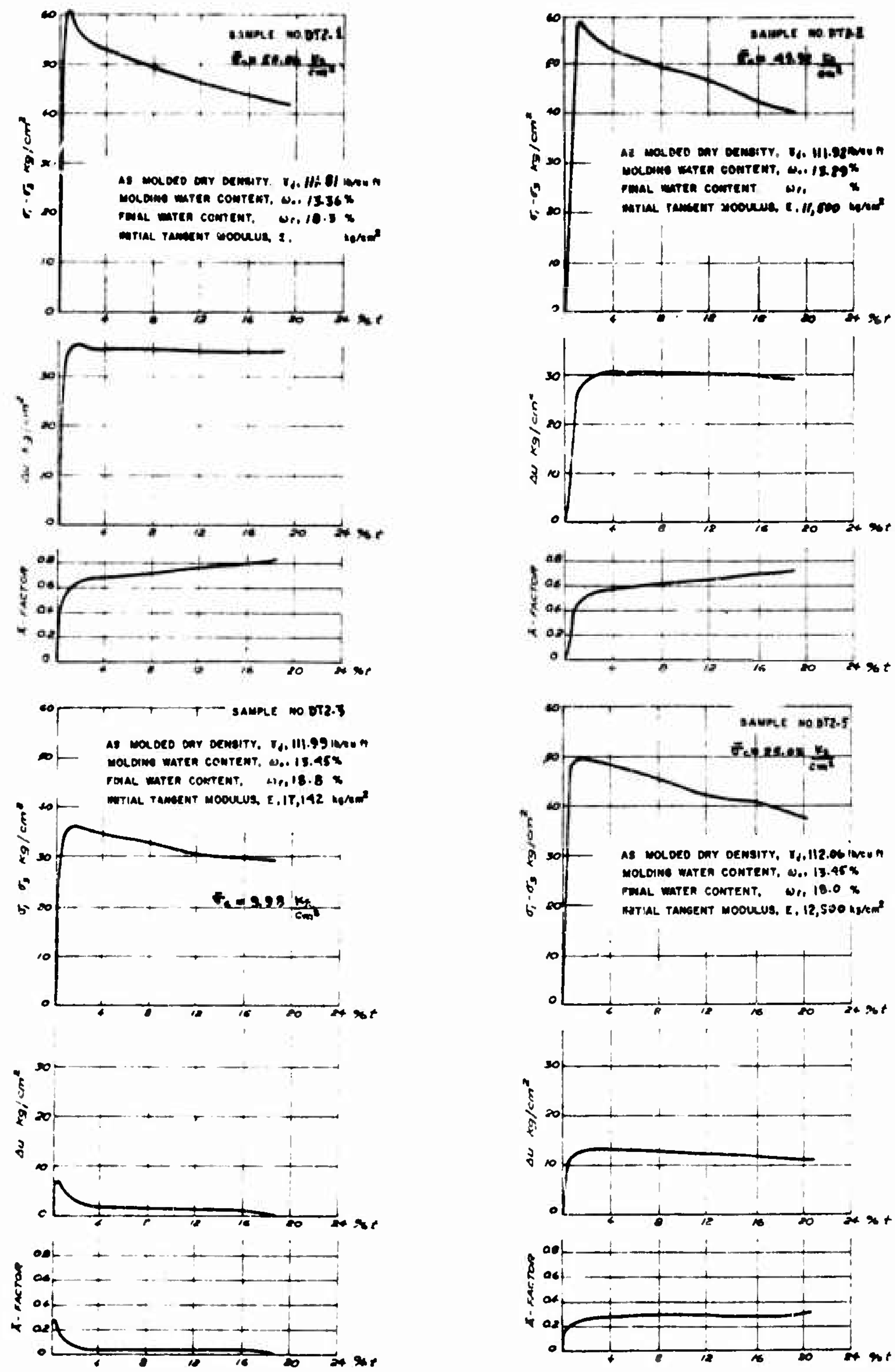

FIG A-16 UNDRAINED STRESS-STRAIN BEHAVIOR OF M-21 + 5% CEMENT. 5 HOURS DELAY TIME TO COMPACTION TO CONSTANT DENSITY

Unclassified

Security Classification

DOCUMENT CONTROL DATA - R & D

(Security classification of title, body of abstract and indexing annotation must be entered when the overall report is classified)

1. ORIGINATING ACTIVITY (Corporate author) Soil Mechanics Division, Department of Civil Engineering, Massachusetts Institute of Technology, Cambridge, Massachusetts	2a. REPORT SECURITY CLASSIFICATION Unclassified 2b. GROUP

3. REPORT TITLE

SOIL STABILIZATION; EFFECT OF MOLDING CONDITIONS ON THE EFFECTIVE STRESS-STRENGTH BEHAVIOR OF A STABILIZED CLAYEY SILT

4. DESCRIPTIVE NOTES (Type of report and inclusive dates)

Phase Report No. 8

5. AUTHOR(S) (First name, middle initial, last name)

Anwar E. Z. Wissa
Samuel Feferbaum-Zyto
Jose Guillermo Paniagua

6. REPORT DATE	7a. TOTAL NO. OF PAGES	7b. NO. OF REFS
January 1970	136	8

8a. CONTRACT OR GRANT NO. DA-IT0611102B52A-01 b. PROJECT NO. I-T-0-1451-B-52-A30 c. d.	9a. ORIGINATOR'S REPORT NUMBER(S) Soils Publication No. 242 Research Report R69-55 9b. OTHER REPORT NO(S) (Any other numbers that may be assigned this report) U. S. Army Engineer Waterways Experiment Station Contract Report No. 3-63, Phase Report No. 8

10. DISTRIBUTION STATEMENT

This document has been approved for public release and sale; its distribution is unlimited.

11. SUPPLEMENTARY NOTES	12. SPONSORING MILITARY ACTIVITY
Conducted for U. S. Army Engineer Waterways Experiment Station, CE, Vicksburg, Mississippi	U. S. Army Materiel Command Washington, D. C.

13. ABSTRACT

The influence of molding water content, as-molded dry density, and delay time prior to compaction after mixing in of the molding water on the effective stress-strength behavior of a clayey silt stabilized with hydrated lime and portland cement is presented in this report. This investigation used the results of high pressure consolidated-undrained triaxial compression tests with pore water pressure measurements. It is shown that molding conditions have no significant effect on the Mohr-Coulomb effective stress-strength parameters, $\bar{c}$ and $\bar{\phi}$, of the untreated compacted soil. For both the cement and lime stabilized systems, the effective cohesion intercept, $\bar{c}$, significantly increases with increases in as-molded dry density while $\bar{\phi}$ does not change. Molding water content per se does not influence either $\bar{c}$ or $\bar{\phi}$. For a given compactive effort, delay time prior to compaction produces a drop in the as-molded dry density of the cement stabilized soil which shows up primarily as a drop in the effective angle of shearing resistance, $\bar{\phi}$. It also lowers the strains required to reach Mohr-Coulomb failure, which is an undesirable characteristic. At ultimate failure (large strains), it is shown that neither molding conditions nor delay time prior to compaction have any significant effect on the effective stress-strength parameters of the stabilized systems.

DD FORM 1 NOV 65 1473 REPLACES DD FORM 1473, 1 JAN 64, WHICH IS OBSOLETE FOR ARMY USE.

Unclassified

Security Classification

Unclassified

Security Classification

14. KEY WORDS	LINK A		LINK B		LINK C	
	ROLE	WT	ROLE	WT	ROLE	WT
Cement soil stabilization						
Clay soils						
Silts						
Soil stabilization						
Soil tests						

Unclassified

Security Classification